



Field trip guidebook to the Upper Fir carbonatite-hosted Ta-Nb deposit, Blue River area, east-central British Columbia

A.S. Rukhlov, T.C. Chudy, H. Arnold, and D. Miller



Ministry of
Energy, Mines and
Petroleum Resources



British Columbia Geological Survey GeoFile 2018-6

**Ministry of Energy, Mines and Petroleum Resources
Mines and Mineral Resources Division
British Columbia Geological Survey**

Recommended citation: Rukhlov, A.S., Chudy, T.C., Arnold, H., and Miller, D., 2018. Field trip guidebook to the Upper Fir carbonatite-hosted Ta-Nb deposit, Blue River area, east-central British Columbia. British Columbia Ministry of Energy, Mines and Petroleum Resources, Geological Survey GeoFile 2018-6, 67 p.

Front cover: Sill-like body of calcite-carbonatite, Howard Creek. Photo by A.S. Rukhlov.

Back cover: Dolomite carbonatite with aligned fluorapatite megacrysts and dark-toned ferrikatophorite prisms set in a recrystallized ferroan dolomite matrix that readily oxidizes brown-red; BS-1 cut, Upper Fir. Photo by A.S. Rukhlov.

This publication is available, free of charge, from the British Columbia Geological Survey website:
www.empr.gov.bc.ca/geology

This guidebook was initially prepared for a field trip sponsored by the Mineralogical Association of Canada as part of the Resources for Future Generations conference held in Vancouver, June 2018.



Ministry of
Energy, Mines and
Petroleum Resources



Field trip guidebook to the Upper Fir carbonatite-hosted Ta-Nb deposit, Blue River area, east-central British Columbia

A.S. Rukhlov
T.C. Chudy
H. Arnold
D. Miller

Ministry of Energy, Mines and Petroleum Resources
British Columbia Geological Survey
GeoFile 2018-6



Field trip guidebook to the Upper Fir carbonatite-hosted Ta-Nb deposit, Blue River area, east-central British Columbia

A.S. Rukhlov^{1a}, T. C. Chudy², H. Arnold¹, and D. Miller¹

¹British Columbia Geological Survey, Ministry of Energy, Mines and Petroleum Resources, Victoria, B.C., V8W 9N3

²Department of Earth, Ocean and Atmospheric Sciences, The University of British Columbia, Vancouver, B.C., V6T 1Z4

^aCorresponding author: Alexei.Rukhlov@gov.bc.ca

Recommended citation: Rukhlov, A.S., Chudy, T.C., Arnold, H., and Miller, D., 2018. Field trip guidebook to the Upper Fir carbonatite-hosted Ta-Nb deposit, Blue River area, east-central British Columbia. British Columbia Ministry of Energy, Mines and Petroleum Resources, Geological Survey GeoFile 2018-6, 67 p.

Abstract

Carbonatites are igneous rocks containing abundant primary carbonate minerals. These rare rocks generally form in intracratonic settings as part of crustal-scale dome and rift systems. Historically regarded as petrogenetic curiosities, recent interest in strategic metals has led to significant exploration for carbonatites. In the Canadian Cordillera, carbonatites were emplaced episodically, at ca. 810-700, 500, and 360-330 Ma, forming part of the British Columbia alkaline province, which defines a long (at least 1000 km), narrow (ca. 200 km) orogen-parallel belt. The ca. 810-700 Ma and 500 Ma carbonatites were injected during protracted breakup of the supercontinent Rodinia and passive margin development on the western flank of Laurentia. In contrast to these and to most carbonatites globally, the 360-330 Ma carbonatites, such as the Blue River area examples, are unusual. They were emplaced near the continental margin during subduction rather than in the cratonic interior during continent breakup. The Blue River carbonatites include at least 18 carbonatite and 2 alkaline, silica-undersaturated-rock occurrences. This field trip considers the characteristics, magmatic evolution, and mineralization of the Blue River carbonatites as represented by the Upper Fir complex, which hosts one of the largest and best studied Nb-Ta deposits in the Canadian Cordillera. Participants will examine outcrops and drill-core sections of amphibolite-grade metacarbonatites, related metasomatic rocks, syntectonic pegmatites, enclosing pelites and amphibolites of the Mica Creek assemblage (750-550 Ma), and Mesozoic-Cenozoic Cordilleran structures. We consider the tectonometamorphic overprinting of igneous features in the Upper Fir carbonatites, as recorded by paragenetic relationships, mineral chemistry, recrystallization, and retrograde deformation.

Exploration by Commerce Resources Corporation at the Upper Fir carbonatite complex established an NI 43-101-compliant resource of 48.4 million tonnes (Indicated) averaging 1,610 ppm Nb₂O₅ and 197 ppm Ta₂O₅ plus 5.4 million tonnes (Inferred) averaging 1,760 ppm Nb₂O₅ and 191 ppm Ta₂O₅. Sill-like carbonatite bodies up to 72 m thick are in isoclinal, recumbent, similar folds (in part roofless) that are refolded by southwest-vergent, open folds with parallel geometries. The deposit has been traced for about 1450 m north-south and about 800 m east-west and consists of mainly dolomite carbonatite and subordinate (<4%) medium- to coarse-grained calcite carbonatite. Calcite carbonatites form lenses up to a few m thick within dolomite carbonatite bodies. The carbonatites show contact-parallel foliation concordant with penetrative schistosity and compositional layering in the enclosing gneisses, schists, and amphibolites. Internal retrograde breccia and shear zones further obscure the original paragenetic record. The carbonatites are recrystallized, and display diverse fabrics. Granoblastic varieties, likely representing magmatic protoliths, occur mainly at the margins of the carbonatite bodies, whereas fine-grained, well-foliated and porphyroclastic varieties typically make up the central portions. This distribution correlates favourably with the composition of amphibole-group minerals and Nb-Ta oxide phases, suggesting that primary compositional zoning within individual dolomite carbonatite bodies controlled rheology and thus strain partitioning during deformation. The Nb-Ta mineralization consists of predominantly ferrocolumbite and pyrochlore-super group minerals.

Isotopic evidence and spatial and temporal associations with large igneous provinces containing ultramafic and alkaline silicate rocks indicate derivation of carbonatite magmas from sub-lithospheric mantle plumes. New isotopic and elemental compositions of minerals from Blue River carbonatites and related rocks are indistinguishable from worldwide carbonatites generated by such deep-mantle plumes. The 360-330 Ma Cordilleran examples formed along the western margin of Laurentia while subduction was taking place immediately to the west. Lithospheric extension related to this Late Paleozoic subduction is considered responsible for rifting the continent margin and initiating the Slide Mountain ocean as a back-arc basin. We suggest that this same back-arc extension triggered emplacement of the Blue River carbonatites, which were derived from a long-lived, deep-level mantle plume that was tapped episodically since the Neoproterozoic.

Keywords: carbonatite, British Columbia alkaline province, mantle plume, Blue River, Upper Fir, Ta-Nb deposit, pyrochlore supergroup, ferrocolumbite, molybdenite

1. Introduction

Carbonatites are rare magmatic rocks that contain abundant primary carbonate minerals, at least 30% (Mitchell, 2005) or 50% (Le Maitre, 2002). Given their extreme geochemistry, carbonatites are unlike other igneous rocks (Tuttle and Gittins, 1966; Heinrich, 1966; Le Bas, 1977; Woolley, 1987, 2001; Bell, 1989; Bell and Keller, 1995; Kogarko et al., 1995; Bell et al., 1998; Wall and Zaitsev, 2004). Carbonatites are generally found in intracratonic regions, such as crustal-scale domal swells and related rift systems (e.g., East African rift valley, Maimecha-Kotui and Kola alkaline provinces). Of more than 530 known occurrences, only two are from oceanic islands, the Cape Verdes and Canary Islands (Woolley and Kjarsgaard, 2008a), which emphasizes the important, yet still enigmatic, role of continental lithosphere in their genesis. Most carbonatites are spatially and temporally associated with much larger volumes of ultramafic and alkaline silicate rocks, suggesting genetic relationships between undersaturated silicate and carbonate magmas (Woolley, 2003; Mitchell, 2005; Woolley and Kjarsgaard, 2008b). Carbonatite magmas can form as low-degree partial melts of a carbonated mantle, as the products of fractional crystallization, or as immiscible liquids separated from carbonated silicate magmas (e.g., Wyllie, 1989). However, their ultimate mantle sources (lithospheric versus sub-lithospheric) remain controversial (e.g., Gerlach et al., 1988; Nelson et al., 1988; Gittins and Harmer, 2003; Bell and Rukhlov, 2004; Bell and Simonetti, 2010; Woolley and Bailey, 2012; Rukhlov et al., 2015; Hulett et al., 2016).

Isotopic evidence provides firm constraints on the origin of these unusual rocks. Found on all continents, carbonatites are well-suited for tracing secular mantle evolution. This is because their extreme enrichment in Sr and REEs, especially light REEs (LREE), buffers Sr and Nd isotopic compositions from changes due to contamination, and because they span ages from 3.0 Ga to the present (Bell et al., 1982; Bell and Blenkinsop, 1987a; Nelson et al., 1988; Bell and Rukhlov, 2004; Rukhlov et al., 2015). The Sr, Nd, Hf, and Pb isotopic signatures of carbonatites worldwide are similar to those of oceanic island basalts (OIBs). The mixing arrays defined by carbonatite data in multi-isotopic space rule out any involvement of the shallow asthenospheric mantle represented by DMM (Depleted Mid-ocean ridge Mantle; Hofmann, 2014), and show mixing in different proportions of depleted, deep-mantle reservoirs such as FOZO (FOCUS ZONE; Hart et al., 1992; Hauri et al., 1994; Campbell and O'Neill, 2012) and EM (Enriched Mantle 1 and 2) and HIMU (high- $^{238}\text{U}/^{204}\text{Pb}$ or μ -mantle) components, which are all found in mantle plumes or hot spots (e.g., Hoernle and Tilton, 1991; Bell and Simonetti, 1996; Bell and Tilton, 2001, 2002; de Ignacio et al., 2006; Rukhlov et al., 2015). The primitive He, N, Ne, Ar, Kr and Xe isotopic compositions in some carbonatites also suggest a relatively un-degassed mantle source, which is difficult to reconcile with an in situ lithospheric origin (Sasada et al., 1997; Marty et al., 1998; Dauphas and Marty, 1999; Tolstikhin et al., 2002). Because of this isotopic evidence and because many

carbonatites are spatially and temporally associated with large igneous provinces (LIPs, see Ernst and Bell, 2010 and Ernst, 2014 for reviews), many favour a sub-lithospheric source for plume-generated carbonatite magmatism (e.g., Gerlach et al., 1988; Nelson et al., 1988; Simonetti et al., 1995, 1998; Marty et al., 1998; Dauphas and Marty, 1999; Bell, 2001; Bizzarro et al., 2002; Tolstikhin et al., 2002; Bell and Rukhlov, 2004; Kogarko et al., 2010; Chen and Simonetti, 2015; Rukhlov et al., 2015; Hulett et al., 2016).

Carbonatites and related rocks are the main sources of REEs (e.g., Bayan Obo mine, Inner Mongolia; Kynicky et al., 2012) and Nb (e.g., Araxá mine, Brazil; Biondi, 2005) and can be economic targets for F, P, Al, Fe, Ti, Zr, V, Cu, Ni, Au, PGE, Ta, Sr, U, Th, phlogopite, vermiculite, olivine, lime, and barite (Mariano, 1989; Pell, 1996; Richardson and Birkett, 1996; Rankin, 2005; Woolley and Kjarsgaard, 2008a). An increasing interest in the strategic commodities has led to the discovery of many carbonatites in western North America, including the Blue River area in the Canadian Cordillera (Fig. 1; McCammon, 1951, 1953, 1955; Rowe, 1958; Currie, 1976; Mariano, 1982; Pell, 1994; Millonig et al., 2013).

The Canadian Cordillera is an accretionary orogen marked by continued subduction and accretion rather than ending with continent-continent collision (for review, see Nelson, 2013). The eastern part of the orogen consists of autochthonous and parautochthonous rocks of Ancestral North America and its Proterozoic to Triassic cover (Fig. 1). To the west are mainly allochthonous terranes accreted to the western margin in the Mesozoic and Cenozoic, and post-accretionary plutons. Carbonatites with ages of ca. 810–700, 500, and 360–330 Ma in the Canadian Cordillera mark breakup of the supercontinent Rodinia and subsequent development of the western margin of Laurentia (e.g., Scammell and Brown, 1990; Pell, 1994; Bell and Rukhlov, 2010; Millonig et al., 2012; Millonig and Groat, 2013; Nelson et al., 2013). The widespread Late Paleozoic carbonatites are unusual. In contrast to most carbonatites, which are restricted to intracratonic regions, they were emplaced in a more active setting along the western margin of Laurentia, during subduction.

Carbonatites and undersaturated silicate alkaline rocks in British Columbia range from intrusive complexes with minor or no associated carbonatites (e.g., Ice River, Trident Mountain, Mount Copeland) to carbonatite complexes with minor or no associated silicate rocks (e.g., Aley, Blue River and Frenchman Cap areas; Fig. 1). All underwent variable degrees of metamorphism and deformation from the Mesozoic through to the Cenozoic (Scammell, 1987, 1993; Scammell and Brown, 1990; Pell, 1994; Millonig et al., 2013). Intrusive complexes made up of mainly undersaturated silicate alkaline rocks, such as the Ice River complex, form small (up to 29 km² at surface), compositionally zoned bodies that are circular to elongate to amoeboid in plan view (Dawson, 1886; Currie, 1975; Peterson and Currie, 1994). Associated dikes composed of REE-rich carbonatites and ultramafic lamprophyres are common (Mumford, 2009). Carbonatites lacking associated

contemporaneous silicate rocks typically form regional swarms of individual occurrences across areas of 1000 km² (e.g., Blue River area; Pell, 1994; Mitchell et al., 2017). Individual occurrences such as the Upper Fir complex form highly strained and recrystallized tabular structures that may have originated as sills. These structures are a few dm to several tens of m thick and extend up to several hundred m along strike. They are typically composed of both calcite carbonatite and dolomite carbonatite end members in variable proportions, commonly with calcite-dolomite hybrids. Carbonatites rich

in apatite and silicate and oxide minerals could be classified as phoscorites (Russell et al., 1954; Krasnova et al., 2004) or silicocarbonatites (>20 wt% SiO₂; Le Maitre, 2002).

This field trip considers the characteristics, magmatic evolution, and mineralization of the Blue River carbonatites as represented by the Upper Fir carbonatite complex (330 Ma), which hosts one of the largest and best studied Nb-Ta deposits in the Cordillera. Participants will examine drill-core sections (Appendix 1) and outcrops of metacarbonatites, related metasomatic rocks, syntectonic pegmatites, enclosing

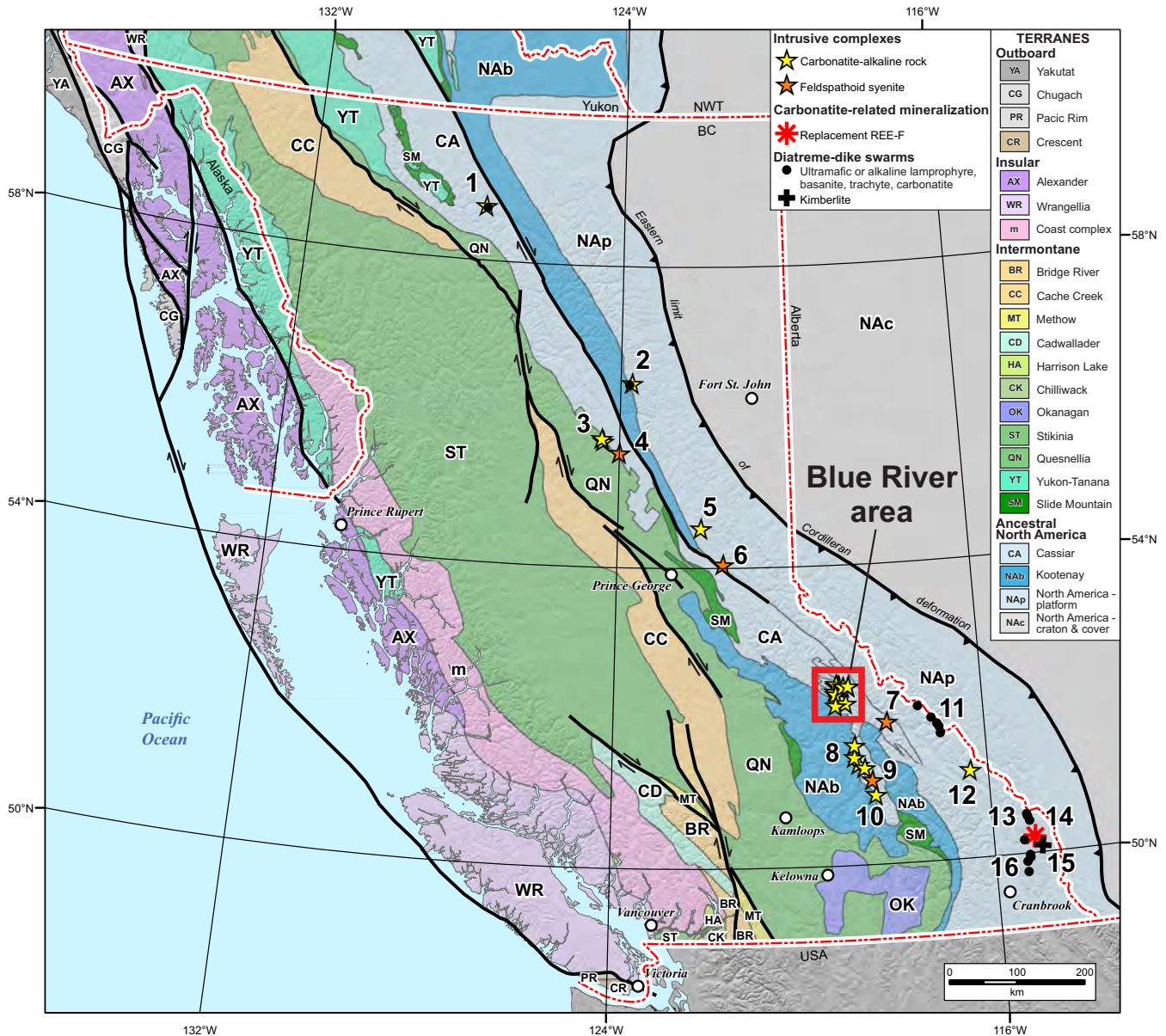


Fig 1. Carbonatite-alkaline complexes and dike-diatreme swarms defining the British Columbia Alkaline province (after Parrish and Scammell, 1988; Pell, 1994; Rukhlov and Bell, 2010; Millonig and Groat, 2013; Rukhlov et al., 2018): 1 – Kechika River; 2 – Aley (~344 Ma) and Ospika diatreme (~366 Ma); 3 – Vergil (~357 Ma) and Lonnie, Manson Creek area; 4 – Mount Bisson; 5 – Wicheeda Lake; 6 – Bearpaw Ridge; 7 – Trident Mountain (~359 Ma); 8 – Mount Grace (~359 Ma), Perry River (~798 Ma), and REN/Ratchford Creek (~698 Ma); 9 – Mount Copeland (~740 Ma); 10 – Three Valley Gap; 11 – Bush River (~410 Ma), Lens Mountain, Mons Creek (~469 Ma), Valenciennes River, and HP (~400 Ma) diatreme-dike swarms; 12 – Ice River (~362 Ma); 13 – Shatch Mountain and Russell Peak diatreme-dike swarms; 14 – Rock Canyon Creek; 15 – Cross diatreme (~245 Ma); 16 – Blackfoot Creek (~400 Ma), Swanson Peak (~400 Ma), Quinn Creek, and Summer Creek diatreme-dike swarms. Terrane geology after Nelson et al. (2013).

(semi)pelites and amphibolites of the Mica Creek assemblage (750–550 Ma) and Mesozoic–Cenozoic structures related to the Cordilleran orogeny. We will consider the tectono-metamorphic overprinting of igneous features in the Upper Fir carbonatites as recorded by paragenetic relationships, mineral chemistry, recrystallization, and retrograde deformation.

2. Field trip overview

The road log (Appendix 2) provides details of the stops and summarizes terranes along the route from Vancouver to Blue River. Throughout the text and in Appendix 2, the attitudes of planar fabrics are given as A°/B° , where A is strike and B is dip in the direction indicated. A magnetic declination of 16.1° east is used.

The highway route from Vancouver to Blue River passes through the Coast and Cascade Mountains, the Interior Plateau, and the Columbia Mountains (Fig. 2), which are underlain by Proterozoic to Cenozoic rocks comprising several Cordilleran terranes. At stops along the way, participants will be able to observe outcrops of Late Paleozoic pillowed basalts that represent remnants of the Slide Mountain ocean, which initiated by back-arc rifting during eastward subduction beneath the western margin of ancestral North America at the same time as carbonatite magmatism farther inboard. We will also examine Pleistocene flood basalts.

The first part of this guidebook establishes the Upper Fir deposit in a global carbonatite context and summarizes the history of work in the Blue River area. We then briefly describe the geology and regional carbonatite occurrences of the Blue River area. The final part outlines the Upper Fir geology, mineralogy and geochemistry based on the findings of Commerce Resources Corp. (Kulla and Hardy, 2015), Chudy (2013) and ongoing studies of the Blue River carbonatites (Rukhlov et al., 2018).

We encourage discussion of mantle sources, evolution of parental carbonate magmas, and the unusual mineralization. In a wider context, the field trip considers the possibility that the back-arc extension responsible for initiating the Slide Mountain ocean also stretched the continental lithosphere farther eastward, triggering emplacement of the Blue River carbonatites by tapping a long-lived (Neoproterozoic to Devonian) mantle plume (Rukhlov et al., 2018).

3. Upper Fir deposit in a global context

Extensive exploration by Commerce Resources Corporation determined an NI 43-101-compliant resource of 48.4 million tonnes (Indicated) averaging 1,610 ppm Nb_2O_5 and 197 ppm Ta_2O_5 plus 5.4 million tonnes (Inferred) averaging 1,760 ppm Nb_2O_5 and 191 ppm Ta_2O_5 (Kulla and Hardy, 2015). The main ore minerals include the Ta±U-rich pyrochlore supergroup and ferrocolumbite, with minor fersmite and nyoboeaschynite (Chudy, 2013). Abundant ferrocolumbite and the unusual Ta-rich pyrochlore (1.05–40.56 wt% Ta_2O_5 , average 20.27 wt% Ta_2O_5), which attains the microlite composition (i.e. $\text{Nb}+\text{Ta} > 2\text{Ti}$ and $\text{Ta} > \text{Nb}$), distinguish the Nb-mineralization at Upper

Fir from that of most carbonatite deposits (Van der Veen, 1963; Bakes et al., 1964; Heinrich, 1966; Mariano, 1982; 1989; Hogarth, 1989; Hogarth et al., 2000; Simandl et al., 2002; Chudy, 2013; Mackay and Simandl, 2014; Chakhmouradian et al., 2015; Mitchell, 2015).

Most primary carbonatite Nb deposits (e.g., Araxá, Brazil; St. Honoré and Oka, Quebec; Aley, British Columbia) have similar or higher Nb grades (0.12–1.6 wt% Nb_2O_5) as those at Upper Fir. Lateritic profiles above primary deposits host the world's richest deposits (e.g., Araxá, Catalão-I and II, and Seis Lagos, Brazil), with extreme Nb enrichment of up to 6.7 wt% Nb_2O_5 (Mariano, 1989; Chakhmouradian, 2006; Mackay and Simandl, 2014; Chakhmouradian et al., 2015; Mitchell, 2015). However, the tantalum contents at Upper Fir are distinctly higher (up to 8,705 ppm Ta; Gorham et al., 2011b), resulting in anomalously low Nb/Ta ratios (0.76–556; average 8.9) relative to most carbonatites (average Nb/Ta = 35; Chakhmouradian, 2006). Examples of other carbonatite deposits with significant Ta enrichment include Crevier in Quebec, Mount Weld in Australia, and Belaya Zima in Russia (Mariano, 1989; Mackay and Simandl, 2014; Chakhmouradian et al., 2015).

Although carbonatitic pyrochlores with up to 26.9 wt% Ta_2O_5 have been reported (Pozharitskaya and Samoylov, 1972), they tend to have <5 wt% Ta_2O_5 , with global averages of 0.85 wt% Ta_2O_5 for 'normal' pyrochlores and 7.92 wt% Ta_2O_5 for U-rich pyrochlores (>2.0 wt% UO_2), resulting in much higher Nb/Ta ratios (typically 200–500) compared with pyrochlores at Upper Fir (Nb/Ta = 0.45–56, average 3.2; Mariano, 1982, 1989; Hogarth, 1989; Simandl et al., 2002; Chudy, 2013; Mackay and Simandl, 2015; Mitchell, 2015). Pyrochlores can have considerable variations in Ta content within a single carbonatite complex, and primary pyrochlore crystals can exhibit both depletion and enrichment in Ta from core to rim (Hogarth, 1989 and references therein; Mariano, 1989; Simandl et al., 2002; Chudy, 2013; Chakhmouradian et al., 2015; Mackay and Simandl, 2015).

The Upper Fir has some similarities to pegmatite-hosted rare-metal deposits, in particular the low Nb/Ta ratios, the sill-like morphology, and the occurrence in clusters or swarms (e.g., Černý, 1992; Černý and Ercit, 2005). The magmatic evolution of rare-metal pegmatites is characterized by progressive Ta-enrichment and roughly concentric zoning due mainly to in-situ differentiation.

Sporadic molybdenite (up to 1.7 cm and up to ~2 vol.%) in carbonatites and fenites (Fig. 3), with up to >2,000 ppm Mo across 2 m (Gorham et al., 2011b) is another peculiar feature of the Upper Fir (Appendix 3f), given that carbonatites are generally poor in Mo (average 12 ppm) and lack molybdenite (Woolley and Kempe, 1989). Although little work has focused on molybdenite from Cordilleran carbonatites (Rukhlov et al., 2018), it has been observed in other carbonatite and related-rock occurrences in British Columbia, including Perry River, Mount Grace, Wicheeda Lake, and the Mount Copeland past producer (Fig. 1; Currie, 1976; White, 1982; Höy, 1988; Trofanenko et al., 2016). With Mo production from a unique carbonatite-hosted

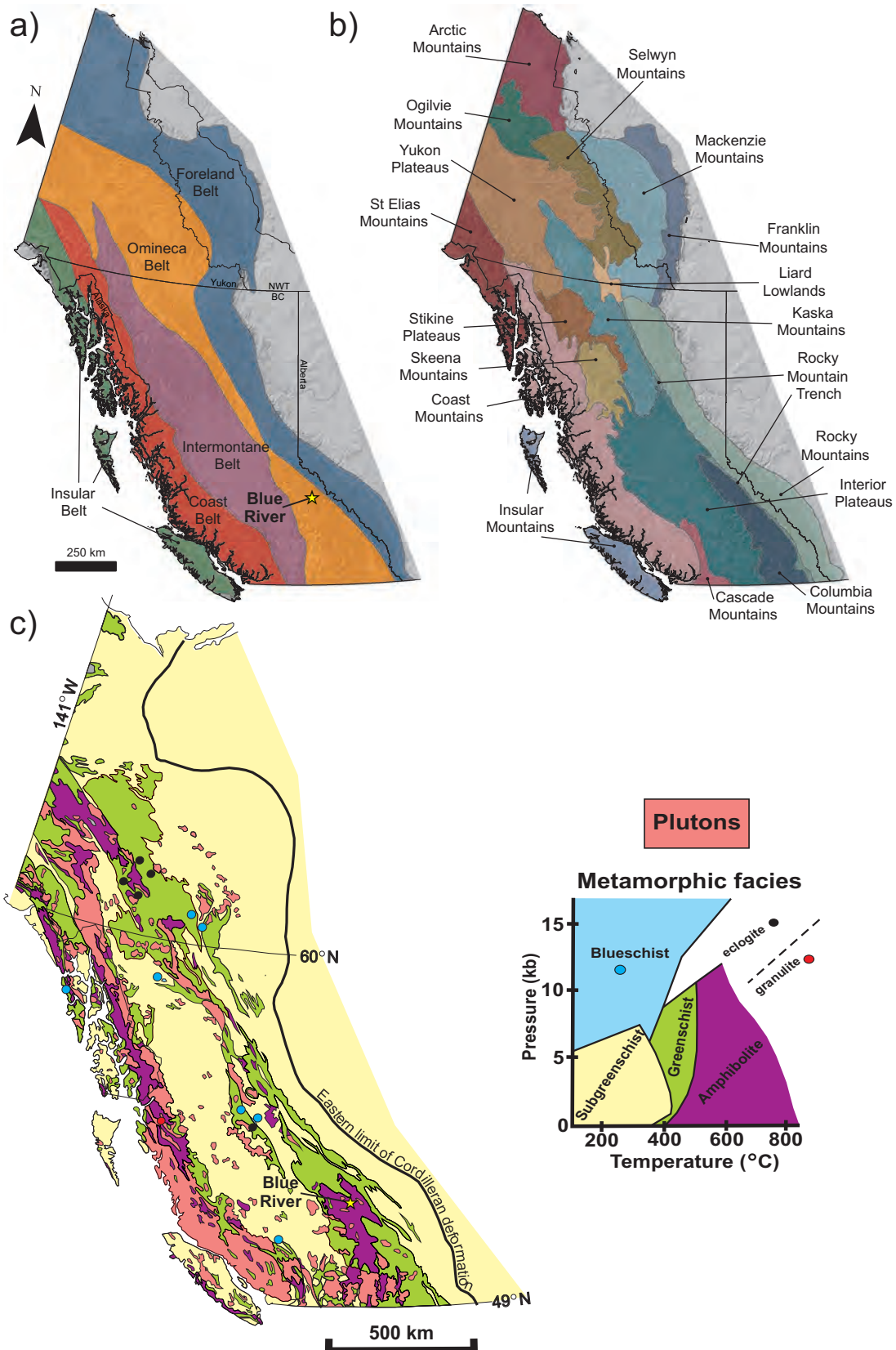


Fig. 2. **a)** Morphogeological belts of the Canadian Cordillera (after Gabrielse et al., 1991; Hickin et al., 2017). **b)** Composite physiographic units (after Mathews, 1986; Hickin et al., 2017). **c)** Metamorphic and plutonic rocks (after Monger and Hutchison, 1971; Read et al., 1991; Monger, 2014).

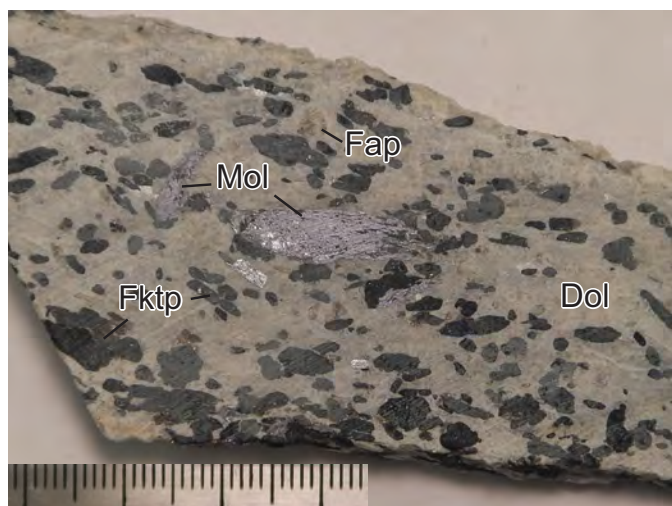


Fig. 3. Molybdenite (Mol) in foliated, ferrikatophorite (Fktp)-rich dolomite-carbonatite, Upper Fir (sample 16-ARU-198; Table 1).

deposit at Huanglongpu in central China (Quinling orogenic belt), the evidence is growing that carbonatite magmatism in atypical tectonic settings, such as cratonic margins or orogenic belts is capable of generating economic Mo deposits (Xu et al., 2010; Song et al., 2016).

Unlike the lower metamorphic-grade carbonatites in the Canadian Cordillera (e.g., Mumford, 2009; Trofantenko et al., 2016), the amphibolite-grade metacarbonatites at Upper Fir lack REE-mineralization, which is often a primary exploration target. Millonig and Groat (2013) suggested that REE-carbonates might be unstable at elevated metamorphic pressures and temperatures. However, it is unclear if the unusually low Nb/Ta ratios of pyrochlore at Upper Fir reflect post-magmatic dissolution-precipitation processes during tectonic reworking at mid-crustal levels (Millonig and Groat, 2013) or are a primary igneous feature of the carbonatites. Likewise, the absence of REE-carbonates or late-stage carbothermal residua might be a hallmark of the Blue River carbonatites and unrelated to regional metamorphism.

Late Paleozoic carbonatites in the Canadian Cordillera, such as those at Upper Fir, did not form in isolation. Similar rocks were emplaced along the length of the British Columbia alkaline province at ca. 810-700 and 500 Ma, during the protracted breakup of Rodinia and creation of a passive margin along the western flank of Ancestral North America (Fig. 1). Furthermore, new isotopic and elemental compositions of minerals from the Blue River carbonatites and related rocks are indistinguishable from worldwide carbonatites generated by deep-mantle plumes (Mitchell et al., 2017; Rukhlov et al., 2018). But the Late Paleozoic carbonatites have an unusual tectonic setting. In contrast to the Neoproterozoic and Cambrian Cordilleran carbonatites and to most carbonatites globally, which are restricted to cratonic interiors, the Late Paleozoic Cordilleran examples formed along the western margin of Laurentia while subduction was taking place immediately to the west. Lithospheric extension related to this

Late Paleozoic subduction is considered responsible for rifting of the continental margin and initiating the Slide Mountain ocean as a back-arc basin (e.g., Nelson et al., 2013). We suggest that this same back-arc extension triggered emplacement of the Blue River carbonatites that were sourced from a long-lived, deep-level mantle plume that was tapped episodically since the Neoproterozoic.

4. History of work in the Blue River area

The first regional (1:253,440 scale) geological map including the Blue River area was completed by Campbell (1968). Subsequent regional mapping and stratigraphic, structural, and metamorphic studies were undertaken by Ghent et al. (1977, 1980), Simony et al. (1980), Pell and Simony (1981, 1984, 1987), Read and Brown (1981), Morrison (1982), Raeside (1982), Raeside and Simony (1983), Digel et al. (1989, 1998), Sevigny and Simony (1989), McDonough et al. (1991a, b, 1992), Crowley et al. (2000), Ghent and Villeneuve (2006), Murphy (2007), and Gervais and Hynes (2013).

Although not recognized as carbonatites in early studies (McCammon, 1951, 1953, 1955; Rowe, 1958), carbonatites in the Blue River area (Fig. 4) have been intermittently explored since 1950 for vermiculite, uranium, niobium, tantalum and phosphate. Discovered by homesteader O.E. French in 1949, the Verity carbonatite occurrences near the Lempriere station, north of Blue River were initially evaluated for vermiculite by the Zonolite Corporation (McCammon, 1951). In 1951, the British Columbia Department of Mines identified uranopyrochlore in a sample of radioactive dolomite carbonatite from Verity, sent to them by O.E. French (McCammon, 1953). The whole-rock analysis returned 0.2 wt% U_3O_8 and 1.7 wt% $Nb_2O_5 + Ta_2O_5$ (Mariano, 1982). Rowe (1958) also reported uraninite-bearing columbite identified in carbonatite specimens sent by O.E. French to the Geological Survey of Canada. Further regional prospecting by the French family resulted in the discovery of the Paradise Lake and other carbonatite occurrences east of the Verity showing (Fig. 4). Between 1952 and 1955, more carbonatite outcrops were found in the area, including the Mill occurrence north of Verity, during uranium exploration by St. Eugene Mining Corporation Ltd. (McCammon, 1955; Rowe, 1958).

The first government reports on the Blue River carbonatites by J.W. McCammon (Mineralogical Branch of the British Columbia Department of Mines) and R.B. Rowe (Geological Survey of Canada) provide many field and mineralogical details, along with the results of vermiculite screen-expansion tests and chemical analyses of whole-rock, uranian pyrochlore, and uranian columbite samples (McCammon, 1951, 1953, 1955; Rowe, 1958). At that time, the idea of magmatic carbonates (Högbom, 1895; Brøgger, 1921; Soellner, 1927) seemed extreme for most to accept, and highly influential petrologists dismissed “these carbonate-bearing rocks as non-igneous” (e.g., Bowen, 1921; Daly, 1933; Johannsen, 1938; Shand, 1943) or considered them to be “limestones remobilized at crustal levels” (Brøgger, 1921). Hence, it is not surprising

that the early studies described the Blue River carbonatites as “bands and lenses of mainly dolomitized limestone” of “a deceptively igneous appearance”, with variable amounts of vermiculite, biotite, white mica, apatite, magnetite, olivine, ilmenite, green amphibole, zircon, pyrrhotite, pyrite, uranian pyrochlore, and uranian columbite (McCammon, 1951, 1953, 1955; Rowe, 1958). Locally cut by pegmatites and coarse-grained hornblende-calcite veins, these carbonatite bodies are up to 46 m thick and extend for at least 300 m along strike. They contain accessory pyrochlore, as pale brown to reddish brown to almost black octahedral crystals typically forming penetration twins or irregular lumps up to 4.5 cm in diameter and disseminated small grains, and amphibole and mica grains lying within the foliation of the enclosing gneisses; an outcrop of sodalite syenite was also noted (McCammon, 1953, 1955; Rowe, 1958).

Several companies and individuals, including Southwest Potash Corporation, Kennco Explorations (Western) Ltd., Falconbridge Ltd., Vestor Exploration Ltd., A.N. Mariano, A. Rich, and J.A. Gower examined carbonatite occurrences at Verity, Paradise Lake, and in the surrounding area between 1955 and 1970 (Mariano, 1982; Kulla and Hardy, 2015). During that time, A.N. Mariano was engaged in carbonatite exploration worldwide on behalf of Kennecott Copper Corporation. He came across a report on the Blue River claims that were briefly evaluated by Kennco Explorations (Western) Ltd. in 1964. Although the Kennco assessment did not find the property of economic interest, A.N. Mariano recognized some of the unique aspects in the structure, geochemistry, and petrology of the carbonatites and initiated a research program to “further understand the nature and genesis of the Blue River occurrences and to reveal the presence of materials of possible economic importance” (Mariano, 1982).

Earl D. Dodson prospected the Howard Creek area to the west of the Paradise Lake occurrences on behalf of Falconbridge Ltd. sometime before 1967, when A. Rich, then a student at the University of Alberta, recognized carbonatites at Howard Creek. Rich carried out an exploration program including geological mapping at Paradise Lake, regional prospecting, and sampling (Rich and Gower, 1968). From 1967 to 1969, A.N. Mariano and J.A. Gower, manager of exploration for Kennco Explorations (Western) Ltd. and Professor of Mineralogy at the University of British Columbia examined the Blue River carbonatites (Mariano, 1979, 1982). They named mineralogically unusual, titanite-rich, calcite-clinopyroxene-amphibole rock intimately associated with carbonatites, ijolites, and nepheline syenites at Howard Creek ‘lemprierite’ after the Mount Lempriere at the Howard Creek headwaters (Fig. 5). Mariano (1982) pointed out that the undersaturated alkaline silicate rock-carbonatite association was at odds with a sedimentary origin of the Blue River carbonatites. Rich and Gower (1968) further confirmed a magmatic origin based on the first isotopic analysis of C, O, and Sr in carbonate and whole-rock fractions from carbonatites and nepheline syenites at Verity, Paradise Lake, and Howard Creek. Their analyses revealed high Sr contents (1,100-5,650

ppm), which are at least ten times that of average sedimentary or metamorphic carbonate rocks, $\delta^{13}\text{C}_{\text{PDB}}$ values of -3.7 to -5.6, and $\delta^{18}\text{O}_{\text{PDB}}$ values of -19.9 to -25.5 (within the range of those from carbonatites elsewhere), and $^{87}\text{Sr}/^{86}\text{Sr}$ values of 0.7035 (Verity carbonatites) and 0.7047 (Paradise Lake nepheline syenite), which are lower than those of crustal rocks (>0.706). These data indicate the sub-crustal origin of the Blue River carbonatites and the associated alkaline silicate rocks (Rich and Gower, 1968).

From 1976 to 1978, John Kruszewski explored for uranium and niobium in the Verity and Paradise Lake areas with ground magnetic and radiometric surveys and more stripping and trenching (Meyers, 1977). In 1979, A.N. Mariano brought the Blue River carbonatites to the attention of Anschutz (Canada) Mining Ltd. Between 1979 and 1982, the company carried out extensive exploration mainly for Ta and Nb in the Blue River area, with road construction, topographic surveys, and 1:4,000-scale mapping, airborne and ground geophysics, and diamond drilling (Ahroon, 1979, 1980; Aaqvist, 1981, 1982a-c). This work defined a resource of about 2.13 million tons of 0.126 wt% Nb_2O_5 and 0.020 wt% Ta_2O_5 for the Verity deposit and in the discovery of the Bone Creek and Fir mineralized carbonatite occurrences (Ahroon, 1980; Aaqvist, 1982a,c).

As part of his research on global carbonatites in the 1960s, A.N. Mariano carried out a detailed petrological, mineralogical, and geochemical study of the Blue River carbonatites that was summarized in confidential reports for Anschutz (Canada) Mining Ltd. (Mariano, 1979, 1982). Intended as a guide to aid Ta-exploration in the Blue River area, Mariano’s (1982) report provided detailed field and petrographic descriptions of the Blue River carbonatites and related rocks, along with a wealth of litho-geochemical and mineral-chemistry data that used spark source mass spectrometry and in situ methods such as cathodoluminescence microscopy, electron probe microanalysis (EPMA) and scanning electron microscopy with energy-dispersive X-ray spectrometry (SEM-EDX) on polished thin sections. These techniques proved very efficient in Blue River carbonatite exploration. Particularly efficient was the use of rapid, qualitative SEM-EDX to identify Ta±U-rich pyrochlore, and cathodoluminescence microscopy or a shortwave UV luminescence to identify fenitization (e.g., apatite), which may be difficult to recognize in the field. Mariano (1982) found anomalously high Ta contents (locally coupled with high U) in pyrochlores from the Blue River carbonatites, which result in unusually low Nb/Ta ratios of about 6. These ratios are unlike most carbonatite pyrochlores which have Nb/Ta ratios of 100-500 (Van der Veen, 1963; Bakes et al., 1964; Heinrich, 1966). Mariano (1982; 1989) also considered pyrochlore, ferrocolumbite, and fersmite to be primary phases in the Blue River carbonatites.

In 1978, J.T. Morton and A.E. Grant discovered the Mud Lake carbonatite occurrence (AEG and JTM claims) based on an anomalous (27 times background) scintillometer reading at a reddish-brown soil exposed in a roadcut along the newly built Mud River logging road about 10 km northeast of Blue

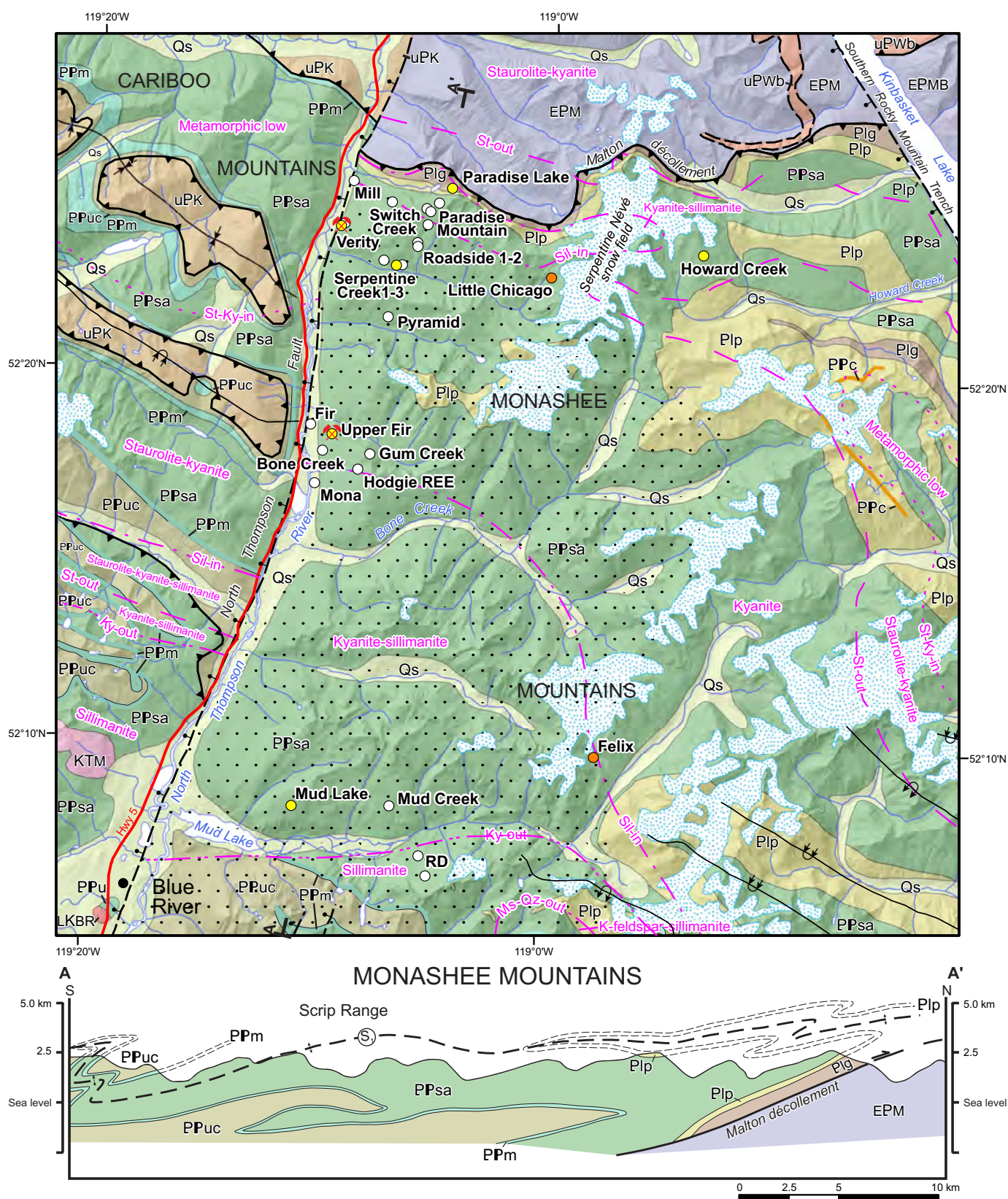


Fig. 4. Carbonatites and related rocks of the Blue River area (after Pell, 1994; Rukhlov and Bell, 2010; Millonig et al., 2012, 2013; Millonig and Groat, 2013; Rukhlov et al., 2018). Geology and metamorphic isograds after Campbell (1968), Simony et al. (1980), Raeside and Simony (1983), Pell and Simony (1987), McDonough and Murphy (1990), McDonough et al. (1991a, b, 1992), Digel et al. (1998), and Murphy (2007).

UNCONSOLIDATED DEPOSITS**Quaternary**

Qs	Undifferentiated sand, silt, clay, gravel, till, and colluvium
-----------	--

INTRUSIVE ROCKS**Cretaceous to(?) Paleogene**

Murtle pluton

KTM	Quartz monzonite and muscovite-biotite granite
------------	--

Late Cretaceous

Blue River pluton

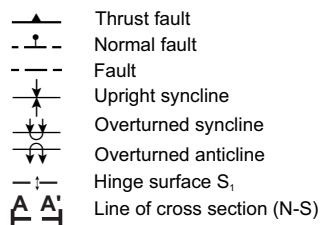
LKBR	Weakly foliated muscovite ± biotite granite
-------------	---

METAMORPHIC ROCKS**Neoproterozoic**

Windermere Supergroup

Kaza Group

uPK	Undivided psammite, grit, pelitic schist, phyllite, slate, marble
------------	---



Undivided basal Windermere Supergroup

uPWb	Grit, conglomerate or diamictite, psammite, mylonitic quartzite at base, pelitic phyllite or schist, marble and calc-silicate rocks
-------------	---

Proterozoic and(?) Paleozoic

PPu	Undivided metamorphic rocks of unknown, probably Proterozoic and possibly Paleozoic age
------------	---

Upper division of Horsethief Creek Group (equivalent units of Mica Creek succession)

Upper clastic unit

PPuc	Quartzofeldspathic psammite and grit, pelitic schist, minor amphibolite
-------------	---

Marble unit

PPm	Marble, calcareous pelite, semipelite, schist, discontinuous interbedded pelite, psammite, grit, quartzite, sandy marble
------------	--

Conglomerate in **PPsa** (Caribboos) and**Plp** (Monashees) units

PPc	Conglomerate with clasts of marble, calc-silicate rock, quartzite and granite
------------	---

REGIONAL METAMORPHISM**Mesozoic isograds**

---St-Ky-in	Staurolite and kyanite in
---St-out	Staurolite out
---Sil-in	Sillimanite in
---Ky-out	Kyanite out
---Ms-Qz-out	Muscovite and quartz out

Paleocene overprint

	Pod sillimanite
--	-----------------

Semipelite-amphibolite unit

PPsa	Quartzose and quartzofeldspathic psammite, grit, pelitic schist, concordant and discordant amphibolite, minor marble, locally marble at base
-------------	--

Proterozoic

Lower division of Horsethief Creek Group (equivalent units of Mica Creek succession)

Lower pelite unit

Plp	Pelitic schist, minor quartzofeldspathic psammite, concordant and discordant amphibolite
------------	--

Lower grit unit

Plg	Quartzofeldspathic psammite and grit, minor pelitic schist and amphibolite, locally prominent diamictite-bearing, conglomeratic horizon at base
------------	---

Paleoproterozoic

Malton gneiss complex

EPM	Undivided foliated granitic augen orthogneiss, mafic orthogneiss, paragneiss
------------	--

Mount Blackman gneiss

EPMB	Amphibolitic mafic gneiss, granitic gneiss
-------------	--

Carbonatite and related-rock occurrence

○	Unknown age
●	ca. 360-330 Ma
●	ca. 500 Ma
✂	Nb-Ta deposit

Fig. 4. Continued

River. The soil formed above a dolomite carbonatite body more than 4 m thick and extending for at least 150 m along strike, (Morton, 1979; White, 1980). Both forsterite and chondrodite were identified by X-ray diffraction of a soil sample containing visually identified phlogopite, pyroxene, and magnetite. Semi-quantitative spectrographic analysis of fresh carbonatite yielded 2.0 wt% P, 0.3-1.0 wt% Sr, 0.03-0.1 wt% Nb, 116 ppm U, 19 ppm Th, and detectable Y and REE (Morton, 1979).

In 1979, G.P.E. White, District Geologist of the Kamloops mining district examined the Mud Lake carbonatite (White, 1980). His report provided further geological details and assay data and quoted an Rb/Sr date of 370 Ma for the Mud Lake carbonatite, which was obtained by R.L. Armstrong and W.J. McMillan at the University of British Columbia and indicated that the carbonatite is significantly younger than the country schists. White (1980) also pointed out that the Mud Lake carbonatite (metabeforsite) has anomalously high Sr contents, similar to those of the Three Valley Gap carbonatite near Revelstoke and to South African dolomite carbonatites. Subsequent studies by White (1981, 1982, 1985) provided many field, mineralogical, and geochronological details for the Blue River carbonatites. Some of the important findings were two U-Pb dates of 325 Ma on zircons from the Verity carbonatites (donated by B. French and analyzed by R. Parrish at UBC), and K/Ar dates of 205±8 Ma on phlogopite from the Howard Creek carbonatite, and 92.5±3.2 Ma and 80.2±2.8

Ma on richterite from the Verity carbonatite obtained by J. Harakal at the University of British Columbia. The K/Ar dates indicate metamorphic overprinting of the Late Mississippian carbonatites during the Cordilleran orogeny, consistent with evidence of transposition of the bodies to a regional foliation, at least three phases of folding, and upper amphibolite-grade (kyanite to sillimanite zone) metamorphism (White, 1982, 1985). Regarding their economic potential, White (1982) noted columbite and pyrochlore in many of the Blue River carbonatites, and an occurrence of molybdenite in drill core from the Fir carbonatite. White's (1985) report also includes a preliminary geological map of the Howard Creek carbonatite-nepheline syenite complex.

Detailed mapping at a scale of 1:24,000 by the Geological Survey of Canada in 1987 and 1988 located two new carbonatite occurrences in the Mount Cheadle area: 1) Serpentine Creek, a <100 m² body east of the Verity occurrence; and 2) Gum Creek, a ~10 m thick layer east of the Bone Creek and Fir carbonatites (Digel et al., 1989). Johnstone et al. (1990a, b) followed up exploration of the Mud Lake carbonatites and related rocks with prospecting, geochemical and geophysical surveys, and detailed petrographic descriptions.

Systematic studies of carbonatites and related rocks in British Columbia by J. Pell, initially at the University of British Columbia and later at the British Columbia Geological Survey, provided further geological maps and general descriptions

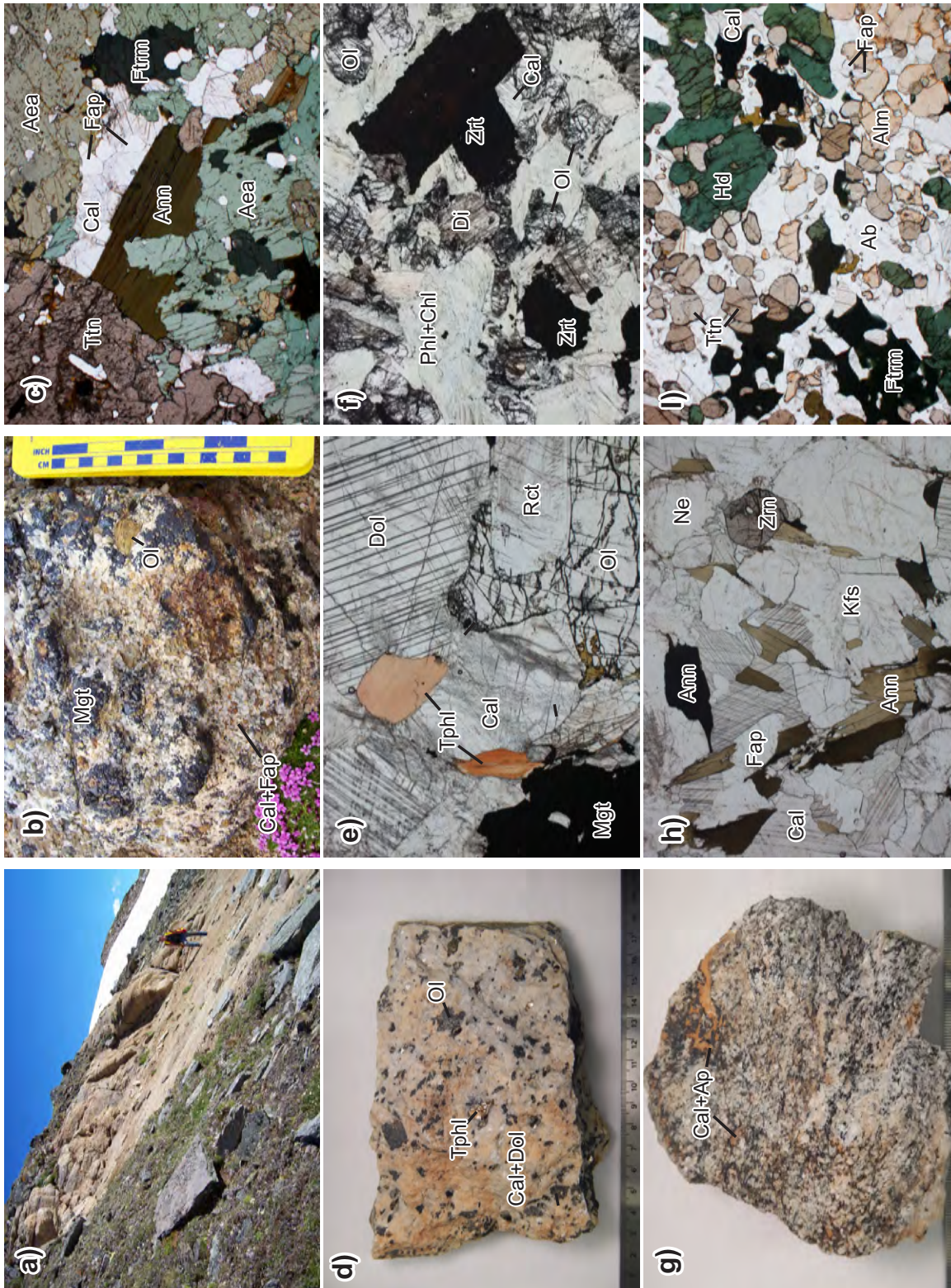


Fig. 5. Examples of carbonates and related rocks of the Blue River area (c, e, f, h, i) photomicrographs, plane-polarized light; field of view 5 mm) a) Sill-like body of calcite-carbonate, Howard Creek. b) Cumulate texture in magnetite-rich phoscorite, Howard Creek. c) Poikilo-porphroblast texture in calcite-titanite-clinopyroxene ('lemprierite'), Howard Creek. d) and e) Granoblastic texture in foliated, olivine- and tetraferriphlogopite-bearing, dolomite-calcite carbonate, Serpentine Creek. f) Zirconolite in foliated, phlogopite- and olivine-rich carbonate, Switch Creek. g) and h) Well-foliated, calcite-bearing nepheline-syenite, Paradise Lake. i) Granoblastic texture in titanite-rich, exocontact fenite, Upper Fir. Aea = aegirine-augite, Ab = albite, Alm = almandine, Ann = annite, Cal = calcite, Chl = chlorite, Di = diopside, Dol = dolomite, Fap = fluorapatite, Ftrm = (ferro)ferritaramite, Hd = hedenbergite, Kfs = K-feldspar, Mg = magnetite, Ne = nepheline, Ol = olivine, Rct = richterite, Tphl = tetraferriphlogopite, Ttn = titanite, Zrt = zirconolite.

of the Blue River rocks and new geochemical analyses and geochronology (Pell, 1985, 1987, 1994; Pell and Höy, 1989). Based on available ages, Pell (1987) attempted to correlate pulses of alkaline and carbonatite magmatism in the Canadian Cordillera with the tectonic evolution of the Pacific and Atlantic margins of North America. Pell (1987) also suggested that variable prospectivity of the carbonatites for Nb, REE, and fluorine may reflect their depth of emplacement and hence the degree of related metasomatism (finitization) based on structural level within the host metamorphic core complex (Frenchman Cap dome) and the younger strata of the Omineca and Rocky Mountain fold-and-thrust belts.

In 2000, prices for Ta raw material spiked several times relative to those prevalent in the 1990s (e.g., Mackay and Simandl, 2014). The favourable Ta market prompted several companies to re-evaluate known carbonatites and to search for new Ta-Nb and REE targets in the Blue River area. In 2002, International Arimex Resources Inc. evaluated the Gum Creek carbonatite for its Ta-Nb-P-REE potential using limited rock and stream-sediment sampling. Reeder and Grywul (2002), Grywul and Reeder (2003), and Thom (2013) described further exploration of the Mud Lake carbonatites and associated rocks.

Extensive exploration undertaken by Commerce Resources Corporation in the Blue River area between 2000 and 2012 included regional prospecting, detailed mapping (1:2,500 scale), road construction, trenching, bulk sampling, drilling, subsurface 3D modelling, metallurgical testing, ground and airborne geophysics, regional drainage heavy-mineral (pan) concentrate- and soil-geochemical surveys, estimating mineral resources, and environmental and economic assessments (Dahrouge, 2001a, b, 2002; Dahrouge and Reeder, 2001; Reeder and Dahrouge, 2002; Smith and Dahrouge, 2002a, 2003; Dahrouge and Wolbaum, 2004; Davis, 2005; Rukhlov and Gorham, 2007; Gorham, 2008; Gorham et al., 2009, 2011a, b, 2013; Kulla and Hardy, 2015 and references therein). This work confirmed known Ta-Nb-P mineralization of the Verity and Fir carbonatites (Dahrouge, 2002; Smith and Dahrouge, 2003) and located many new carbonatites, such as Upper Fir, which was discovered in 2002 (Smith and Dahrouge, 2003). The Upper Fir deposit was delineated by extensive drilling between 2005 and 2011 and, thus far, represents the largest Ta-Nb deposit in the Blue River area (Kulla and Hardy, 2015). Other examples include the Felix, Little Chicago, Mona, Mud Creek, and RD carbonatites, and the Hodgie Zone REE showing (Gorham et al., 2009, 2011a, b). In addition, the extensive Mount Cheadle and Hellroar Creek Ta-Nb soil geochemical anomalies likely indicate near-surface carbonatite bodies (Gorham et al., 2009, 2011a, b). Commerce Resources Corp. (Zimtu Capital Corp.) co-funded several academic studies of the Blue River carbonatites and local geology (e.g., Millionig et al., 2012, 2013; Chudy, 2013; Gervais and Hynes, 2013; Millionig and Groat, 2013; Mitchell et al., 2017).

Further data on various aspects of the Blue River carbonatites were contributed by Hogarth (1989), Mariano (1989), Hogarth et al. (2000), Simandl et al. (2002, 2010), Rukhlov and Bell

(2010), Millionig et al. (2012, 2013), Reguir et al. (2012), Chudy (2013), Millionig and Groat (2013), Mitchell (2015), Mackay and Simandl (2015), Fajber et al. (2015), Rukhlov et al. (2015, 2018), Chakhmouradian et al. (2016a, b, 2017), Mao et al. (2016), and Mitchell et al. (2017). Importantly, the compositional variations in pyrochlores from the Verity carbonatite were interpreted to represent primary zoning that was preserved despite high-grade metamorphism (Hogarth, 1989; Hogarth et al., 2000). Chudy (2013) provided details on the mineralogy, geochemistry, and petrogenesis of the Upper Fir carbonatite complex. Mitchell et al. (2017) presented trace-element and Sr-Nd isotopic compositions of apatites from several Blue River carbonatites. These data rule out the possibility that these rocks evolved from a single parental magma and suggest a depleted mantle source similar to that of carbonatites worldwide. These findings were corroborated with further petrogenetic constraints in an ongoing mineralogical and O-C-S-Sr-Pb-Nd isotopic study of the Blue River carbonatites (Rukhlov et al., 2018).

5. Blue River area

5.1 General geology

The Blue River area is in the Omineca belt of the Canadian Cordillera, at the northeastern margin of the Shuswap metamorphic complex, in the Monashee Mountains (Fig. 2). The region saw multiple episodes of penetrative deformation from the Jurassic through to the Eocene (e.g., Monger and Price, 1979; Monger et al., 1982; Raeside and Simony, 1983; Scammell, 1993; Pell, 1994; Digel et al., 1998; Crowley et al., 2000; Evenchik et al., 2007; Simony and Carr, 2011). Barrovian metamorphism (garnet-staurolite-kyanite-sillimanite rocks) reached conditions for anatexis, which resulted in syntectonic plutonism (e.g., Ghent et al., 1980; Simony et al., 1980; Carr, 1992; Digel et al., 1989, 1998; Sevigny and Simony, 1989; Sevigny et al., 1989, 1990; Scammell, 1993; Ghent and Villeneuve, 2006; Gervais and Hynes, 2013). Consequently, the ca. 500 Ma and 360-330 Ma metacarbonatites and the enclosing (semi) pelites and amphibolites of the Mica Creek assemblage (750-550 Ma) record protracted deformation at mid-crustal and retrograde conditions (Ghent et al., 1977; Simony et al., 1980; Pell and Simony, 1981, 1987; Pell, 1994; Digel et al., 1989, 1998; Kraft, 2011).

The supracrustal rocks form part of a continuous belt containing the Horsethief Creek and the overlying Kaza groups (Neoproterozoic) and extending from the northern Selkirk Mountains in the southeast, through the Monashee Mountains, and into the Cariboo Mountains in the northeast (Campbell, 1968; Pell and Simony, 1981, 1987; Raeside and Simony, 1983; Digel et al., 1989, 1998; McDonough et al., 1991a, b, 1992; Murphy, 2007). These rocks are cut by steeply dipping, northwest-trending, west-side-down Eocene normal faults (North Thompson fault on the west; Southern Rocky Mountain Trench fault on the east) and are juxtaposed against imbricated North American basement (Malton gneiss complex) by the south-dipping Malton décollement, a mylonitic thrust zone to

the north (Fig. 4; Morrison, 1982; McDonough and Simony, 1988).

The lower pelite unit and the stratigraphically overlying semipelite-amphibolite unit (at least 1 km thick) of the Mica Creek assemblage, the lower division of the Horsethief Creek Group, underlie much of the Blue River area (Fig. 4; Simony et al., 1980; Raeside and Simony, 1983; Pell and Simony, 1987; McDonough and Murphy, 1990; McDonough et al., 1991a, b, 1992). These rocks represent turbidites and mafic rocks formed during breakup of the supercontinent Rodinia and subsequent development of the western margin of Laurentia from ca. 750 to 550 Ma (Bond and Kominz, 1984; Scammell, 1987; Scammell and Brown, 1990; Ross, 1991; Colpron et al., 2002). The ca. 500 Ma and the more widespread 360–330 Ma carbonatites and related rocks, including the Upper Fir complex (ca. 330 Ma) in the Blue River area were emplaced in a continent-margin setting (Pell, 1985, 1987, 1994; Pell and Höy, 1989; Rukhlov and Bell, 2010; Millonig et al., 2012, 2013; Millonig and Groat, 2013; Mitchell et al., 2017; Rukhlov et al., 2018).

Structural studies in the Blue River area recognized the Scrip nappe, a regional (>50 km long) southwest-vergent structure that has been attributed to Jurassic deformation and exhumation due to collision of the western margin of Ancestral North America with offshore Intermontane terranes (Raeside and Simony, 1983; Diegel et al., 1989, 1998; Nelson et al., 2013; Monger, 2014; Sigloch and Mihalyuk, 2017). Subsequent protracted convergence of the Pacific and the North American plates resulted in crustal thickening and regional uplift in the mid-Cretaceous through to the Paleocene, refolding by at least two generations of isoclinal to open folds, a penetrative northeast to southeast dipping foliation, which developed at mid-crustal conditions, and retrograde reverse faults (e.g., Simony et al., 1980; Raeside and Simony, 1983; Diegel et al., 1989, 1998; Kraft, 2011). In addition, 3D modelling of the Upper Fir carbonatite revealed late SE–NW contraction (Gorham et al., 2013; Kulla and Hardy, 2015). The latest brittle structures (with <1 m displacement) generally parallel the North Thompson valley and are probably related to Eocene extension and uplift, although some studies argue for continued contraction, until about 50 Ma (e.g., Parrish et al., 1988; Diegel et al., 1998; Kraft, 2011). Syntectonic syenitic and granitic intrusions were emplaced throughout the Jurassic–Eocene orogenesis; at least some of these intrusions lack folds (Carr, 1992; Scammell, 1993; Diegel et al., 1998; Gervais and Hynes, 2013).

Polyphase but localized metamorphism has been identified in the Blue River area. Metamorphism was between ca. 160 Ma and 56 Ma, with peak conditions of about 540–700°C at 6–8 kbar (e.g., Ghent et al., 1983; Diegel et al., 1998; Scammell, 1993; Crowley et al., 2000; Tinkham and Ghent, 2005; Ghent and Villeneuve, 2006; Millonig et al., 2012, 2013; Gervais and Hynes, 2013). Deformation and metamorphic processes overprinted most of the primary igneous features of the carbonatites, which now comprise tightly folded layers up to several tens of m thick with contact-parallel foliation concordant with penetrative fabrics in the country gneisses,

schists, and amphibolites (Rukhlov and Gorham, 2007; Gorham et al., 2013). Internal retrograde breccia and shear zones further obscure the original paragenetic record (Chudy, 2013).

5.2 Carbonatites and related rocks

The Blue River carbonatites include at least 18 carbonatite and 2 alkaline, silica-undersaturated-rock occurrences (Fig. 4; Mitchell et al., 2017). Table 1 provides details of some of the 360–330 Ma carbonatites, related rocks, and regional Neoproterozoic marbles. For additional details about these and other occurrences, the reader is referred to McCammon (1953, 1955), Rowe (1958), Rich and Gower (1968), Mariano (1979, 1982), White (1980, 1982, 1985), Aaquist (1982a), Johnston et al. (1990a, b), Pell (1994), Simandl et al. (2002), Rukhlov and Gorham (2007), Millonig et al. (2012, 2013), Chudy (2013), Millonig and Groat (2013), and Mitchell et al. (2017). Generally, they form folded, concordant bodies of dolomite and calcite carbonatites, mainly a few m thick and extending for up to a few 100 m along strike within the enclosing gneisses, schists and amphibolites of the Mica Creek assemblage (Figs. 5a, 6 and 7; Simony et al., 1980; Raeside and Simony, 1983; Pell and Simony, 1987; Diegel et al., 1989, 1998; McDonough and Murphy, 1990; McDonough et al., 1991a, b, 1992). Alkaline



Fig. 6. Examples of alpine carbonatite exposures in the Blue River area (photos courtesy of L.J. Millonig). **a)** Dolomite carbonatite boudin mantled by zoned clinopyroxene (Cpx)-amphibole (Amp) skarn in country gneiss, Little Chicago (ca. 496 Ma). **b)** Deformed, banded calcite carbonatite with modal layering of magnetite, phlogopite, and zircon, and with amphibolite boudins cut by syntectonic pegmatite veins, Felix (ca. 498 Ma). Note oxidation of a skarn between the carbonatite and pegmatite bodies



Fig. 7. Verity carbonatite (ca. 350 Ma). **a)** Tan weathered dolomite carbonatite made up of ferroan dolomite, fluorapatite, F-Fe²⁺-rich tetraferriphlogopite, K-fluorrichterite, and accessory dark-red to almost black F±U±Ta-rich primary pyrochlore (contains inclusions of Mg-rich ferrocolumbite), orange F-Sr-rich late-stage pyrochlore, magnetite, and pyrrhotite, crosscut by a folded pegmatite dike, Specimen Pit. **b)** Foliated calcite carbonatite with hydroxylapatite transitional to fluorapatite, Na-rich phlogopite, olivine (Fo₈₅), diopside, and accessory Mg-Mn-V-Al-bearing and Ti-rich magnetite, Nb-bearing and Mg-rich ilmenite, Nb-rich zirconolite, and pyrrhotite in a road cut about 250 m northeast from the Specimen Pit. Note flat-lying gneissosity and the apparent competency contrast between dm-thick zones due to subtle modal variations.

metasomatic rocks (fenites), including glimmerites and Na-rich amphibolites typically have sharp contacts with carbonatites and grade into unaltered country rocks across a few cm to a few m (Fig. 8). Clumps of magnetite±ilmenite±olivine±apatite several cm in diameter are common and represent fragmented cumulates (e.g., Fig. 5b; Mitchell et al., 2017). Coarse-grained, calc-silicate veins up to several dm wide (Fig. 9) commonly cut Fe-rich dolomite carbonatites, which weather to a reddish-brown saprolite with enrichment in apatite and silicate and oxide minerals. In contrast, Fe-poor calcite carbonatites typically weather to gravel (Fig. 10). Nepheline syenites



Fig. 8. Contact between foliated, calcite carbonatite and banded, fenitized country gneiss, Paradise Lake (ca. 360 Ma).

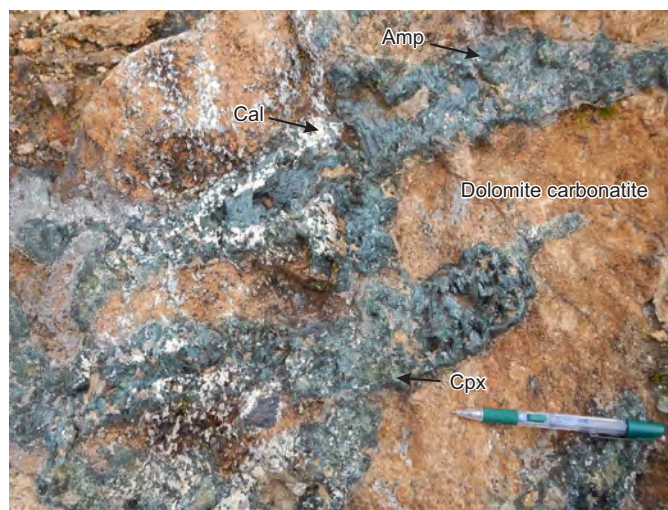


Fig. 9. Dolomite carbonatite crosscut by calcite (Cal)-clinopyroxene (Cpx)-amphibole (Amp) veins, Upper Fir.

associated with carbonatites and diverse ultramafic rocks are only at the Paradise Lake and Howard Creek occurrences (Figs. 5g, h and 11). Outcrops at most showings are discontinuous, due to extensive weathering, locally thick overburden and, at lower elevations, dense vegetation.

The coarse-grained, granoblastic or gneissic to strongly foliated porphyroclastic textures in the carbonatites and related alkaline silicate rocks record equilibrium metamorphic recrystallization and localized retrograde shearing (Chudy, 2013). Regardless of the metamorphic overprinting, the carbonatites retain primary paragenetic relationships, mineral chemistry, and isotopic compositions (Chudy, 2013; Mitchell et al., 2017; Rukhlov et al., 2018). The Upper Fir carbonatite is described in detail below.

Table 1. Petrography of selected carbonatites, related rocks, and regional marbles of the Blue River area after Rukhlov et al. (2018).

Rock type	Sample	Texture	Mineralogy		Notes	Equilibrium T°C (logfO ₂)	
			Major	Minor/accessory		Cal _{Mg-Fe}	Mgt-Ilm _{Fe-Ti}
Gum Creek (119°07'48.45" W, 52°17'48.20" N)							
Calcite	16-ARU-123	Foliated,	Cal, Fap-Hap,	Phl (Tpfl), Pcl,	Dol ex in Cal; brown-red U-Ti-	604-696	
carbonatite	16-ARU-133	porphyroclastic	Fktp-Marf	Fcl, Zrn, Ilm, Ep, Po, Ccp	rich Pcl; Fe ²⁺ -Ti±Na-rich Phl or Tpfl; Mg-Ti-rich Fcl; Nb-bearing, Fe ³⁺ -rich Ilm		
Howard Creek (118°53'17.67" W, 52°23'17.00" N)							
Calcite	16-ARU-046	Foliated, coarse-grained, granoblastic	Cal, Fap-Hap, Ol, Mgt	Ilm, Phl, Ed, Zrn, Bdy, Zrt, Po	For ₈₆ ; Na-rich Phl; low-X (Fe-rich) Po; Hf-rich Zrn (1 cm)	571-645 (-18 to -22)	
Calcite-nepheline syenite	16-ARU-040	Coarse-grained, poikiloblastic	Cal	Fap, Aea, Ttn, Sep, Ccn, Ann, Po	Fe-Nb-Zr-rich Ttn; Sr-rich Fap; Al-Fe ²⁺ -Mg-rich Aea		
Calcite-titanite-amphibole clinopyroxenite	16-ARU-042-2	Coarse-grained, poikiloblastic	Aea, Ftrm, Ttn, Fap, Ab Ann, Cal		Al-Fe ²⁺ -Mg-rich Aea; Mg-Ti-rich Ann		
Phoscorite	16-ARU-044-2	Coarse-grained, sideronitic-cumulate	Ol, Mgt, Ilm, Cal	Fap-Hap, Ath, Zrn, Bdy, Chn	For ₈₃₋₈₄ ; Zn-bearing, Mg-rich Ilm; V-bearing Mgt	472-662 (-23 to -13)	
Mill (119°08'51.22" W, 52°25'10.61" N)							
Calcite clinopyroxenite	16-ARU-171	Coarse-grained, cumulate-nematoblastic	Aea-Omp, Cal, Fap-Hap	Phl	Na-Al-Fe ²⁺ -Ti-rich Phl; Fe ³⁺ -Mg-rich Omp to Al-Mg-rich Aea		
Paradise Lake (119°05'03.28" W, 52°24'37.95" N)							
Calcite	16-ARU-116A	Foliated, coarse-grained,	Cal, Fap, Mgt, Phl (Tpfl)	Ol, Chn, Ed, Zrn, Po, Gth	For ₈₅ ; sub-µm Dol ex in Cal; Na-rich Phl or Tpfl; Zn-bearing, Mg-rich Ilm or Fe-rich Gk ex in	486-508 (-23 to -25)	
carbonatite	16-ARU-120	granoblastic to porphyroclastic			V±Mg±Zn-bearing Mgt	623-627 (-14)	
Dolomite-calcite carbonatite	16-ARU-119	Foliated, coarse-grained, porphyroclastic	Cal>Dol, Ol, Cal	Tppl, Fap, Zrn, Po, Ccp, Cbn, Srp	Dol ex in Cal; Hf-rich Zrn; low-X (Fe-rich) Po; Nb±Cr-bearing, Mg±Fe ³⁺ -rich Ilm	692-721	
Dolomite carbonatite	16-ARU-122	Coarse-grained, granoblastic to foliated, porphyroclastic	Dol, Fap, Tr-	Krct, Mgt, Po, Py, Ilm, Tppl (Phl), Fcl, Gth, Chl	Fe-rich Dol; V-bearing Mgt; Nb-bearing, Fe ³⁺ -rich Ilm, Co-rich Py	482 (-21)	
Silicocarbonatite	16-ARU-177	Coarse-grained, sideronitic-cumulate to foliated, poikiloblastic	Cal, Dol, Ol, Rct, Mgt, Chn, Fap	Zrn, Phl, Srp, Chl	For ₈₀₋₈₁ ; Ti-bearing Mgt; Ti-Fe-rich Chn; Hf-rich Zrn; Fe ³⁺ -Na±Fe ²⁺ -rich Di to Aug; Fe ²⁺ -Ti-rich Phl		
	16-ARU-183						

Equilibrium temperature and oxygen fugacity (logfO₂, in parentheses) based on Fe-bearing calcite-dolomite solvus (Anovitz and Essene, 1987), assuming 0-10 vol% reintegrated dolomite, and magnetite-ilmenite solid solutions (Andersen and Lindsley, 1985).¹ See Rukhlov et al. (2018) for details of drill-core samples. Abbreviations: **Aea** = aegirine-augite, **Ab** = albite, **Act** = actinolite, **Alm** = almandine, **Ann** = annite, **Ath** = anthophyllite, **Aug** = augite, **Bdy** = baddeleyite, **Cal** = calcite, **Cbn** = cubanite, **Ccn** = cancrinite, **Ccp** = chalcopyrite, **Chl** = chlorite, **Chn** = chondrodite, **Di** = diopside, **Dol** = dolomite, **Ed** = edenite, **Ep** = epidote, **ex** = exsolution, **Fap** = fluorapatite, **Fcl** = ferroclumbite, **Fktp** = ferrikataphorite, **Fo** = forsterite end-member (mol%) in olivine, **Frs** = ferrosilite, **Ftrm** = (ferro)ferriaramite, **Fwnc** = ferriwincite, **Gk** = geikielite, **Gr** = graphite, **Gth** = goethite, **Hap** = hydroxylapatite, **Hd** = hedenbergite, **Ilm** = ilmenite, **Kfs** = K-feldspar, **Kfct** = K-fluorichterite, **Kret** = K-richterite, **Marf** = magnesio-arfvedsonite, **Mfbb** = magnesioferrihornblende, **Mgt** = magnetite, **Mhs** = magnesiohastingsite, **Mol** = molybdenite, **Ms** = muscovite, **Ne** = nepheline, **Ol** = olivine, **Omp** = omphacite, **opq** = opaque, **Pel** = pyrochlore, **Phl** = phlogopite, **Po** = pyrrhotite, **Py** = pyrite, **Qz** = quartz, **Rct** = richterite, **Sdl** = sodalite, **Sep** = scapolite, **Srp** = serpentine, **Tr** = tremolite, **Tpfl** = tetraferriphlogopite, **Ttn** = titanite, **Zm** = zircon, **Zrt** = zirconolite.

Table 1. continued

Rock type	Sample	Texture	Mineralogy		Notes	Equilibrium T°C (logfO ₂)	
			Major	Minor/accessory		Cal _{Mg-Fe}	Mgt-Ilm _{Fe-Ti}
Phoscorite	16-ARU-138	Coarse-grained, sideronitic-cumulate	Ol, Mgt, Cal, Fap-Hap, Rct	Pcl, Tphl, Py, Po, Zrn, Zrt, Srp	For ₈₄₋₈₅ ; Dol ex in Cal; orange-brown U-Ta-Ti-rich Pcl; Ta-Nb-rich Zrt; Na-rich Tphl; Mn-Fe ²⁺ -Fe ³⁺ -rich Gk to Mn-Mg±Fe ³⁺ -rich Ilm ex in V±Mg-bearing Mgt	714-733	488-628 (-25 to -16)
Fenite	16-ARU-126	Foliated, medium-grained, nematoblastic	Rct-Fktp, Aea, Cal, Fap	Ab, Kfs, Zrn	Al-Mg±Fe ²⁺ -rich Aea		
Calcite-nepheline syenite	16-ARU-186	Foliated, medium-grained, porphyroclastic Sdl, Ann, Cal, Fap	Ab, Kfs, Ne, Fap	Zrn, Ccn, Pcl, opq	Mg-Al-Ti-rich Ann; Hf-rich Zrn; red-brown Pcl		
Roadside 1 (119°05'57.74" W, 52°23'32.96" N)							
Calcite carbonatite	16-ARU-155	Foliated, coarse-grained, porphyroclastic	Cal, Fap, Ol	Zrn, Tphl, Rct, Py, Po, Mgt, Pcl	Dol ex in Cal; orange Pcl; ubiquitous Zrn; Na-rich Tphl; Zn-bearing, Mg-Fe ³⁺ -rich Ilm ex in V±Mg±Mn-bearing Mgt	668-731	725 (-13)
Serpentine Creek 3 (119°06'52.71" W, 52°22'55.33" N)							
Calcite carbonatite	16-ARU-152	Foliated, porphyroclastic	Cal, Fap, Ol, Di, Phl, Mgt	Ed, Ilm, Po, Zrn, Srp	For ₈₅₋₈₆ ; ubiquitous fine-grained Zrn aggregates; Na-rich Phl; Zn-bearing, Mg-rich Ilm ex in V±Zn±Al-bearing Mgt; Nb-bearing, Mg-Fe ³⁺ -rich Ilm		557 (-19)
Dolomite-calcite carbonatite	16-ARU-150	Foliated, coarse-grained, porphyroclastic	Cal>Dol, Ol, Tphl, Rct-Kret, Mgt, Ilm	Fap, Po, Ccp	For ₇₇₋₇₈ ; coarse to sub-µm Dol ex in Cal; rare PbS-SnO ₂ globules (~1 mm); Mg-rich Ilm ex in Cr-V-bearing Mgt; Nb-bearing, Mg-Fe ³⁺ -rich Ilm	569-714	538 (-19)
Switch Creek (119°07'15.28" W, 52°24'40.72" N)¹							
Silicocarbonatite	16-ARU-093	Foliated, medium-grained, cumulate-porphyroclastic	Ol, Phl, Di, Cal, Zrt, Chl, Srp	Fap, Mgt, Ilm	For ₈₄ ; Na-rich Phl; Mg-rich Ilm (Mn-rich inclusions in Zrt); V±Mg±Mn-bearing, ±Ti-rich Mgt; Nb-rich Zrt		511-558 (-23 to -21)

Table 1. continued

Rock type	Sample	Texture	Mineralogy		Notes	Equilibrium T°C (logfO ₂)	
			Major	Minor/accessory		Cal _{Mg-Fe}	Mgt-Ilm _{Fe-Ti}
Upper Fir (119°09'28.13" W, 52°18'17.40" N) ¹							
Dolomite	16-ARU-006	Foliated,	Dol, Fap, Fktp, Po, Mgt, Pcl, Cal,		Fe-rich Dol; orange-red, U-		
carbonatite	16-ARU-072	porphyroclastic to	Rct (Fwnc, Phl, Zrn, Fcl, Frs,		Ta±Ti±F-rich Pcl; orange, Na-		
	16-ARU-089	coarse-grained,	Mfthb, Act)	Ccp, Mol	deficient, Fe-Ti-Ta-rich Pcl;		
	16-ARU-104	granoblastic			Fe ²⁺ -rich Phl; V-bearing Mgt;		
	16-ARU-111				Mg±Ta-rich Fcl; Ni-rich Po; Py		
	16-ARU-144				mantle on Fap inclusion in Pcl;		
	16-ARU-198				up to 17 mm wide Mol (~2		
					vol.%) in Fktp segregation		
Calcite-dolomite	16-ARU-101	Coarse-grained,	Dol, Cal, Fap, Pcl, Ilm, Zrn, Fcl,		Lamellar or coarse to sub-µm	660-684	462-706
carbonatite	16-ARU-082	sideronitic-granoblastic	Fktp, Rct, Mgt Po, Phl, Ccp		Dol ex in Cal; Fe-rich Dol;		(-28 to -13)
		to porphyroclastic;			orange, U-Ta-rich Pcl; Na-Ca-		
		massive Po-Fap-Mgt			deficient, U-Fe-Ta-rich Pcl;		
		clumps up to 4 cm wide			Fe ²⁺ -Na-rich Phl; Fe ³⁺ -rich Ilm;		
					Ilm ex in Ti-bearing Mgt; Mg-		
					Ta-rich Fcl		
Fenite	16-ARU-062-1	Medium-grained,	Hd, Alm, Ttn, Cal, Ftrm?, Kfs,		Mg-Fe ³⁺ ±Na-rich Hd		
		granoblastic	Ab	Fap, Po			
Verity (119°09'20.93" W, 52°23'57.10" N)							
Calcite	16-ARU-143B	Foliated, coarse-	Cal, Hap-Fap, Mgt, Po?, Srp, Ilm, Fo _{ss} ;		Na-rich Phl; Nb-rich Zrt;		599 (-20)
carbonatite		grained, porphyroclastic	Ol, Phl, Di	Zrt	Nb-bearing, Mg-rich Ilm; Mg-		
					Mn-V-Al-bearing, Ti-rich Mgt		
Dolomite	16-ARU-175	Foliated,	Dol, Fap, Tphl	Kfrct, Mgt, Po,	Fe-rich Dol; Fe ²⁺ -F-rich Tphl;		
carbonatite		porphyroclastic		Pcl, Fcl	brown-red, F±U±Ta-rich Pcl;		
					orange, F-Sr-rich Pcl; Mg-rich		
					Fcl (inclusions in brown-red Pcl)		
Oventop Ridge (118°43'47.41" W, 52°19'55.43" N)							
Dolomite-calcite	16-ARU-050	Foliated, coarse-	Cal>Dol, Tr	Phl, Gr?	Dol ex in Cal	667-709	
marble		grained, porphyroclastic					
Windfall Creek (118°52'24.91" W, 52°24'12.94" N)							
Calcite marble	16-ARU-048	Foliated, medium-	Cal	Gr, Qz, Ab, Kfs,			
		grained, granoblastic		Ms, Py			



Fig. 10. a) Weathered surface of foliated dolomite carbonatite with apatite (white) and magnetite (Mgt) porphyroclasts, Upper Fir. **b)** Gravelly weathered calcite carbonatite, Roadside.

6. Upper Fir carbonatite complex

6.1 Geology

The Upper Fir carbonatite complex (Figs. 12, 13) contains tabular bodies up to 72 m thick that are in isoclinal recumbent similar (in part rootless) folds that are refolded by southwest-vergent, open folds with parallel geometries (Gorham et al., 2013). Fold (F_3) hinges in the Upper Fir area have an average trend of 125° and an average plunge of 17° (Kraft, 2011). The carbonatite has been traced for about 1450 m north-south and about 800 m east-west.

Compositionally very similar to the Upper Fir, the Fir and Bone Creek carbonatites immediately to the west (Fig. 4) are probably part of a single complex. The Upper Fir complex consists of mainly dolomite carbonatite and subordinate (<4%) medium- to coarse-grained calcite carbonatite. Calcite carbonatites form lenses up to a few m thick within dolomite carbonatite bodies (Fig. 13); contacts between the two may be sharp or gradational (Fig. 14; Rukhlov and Gorham, 2007;

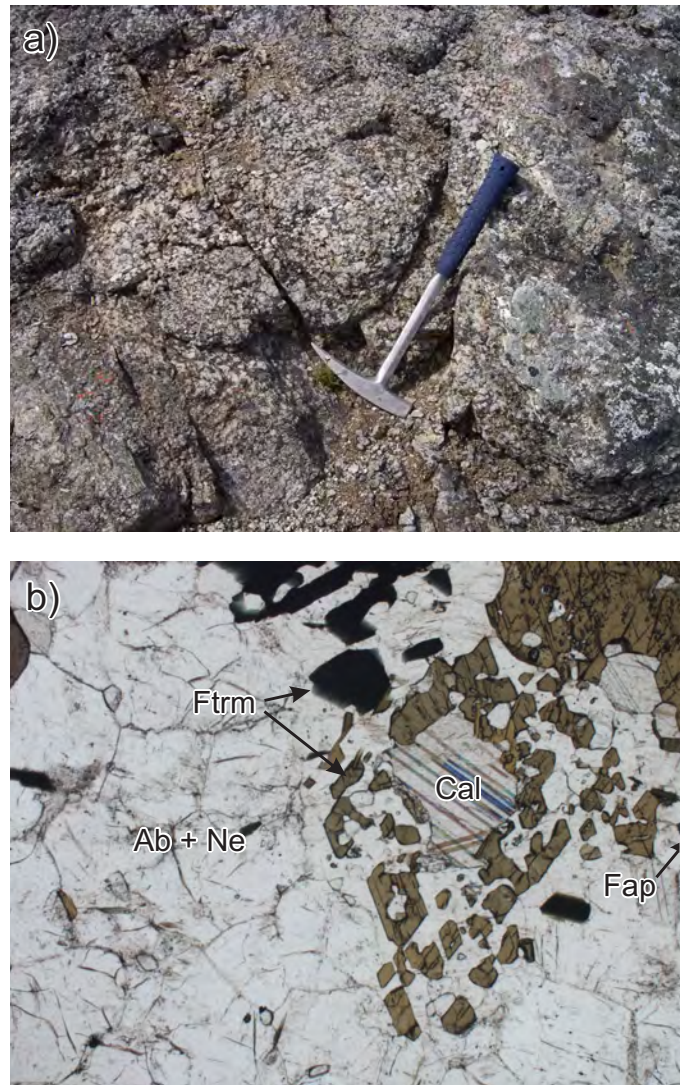


Fig. 11. The Howard Creek calcite-nepheline syenite: a) Coarse-grained texture in a heterogeneous dike (ca. 1 m wide) crosscutting calcite carbonatite. **b)** Photomicrograph of poikilo-granoblastic texture in sample 16-ARU-040 (see Table 1 for details) with mosaic albite (Ab), nepheline (Ne) and calcite (Cal), poikiloblasts of (ferro) ferritaramite (Ftrm), and minor Sr-rich fluorapatite (Fap). Plane-polarized light; field of view 5 mm.

Chudy, 2013). The carbonatites display a foliation that is concordant with penetrative schistosity and compositional layering in the enclosing gneisses, schists, and amphibolites. They are recrystallized, and display fabrics ranging from granoblastic (likely preserving magmatic protoliths) to porphyroclastic and medium- to coarse-grained gneissic, to fine-grained and well foliated (see below). Granoblastic varieties occur mainly at the margins of the carbonatite bodies, whereas the porphyroclastic and fine-grained well-foliated varieties typically make up the central portions of >10 m-thick bodies. This distribution correlates favourably with the composition of amphibole-group minerals and the Nb-Ta oxide phases (see below for details), strongly suggesting that primary compositional zoning within individual dolomite carbonatite

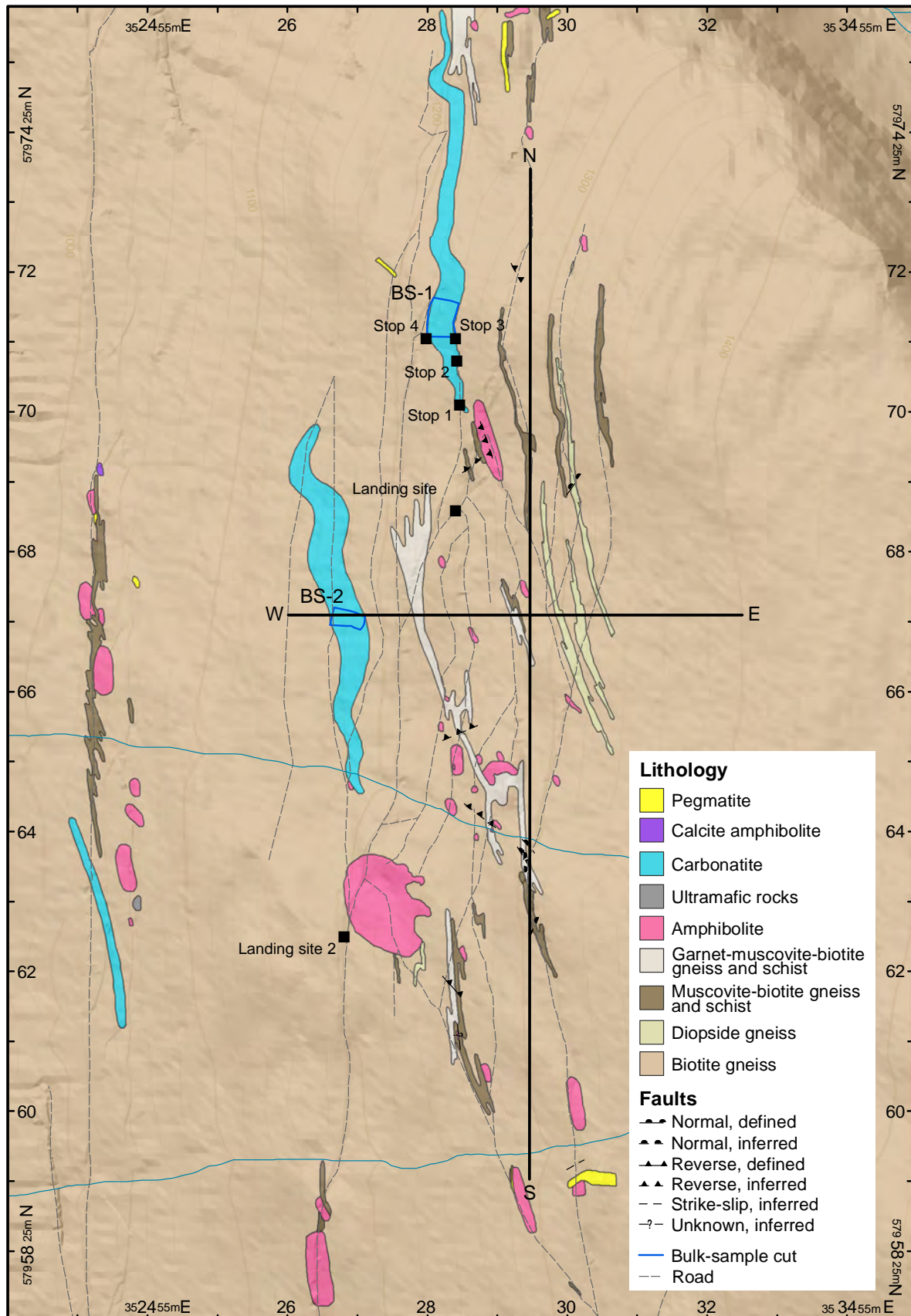


Fig. 12. Stops and positions of north-south and east-west cross sections in the Upper Fir area (NAD83 UTM, Zone 11 coordinates). **a)** Bedrock geology modified from Kraft (2011) and Gorham et al. (2013).

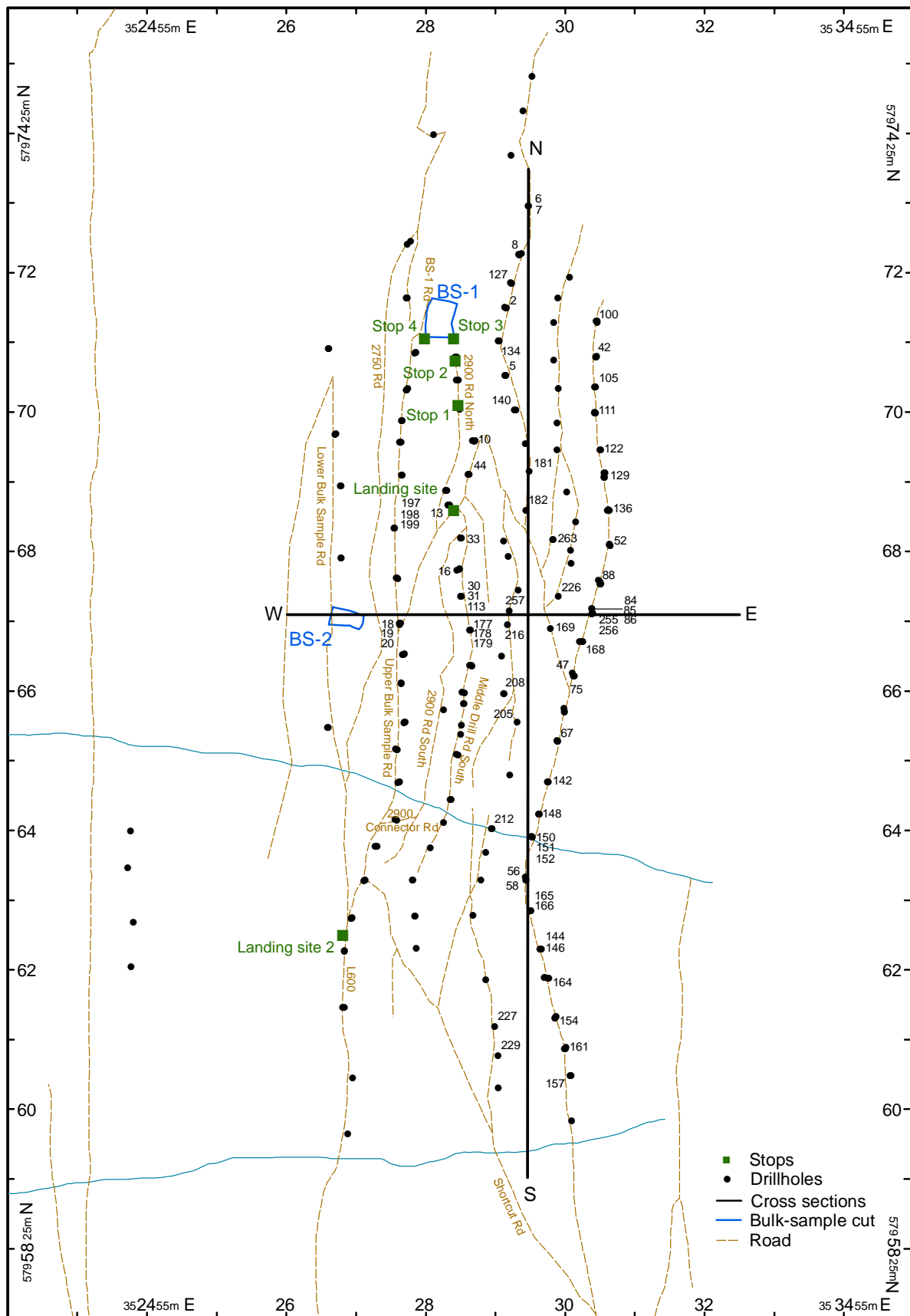


Fig. 12 continued. b) Road network and diamond drill-holes after Gorham et al. (2011b, 2013).

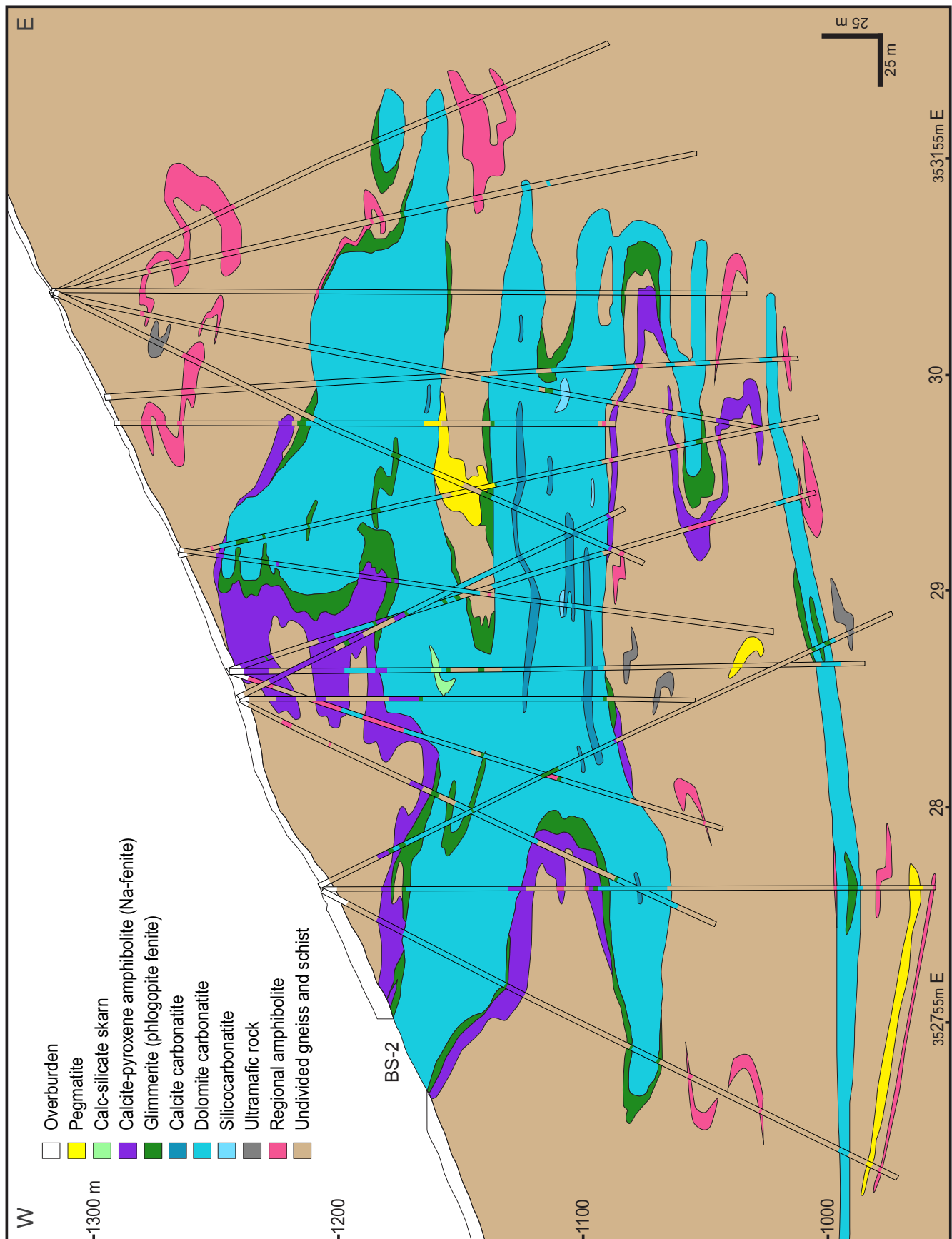


Fig. 13. Geological cross-sections through the Upper Fir carbonatite complex based on 3D view of drill-hole data (Commerce Resources Corp., pers. comm.) in 100-150 m wide corridor. Lithological logs are shown only for a 10 m wide corridor for clarity (NAD83 UTM, Zone 11 coordinates). **a)** East-west. **b)** North-south.

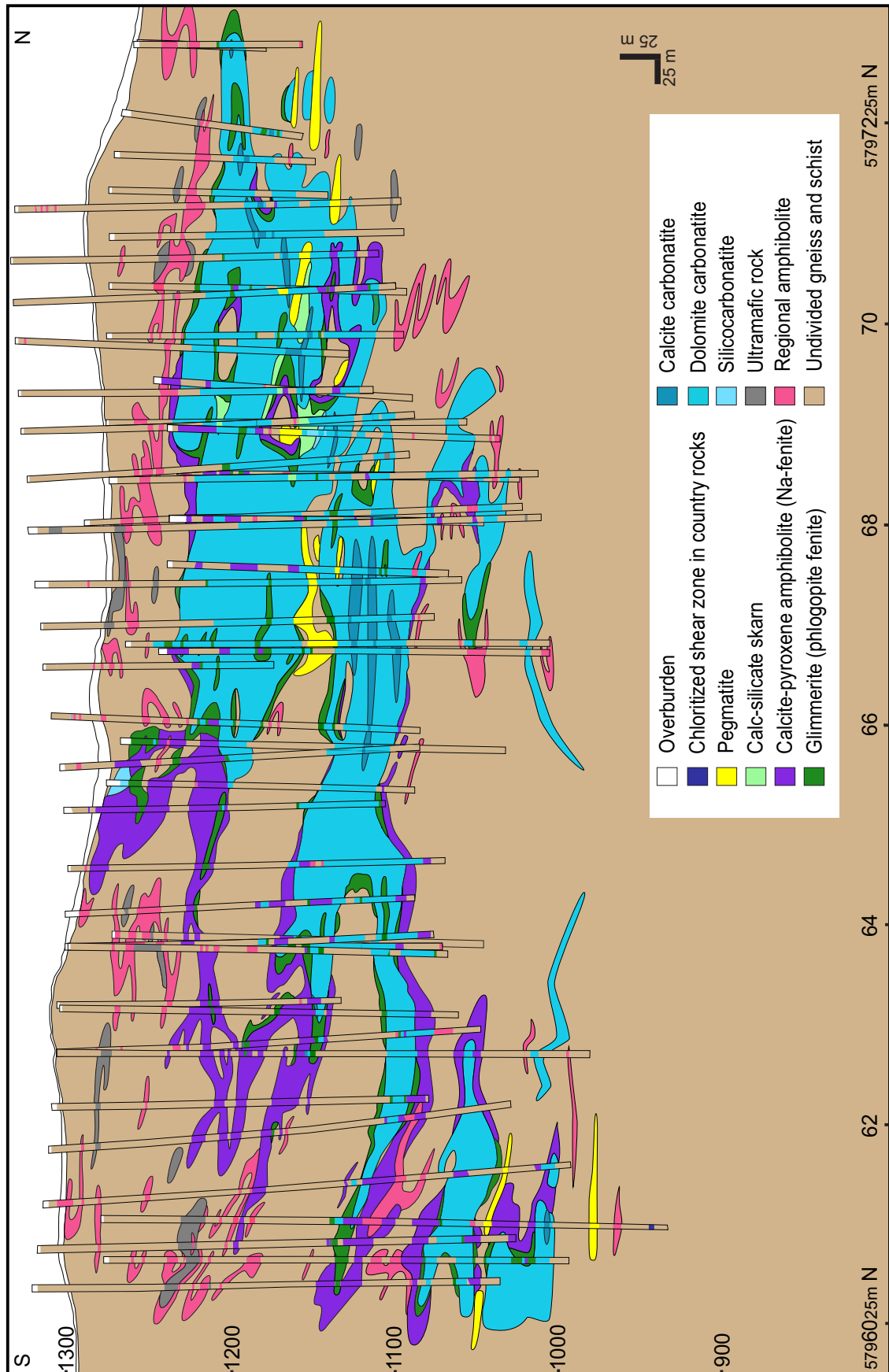


Fig. 13. b

bodies controlled original rheology and thus strain partitioning.

Discontinuous zones (typically <1 m thick) of compositionally heterogeneous phlogopite schist with minor calcite, dolomite, fluorapatite, and amphibole (i.e. phlogopite fenite) mantle carbonatite sills (Fig. 13). These fenites range from phlogopite or 'glimmerite', made up of mostly phlogopite, to banded schists with thin layers of dolomite carbonatite, amphibolite, and biotite-rich gneiss. They are generally strongly foliated and locally crenulated (Fig. 15).

Heterogeneous medium- to coarse-grained, equigranular and porphyroblastic, calcite±clinopyroxene-amphibole rocks

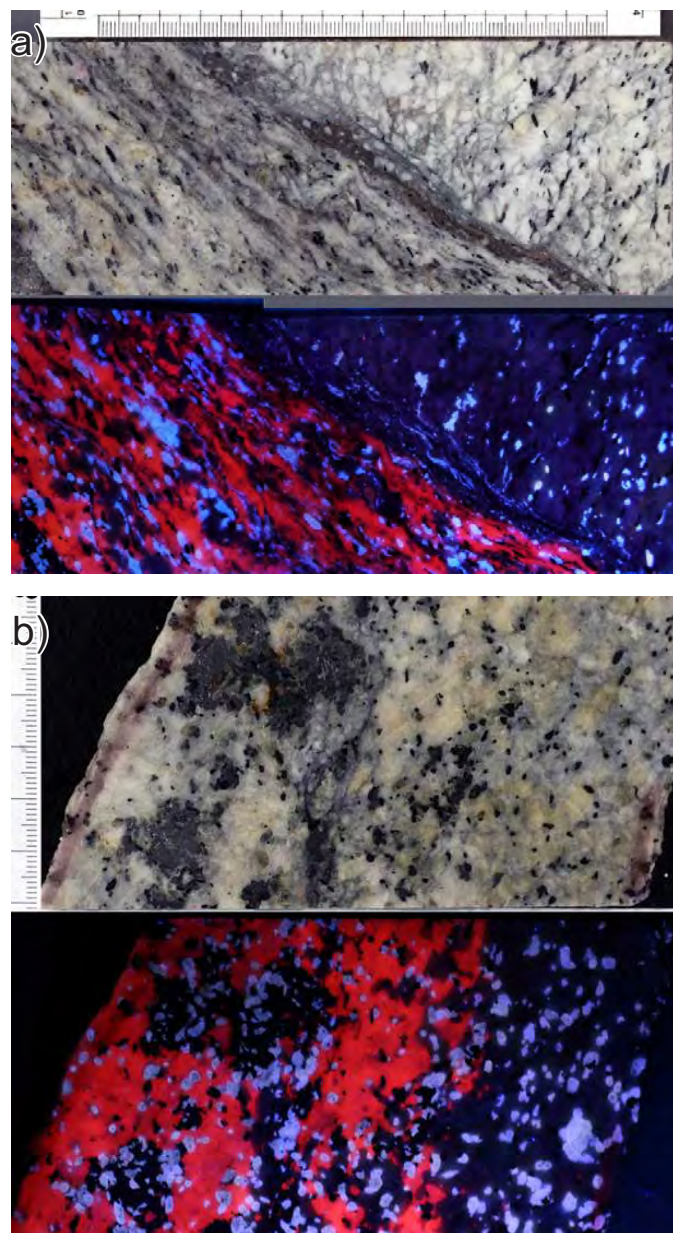


Fig. 14. Drill core slabs (scale in mm and cm) in normal and UV light showing relationships between calcite and dolomite carbonatites, Upper Fir (Chudy, 2013). **a)** Abrupt fault contact between dolomite carbonatite (right) and calcite carbonatite (left). **b)** Gradational contact; calcite is red luminescent, fluorapatite is light-blue, and amphibole and magnetite are black.

are closely associated with carbonatites, typically enveloping glimmerites. These heterogeneous amphibolites, commonly interbanded with glimmerites and country gneisses, contain variable amounts of Ca to Na-Ca amphibole, hedenbergite, titanite, albite, calcite, almandine, potassium feldspar, phlogopite, and fluorapatite (Figs. 5i and 16) and probably represent an outer, Na-fenite aureole. Alternatively, the amphibolites could represent metamorphosed alkaline rocks of the Mica Creek assemblage and thus be unrelated to the Upper Fir carbonatite complex, but their association with glimmerites and carbonatites favours a metasomatic origin. The coarse-grained clinopyroxene-calcite amphibolites are also distinct from foliated amphibolites of the Mica Creek assemblage (Rukhlov and Gorham, 2007).

Carbonatites typically have sharp contacts with fenites, which tend to have gradational contacts with the country rocks. Strongly heterogeneous zones of fenitization also occur at a distance to carbonatites, where they can be up to tens of m thick and consist of massive phlogopite fenite intercalated with thin (up to 30 cm), coarse-grained dolomite carbonatite lenses, variably fenitized country gneisses, and clinopyroxene-calcite

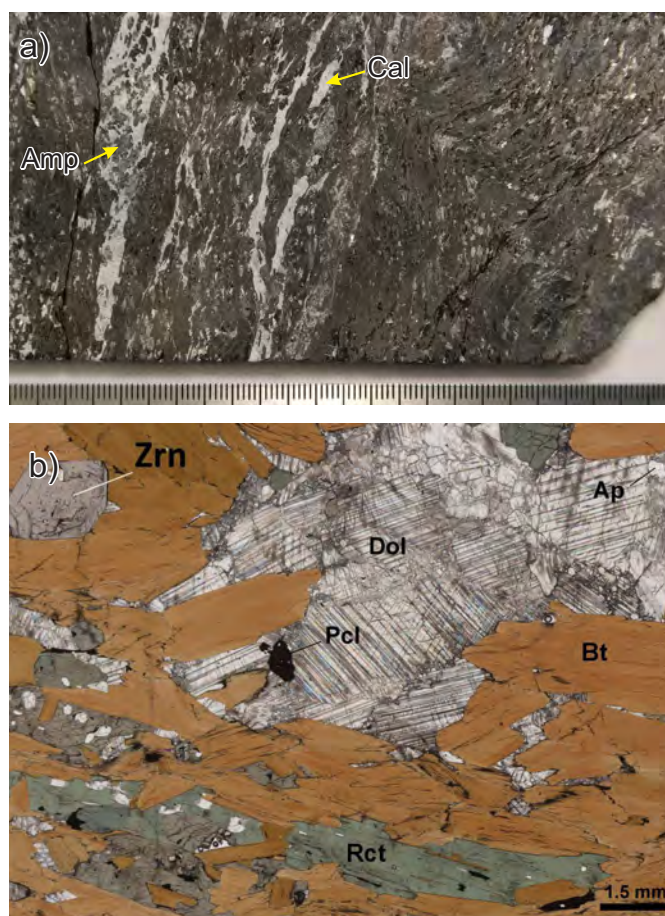


Fig. 15. Examples of exocontact glimmerites (phlogopite fenites) at Upper Fir. **a)** Crenulated glimmerite with calcite (Cal) and amphibole (Amp). **b)** Lepidoblastic texture in glimmerite with biotite (Bt), richterite (Rct), dolomite (Dol), and accessory apatite (Ap), zircon (Zrn), and pyrochlore (Pcl); plane-polarized light photomicrograph (Chudy, 2013).

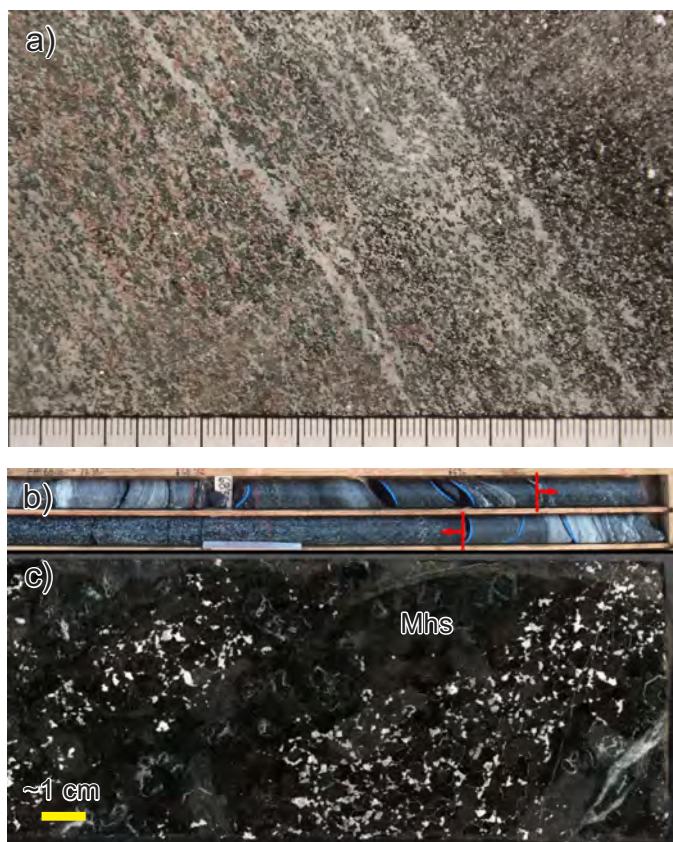


Fig. 16. Examples of Na-fenites at Upper Fir. **a)** Banded, medium-grained fenite with variable amounts of hedenbergite, almandine, Ca to Na-Ca amphibole, albite, titanite, and minor potassium feldspar. **b)** Interval of a coarse-grained porphyroblastic hornblendite (marked with red arrows) in drill core. **c)** Close-up of **b)** showing coarse-grained magnesiohastingsite (Mhs) with interstitial albite and calcite (white minerals; Chudy, 2013).

amphibolites (Na-fenites).

Locally, a coarse-grained, amphibole-pyroxene \pm phlogopite \pm calcite skarn (usually <1 m thick) is developed between the carbonatites and the country rocks, where the glimmerite is lacking. Similar skarn, commonly exhibiting compositional zoning, also mantles carbonatite contacts with crosscutting syenitic and granitic pegmatites (up to 15 m wide). Sharp contacts between carbonatites and unaltered host rocks are likely faults. Ubiquitous veins (several cm wide) composed of aligned amphibole crystals up to 2.5 x 3.0 cm (\pm pyroxene \pm phlogopite \pm pyrrhotite) crosscut the carbonatites (Fig. 9; Appendix 2).

6.2 Textural evolution of the carbonatites

One of the most striking features of the Blue River carbonatites is their textural diversity, which likely records prolonged tectonometamorphic reworking. Compared to the smaller occurrences in the area, the Upper Fir carbonatites exhibit at least four major textural types. The historical nomenclature of the carbonatites recognized texturally distinct rauhaugite (medium- to coarse-grained dolomite carbonatite), beforseite (fine-grained dolomite carbonatite), sövite (medium- to coarse-

grained calcite carbonatite), and alvikite (fine-grained calcite carbonatite), suggesting different intrusion phases within individual carbonatite complexes (e.g., Kresten, 1983). Below, we briefly summarize the fabric types and their characteristics, based on detailed textural analysis by Chudy (2013).

The most common fabric is a medium- to coarse-grain size and a shape-preferred orientation of dolomite grains that gives the rock a gneissic appearance. Minor and accessory phases such as elongated amphibole and apatite crystals are aligned within the gneissosity resulting in a penetrative foliation (Figs. 17a, b). Rarely, dolomite and minor phases lack a preferred orientation resulting in a granoblastic texture. Granoblastic rocks are generally restricted to the smaller (<30 cm thick), coarse-grained dolomite lenses that are completely embedded in glimmerite at the margins of the major sills or within extensive zones of fenitization.

Rocks with a porphyroclastic texture display medium- to coarse-grained milky-white dolomite grains set in a very fine-grained, bluish-grey matrix (Fig. 17c). The porphyroclast-to-matrix ratio is highly variable and compositional banding is preserved. The fabric overprints the gneissic fabric due to dynamic recrystallization.

Fine- to very fine-grained dolomite carbonatites with no or only minor dolomite clasts set in a bluish-grey matrix represent zones of localized retrograde strain. Aligned dolomite clasts, minor and accessory phases, and pyrrhotite and magnetite define a well-developed foliation (Fig. 17d). The gneissic fabric is the result of re-equilibration under metamorphic conditions. The primary igneous fabric of the dolomite carbonatite cannot be unequivocally determined, but the occurrence of dolomite carbonatites with the granoblastic texture suggests that it was a coarse-grained to pegmatitic rock. Following the peak of metamorphism, continued ductile to brittle deformation resulted in the development of localized shear zones. These zones formed a continuum of fabrics ranging from variably porphyroclastic to very fine-grained foliated rocks. The transitions between the fabric types are commonly gradational, but sharp transitions juxtaposing a gneissic fabric against well-foliated rocks can also be observed. Furthermore, the retrograde shear zones are heterogeneous in terms of their vertical zoning and lateral distribution. They transect the Upper Fir carbonatite complex oblique to the regional foliation and result in the displacement of different mineralogical facies.

The syntectonic pegmatites, syenites and leucogranites crosscutting the carbonatites and related metasomatic rocks constrain the timing of retrograde shearing. The shearing must have occurred after emplacement of the syntectonic quartz veins and pegmatites because the shear zones contain fragments of skarn typically found at vein/pegmatite contacts with dolomite carbonatite. It is important to note that the syntectonic intrusions had a stabilizing effect on the carbonatite during shearing. The carbonatite zones that are intersected by thicker felsic dikes or pegmatite veins (>1 m wide) always preserve their gneissic fabric and the original compositional zoning is intact.

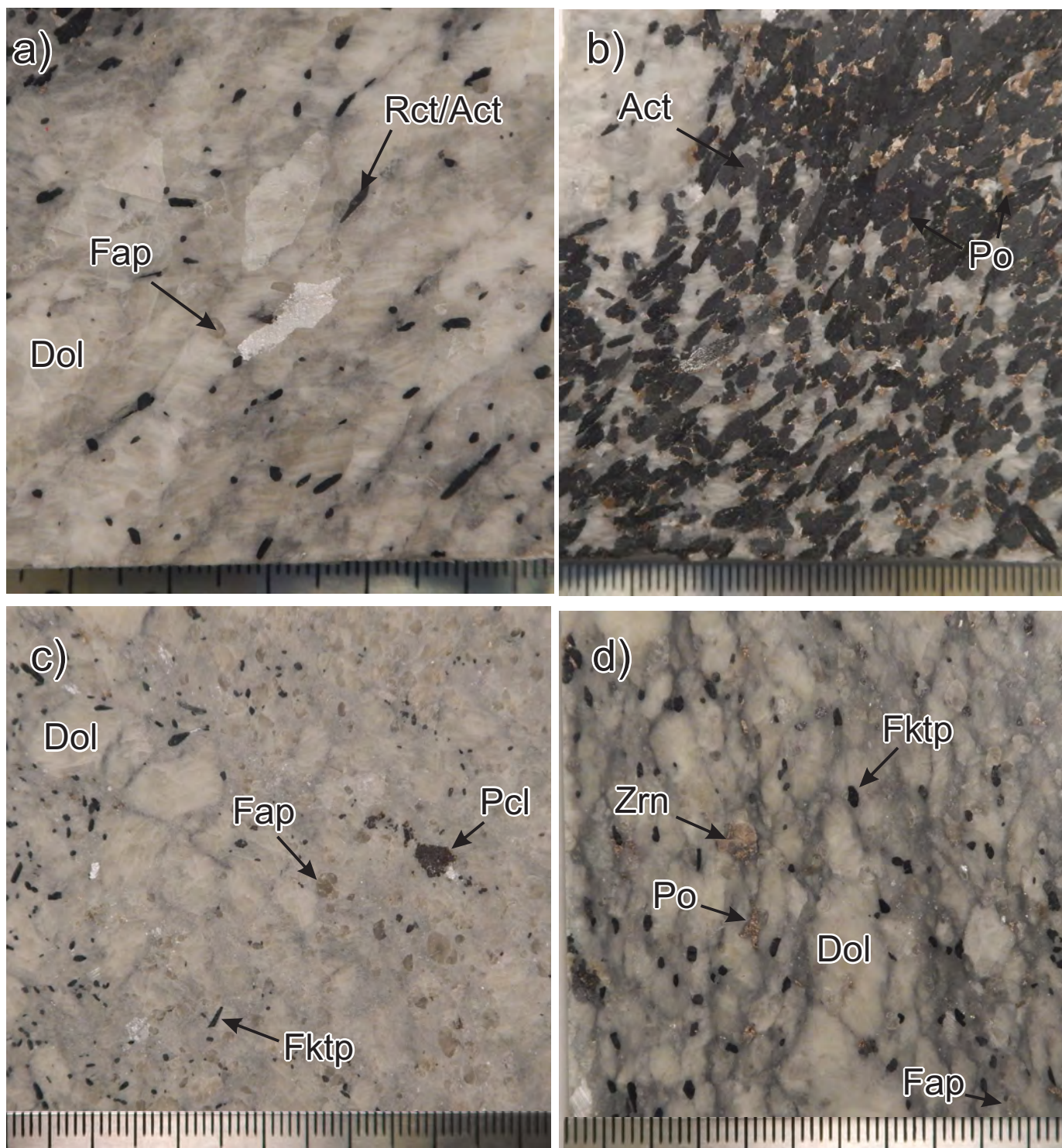


Fig. 17. Typical fabrics in the Upper Fir dolomite carbonatites: **a)** Foliated, coarse-grained granoblastic or gneissic texture (sample 16-ARU-104, Table 1). **b)** Foliated, coarse-grained pyrrhotite-actinolite segregation in a). **c)** Porphyroclastic texture. **d)** Foliated, fine-grained porphyroclastic texture. **Act** = actinolite, **Dol** = Fe-rich dolomite, **Fap** = fluorapatite, **Fktp** = ferrikatophorite, **Pcl** = pyrochlore, **Po** = pyrrhotite, **Rct** = richterite, **Zrn** = zircon. Scale in mm and cm.

6.3 Mineralogy

The Upper Fir carbonatite complex consists mainly of dolomite carbonatite with only subordinate calcite carbonatite. Ferroan dolomite is the main constituent of the dolomite carbonatite. Within the dolomite carbonatite, three major mineralogical facies are distinguished, based on minor and accessory phases: 1) anchimonomineralic facies, 2) ferriwinchite facies, and 3) ferrikatophorite facies (Chudy, 2013).

The anchimonomineralic facies contains very coarse-grained (up to 2 cm) Fe-rich dolomite and minor amounts of accessory phases such as amphibole, fluorapatite, and phlogopite (Fig. 18a). The accessory minerals are concentrated into layers, lenses, and veinlets a few cm thick. The amphiboles are fine grained (<1 mm), pale-green in hand specimen, and belong to the calcium group (actinolite with minor tremolite). They are situated predominantly between the coarse-grained dolomite. Fluorapatite is fine grained (<1 mm) and forms

granular accumulations, commonly with substantial amounts of ferrocolumbite and minor amphibole. This assemblage typically forms foliation-parallel lenses or layers, and in some instances, vein-like features in granoblastic or slightly gneissic sections. Accessory pyrrhotite forms anhedral masses (<1 mm) in interstices between the dolomite grains. Isolated flakes of phlogopite, up to 5 mm long, are rare and might be xenocrystic. The anchimonomineralic dolomite carbonatite facies generally occurs within fenite selvages and at the margins of the carbonatite bodies.

Both the ferriwinchite and ferrikatophorite facies contain 5-10 vol.% of fine- to medium-grained (<4 mm), euhedral to subhedral amphiboles, 10-15 vol.% fluorapatite typically as 3-5 mm-long ovoid grains, and variable amounts of pyrrhotite, Nb-Ta oxide phases, zircon, baddeleyite, phlogopite, magnetite, olivine, ilmenite and monazite (Fig. 18b and c). These minerals are generally evenly disseminated and fully enclosed within

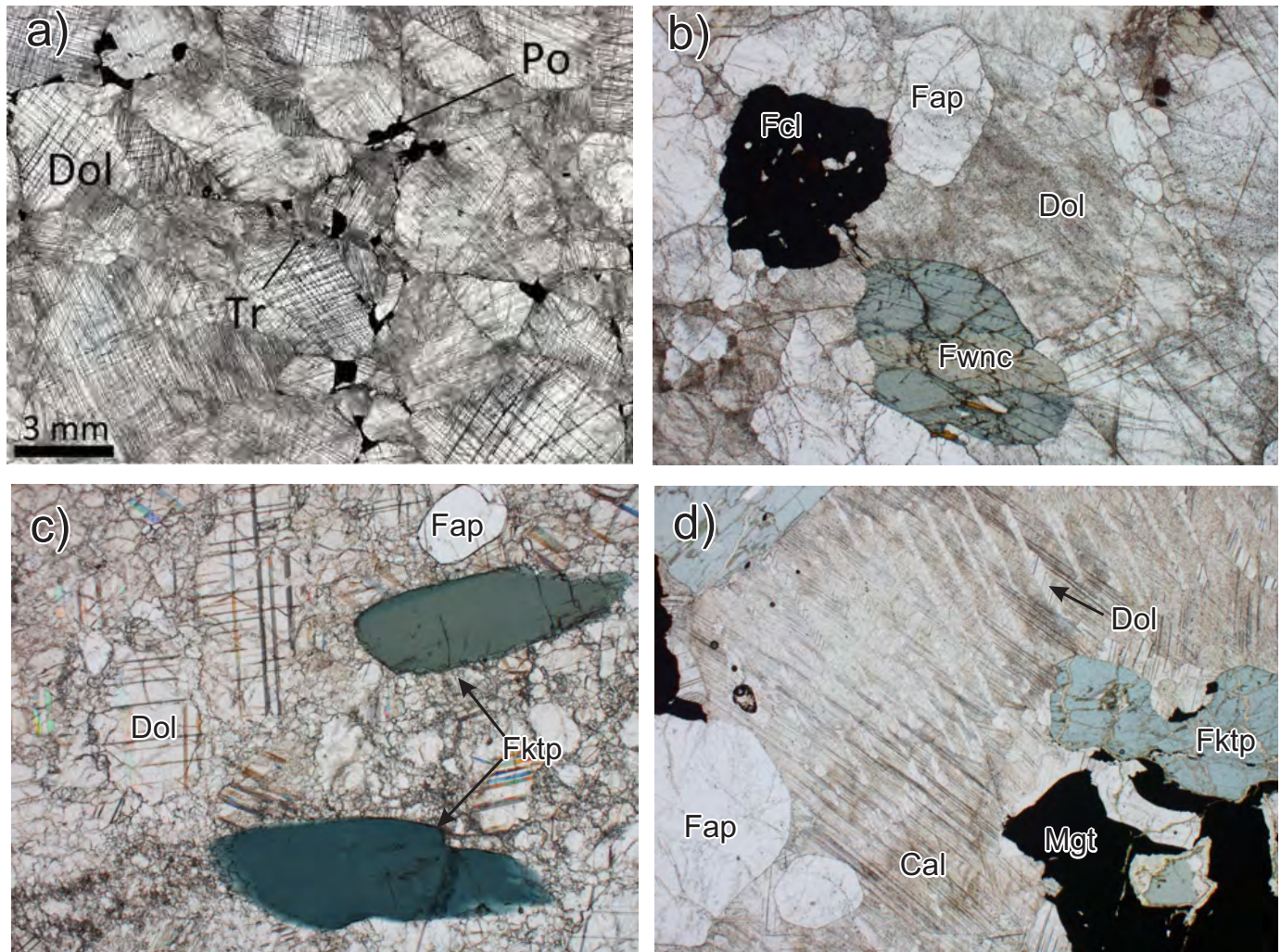


Fig. 18. Plane-polarized light photomicrographs of the main mineralogical types of carbonatites at Upper Fir (**b, c, d** field of view 5 mm; see Table 1 for sample details). **a)** Mosaic texture in anchimonomineralic dolomite carbonatite (Chudy, 2013). **b)** Granoblastic texture in dolomite carbonatite, containing ferriwinchite to actinolite and Mg±Ta-rich ferrocolumbite (sample 16-ARU-072). **c)** Porphyroclastic texture in pyrochlore- and ferrikatophorite-bearing dolomite carbonatite (sample 16-ARU-006). **d)** Granoblastic texture in dolomite-calcite carbonatite, containing Ti-bearing magnetite, ferrikatophorite and lamellar dolomite exsolutions in calcite (sample 16-ARU-082). **Dol** = Fe-rich dolomite, **Fap** = fluorapatite, **Fcl** = Mg±Ta-rich ferrocolumbite, **Fktp** = ferrikatophorite, **Fwnc** = ferriwinchite, **Mgt** = Ti-bearing magnetite, **Po** = pyrrhotite, **Tr** = tremolite.

Fe-rich dolomite, or form aggregates in layers or lenses up to 10s of cm thick, resulting in a compositional banding parallel to contacts of carbonatite bodies and to foliation in the carbonatite. Magnetite porphyroclasts typically form sheared and tightly folded lenses. Subhedral to anhedral ilmenite (<1 vol.%) occurs as inclusions in dolomite and amphibole. Nickel-rich pyrrhotite (average 0.5 vol. %) is a ubiquitous accessory phase, forming anhedral disseminated grains and sideronitic segregations with rare pyrite and chalcopyrite. Molybdenite books (up to 1.7 cm long) occur sporadically in both amphibole-rich accumulations and fenites (Fig. 3).

The ferriwinchite-facies dolomite carbonatite contains the sodium-calcium amphibole ferriwinchite or rare magnesioferrihornblende transitional to actinolite, which forms fine- to medium-grained (5-10 mm), subhedral to euhedral prisms showing Na-enrichment (transitional to richterite) at their margins. Ferrocolumbite ($\text{Mg} \pm \text{Ta}$ -rich) is the main Nb-Ta oxide phase in the ferriwinchite-bearing dolomite carbonatite. In contrast, the ferrikataphorite-facies dolomite carbonatite

contains the sodium-calcium amphibole ferrikataphorite transitional to richterite and magnesio-arfvedsonite at rims and predominantly U-Ta \pm Ti-rich pyrochlore. A 1-5 m wide transition zone between the two facies contains texturally variable pyrochlore-ferrocolumbite intergrowths (Fig. 19).

Volumetrically minor, calcite carbonatite at Upper Fir (Fig. 13; Appendix 1) is a heterogeneous rock with abundant (up to 20 vol.%), medium- to coarse-grained masses of anhedral Ti-bearing magnetite enclosing fluorapatite, richterite, pyrrhotite, and pyrochlore that are unevenly distributed within the calcite carbonatite matrix or form massive layers and lenses. These apatite-magnetite masses thus resemble phoscorite (Krasnova, 2004). Other than Ti-bearing magnetite with ilmenite exsolutions, the calcite carbonatite contains fluorapatite, ferrikataphorite transitional to richterite, pyrrhotite, ubiquitous orange, U-Ta-rich and rare Na-Ca-deficient, Fe-rich pyrochlore, Fe^{3+} -rich ilmenite, zircon, chalcopyrite, and Fe^{2+} -Na-rich phlogopite in similar amounts to those of the ferrikataphorite-bearing dolomite carbonatites. The carbonates

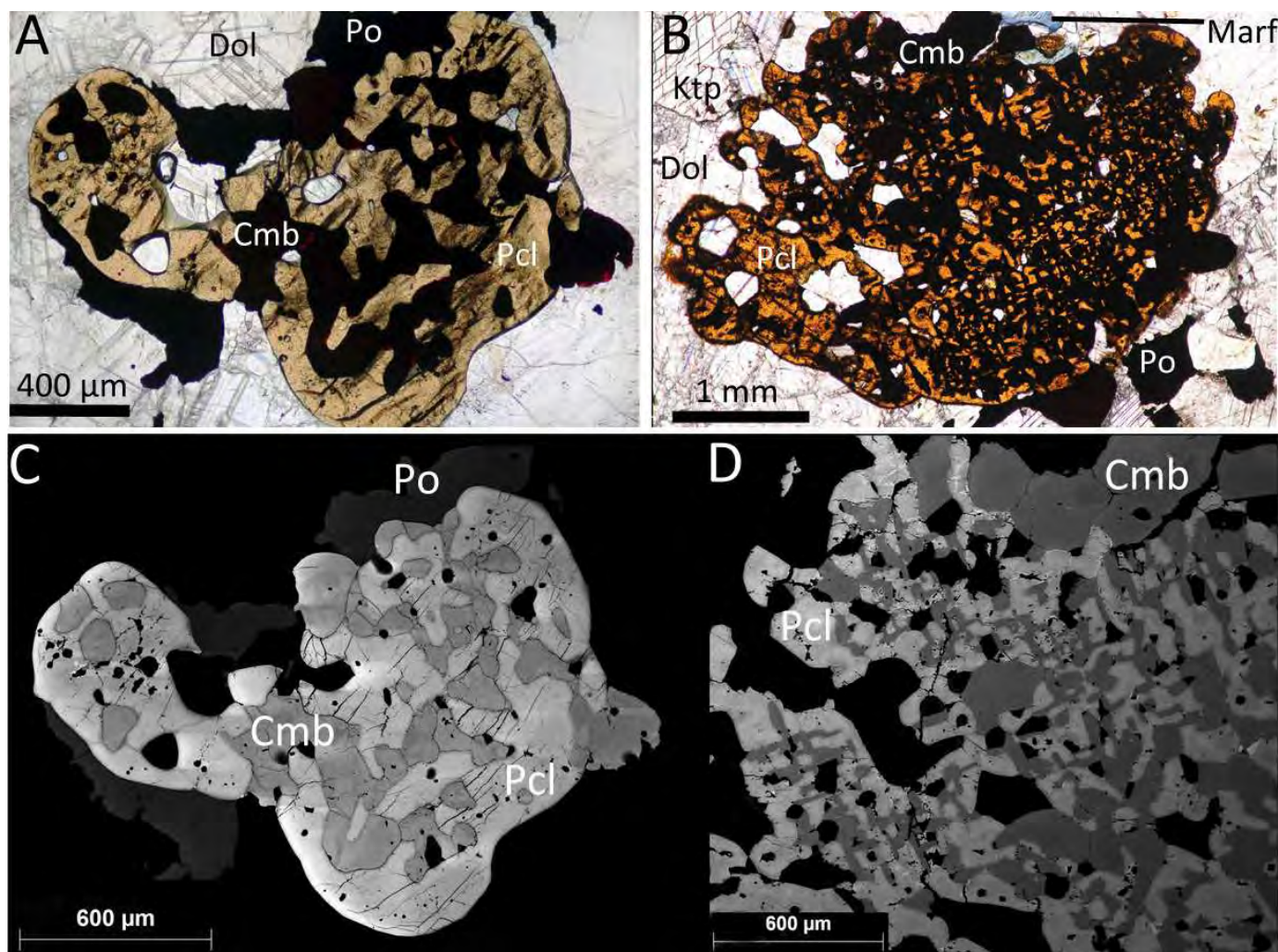


Fig. 19. Examples of pyrochlore-ferrocolumbite composite grains in the Upper Fir dolomite carbonatites (a, b plane-polarized light photomicrographs, c, d corresponding BSE images; Chudy, 2013): **a)** and **c)** Ferrocolumbite (Cmb) and other mineral inclusions in pyrochlore (Pcl) enclosing matrix and partially mantled by pyrrhotite (Po). **b)** and **d)** Fine-grained ferrocolumbite intergrown with pyrochlore. Note enclosed matrix phases and associated pyrrhotite, ferrikataphorite (Ktp) and magnesio-arfvedsonite (Marf).

are mostly calcite, containing coarse to sub- μm , irregular and lamellar dolomite exsolutions (Fig. 18d), and minor amounts of Fe-rich dolomite, and typically form a heterogeneous porphyroclastic matrix. The minor and accessory phases tend to form aggregates.

6.4 Niobium-tantalum mineralization

The Nb-Ta mineralization at the Upper Fir complex consists predominantly of ferrocolumbite and pyrochlore-supergroup minerals. The proportion of these minerals generally depends on position relative to the margins of the carbonatite bodies or on mineralogical facies of the carbonatites. Rare fersmite replaces ferrocolumbite. The two main Nb-Ta oxide minerals vary widely in grain size (sub-mm to cm), with ferrocolumbite typically forming coarser grains than pyrochlore. Pyrochlore forms disseminations and clusters.

Ferrocolumbite occurs mainly in the ferriwinchite-facies dolomite carbonatite and forms massive, subhedral or xenomorphic, commonly skeletal to strongly poikilitic grains (up to 3 cm) that enclose all other phases in the dolomite carbonatite (Figs. 18b and 20). Ferrocolumbite concentrations occur in fluorapatite layers and lenses within the anchimonomineralic and ferriwinchite facies, and within the phlogopite fenite. Compositional variation in terms of Nb/Ta and Fe/Mn ratios is relatively minor compared to that of rare metal pegmatites (Fig. 21). The X_{Ta} (Ta/(Ta+Nb) in a.p.f.u.) ranges from <0.002 to 0.068, and the X_{Mn} (Mn/(Mn+Fe) in a.p.f.u.) ranges from 0.054 to 0.123. Titanium and iron show no systematic variation and range between 0.022–0.083 a.p.f.u. Ti and 0.703–0.932 a.p.f.u. Fe. Altered ferrocolumbite crystals have distinctly higher X_{Ta} values (up to 0.179) compared to those of primary ferrocolumbites, and are associated with secondary Ta-rich pyrochlore together with monazite and thorite inclusions (Fig. 20). Subordinate amounts of ferrocolumbite occur also as exsolution lamellae in ilmenite.

The transition zone between the two amphibole facies of dolomite carbonatites displays intergrown ferrocolumbite-pyrochlore aggregates (Fig. 19). The proportion of the two Nb-Ta oxide phases varies widely with unclear replacement relationships between these phases. The composition of ferrocolumbite in the aggregates is within the range of that for primary ferrocolumbite and does not show elevated Ta concentrations. The composition of pyrochlore in the aggregates is also similar to that of free pyrochlore grains disseminated in the matrix of the ferrikatophorite-bearing dolomite carbonatite.

Pyrochlore in the Upper Fir carbonatites (Fig. 22) shows a wide range of compositions extending from the Nb end member to the Ta-rich compositions attaining that of microlite (i.e. $\text{Ta} \geq \text{Nb}$ and $(\text{Nb} + \text{Ta}) \geq 2\text{Ti}$) accompanied by an increase in Ti (Fig. 23). Chudy (2013) distinguished primary and secondary pyrochlores at Upper Fir. The primary pyrochlore forms sub-mm to cm-sized euhedral to subhedral grains, ranging from yellow through red-brown to black, that are disseminated in the carbonate matrix and form inclusions in fluorapatite, amphibole, magnetite, and zircon (Fig. 22a-d and f). Some

pyrochlores contain inclusions of dolomite, calcite, and apatite. Clusters and seams of larger pyrochlore clumps are common, resulting in discontinuous high-grade zones with up to 1.06 wt.% Ta_2O_5 and 17.57 wt.% Nb_2O_5 across a single 1 m drill-core interval (Gorham et al., 2013). The secondary pyrochlore transitional to microlite is exclusively associated with altered ferrocolumbite, forming subhedral grains less than 100 μm (Fig. 22g). The A-site cations of primary pyrochlore are mostly occupied by Ca and Na in equal amounts, with a tendency of the enrichment in Ca and a small percentage of vacancies (Chudy, 2013; Rukhlov et al., 2018). Minor elements include Sr, Th, REE, Fe, and Mn.

Most pyrochlores in the dolomite carbonatite at Upper Fir have a Nb/Ta ratio between 6.0–6.5 with relatively high Nb (up to 1.659 a.p.f.u.) and fluorine (up to 0.767 a.p.f.u.), and relatively low Ti (<0.083 a.p.f.u.) and U (<0.043 a.p.f.u.) contents (Chudy, 2013). Rare pyrochlore grains that form a locally restricted paragenetic assemblage together with zircon and ferrikatophorite are enriched in Ta (Nb/Ta ratio = 2.8–5) and have higher Ti (up to 0.310 a.p.f.u.) and U (0.360 a.p.f.u.), and lower F (<0.55 a.p.f.u.) concentrations. They are compositionally similar to pyrochlores in the calcite carbonatite. Pyrochlore intergrown with ferrocolumbite in composite grains from the transition zone between the carbonatite facies has relatively high Nb/Ta ratios (up to 8.5) and low Ti (<0.14 a.p.f.u.) and U (<0.045 a.p.f.u.) contents (Chudy, 2013).

Secondary pyrochlore, which formed during the alteration of ferrocolumbite, is strongly enriched in Ta, resulting in the low Nb/Ta ratios of <3 (Fig. 22g). Some compositions with up to 0.840 a.p.f.u. Ta and 0.753 a.p.f.u. Nb are thus classified as microlite. Secondary pyrochlore is also typically enriched in Ti (0.34 – 0.57 a.p.f.u.), U (0.125 – 0.49 a.p.f.u.), Th (0.04 – 0.17 a.p.f.u.), La+Ce (up to 0.09 a.p.f.u.), and have detectable Mn and Fe (Chudy, 2013). Generally, pyrochlores from the Upper Fir are unique in possessing distinctly higher Ta contents compared to those from other carbonatites in the Blue River area and to most carbonatites elsewhere (Fig. 23).

6.5 Whole rock geochemistry

Based on whole-rock geochemistry, the Upper Fir carbonatites classify as magnesiocarbonatite and ferrocarbonatite (Fig. 24). The classification of the calcite carbonatites as ferrocarbonatite is due to abundant magnetite (up to 30 vol.% across 1 m intervals). Likewise, the compositionally heterogeneous dolomite carbonatites with clusters and bands of minor and accessory phases results in a considerable range of major- and trace-element concentrations. Appendix 1 provides examples of downhole geochemical variations in the Upper Fir carbonatites and related fenites for selected elements. Appendix 3 also shows 3D interpolated gridding of drill-core assay data (99th percentile) for selected elements by the inverse-distance method using GOCAD® software in the east-to-west cross section (see Fig. 13a for geological interpretation). The CaO/MgO ratio and total Fe expressed as Fe_2O_3 contents discriminate between the calcite and dolomite carbonatites, whereas the $\text{Na}_2\text{O}/\text{SiO}_2$ ratio

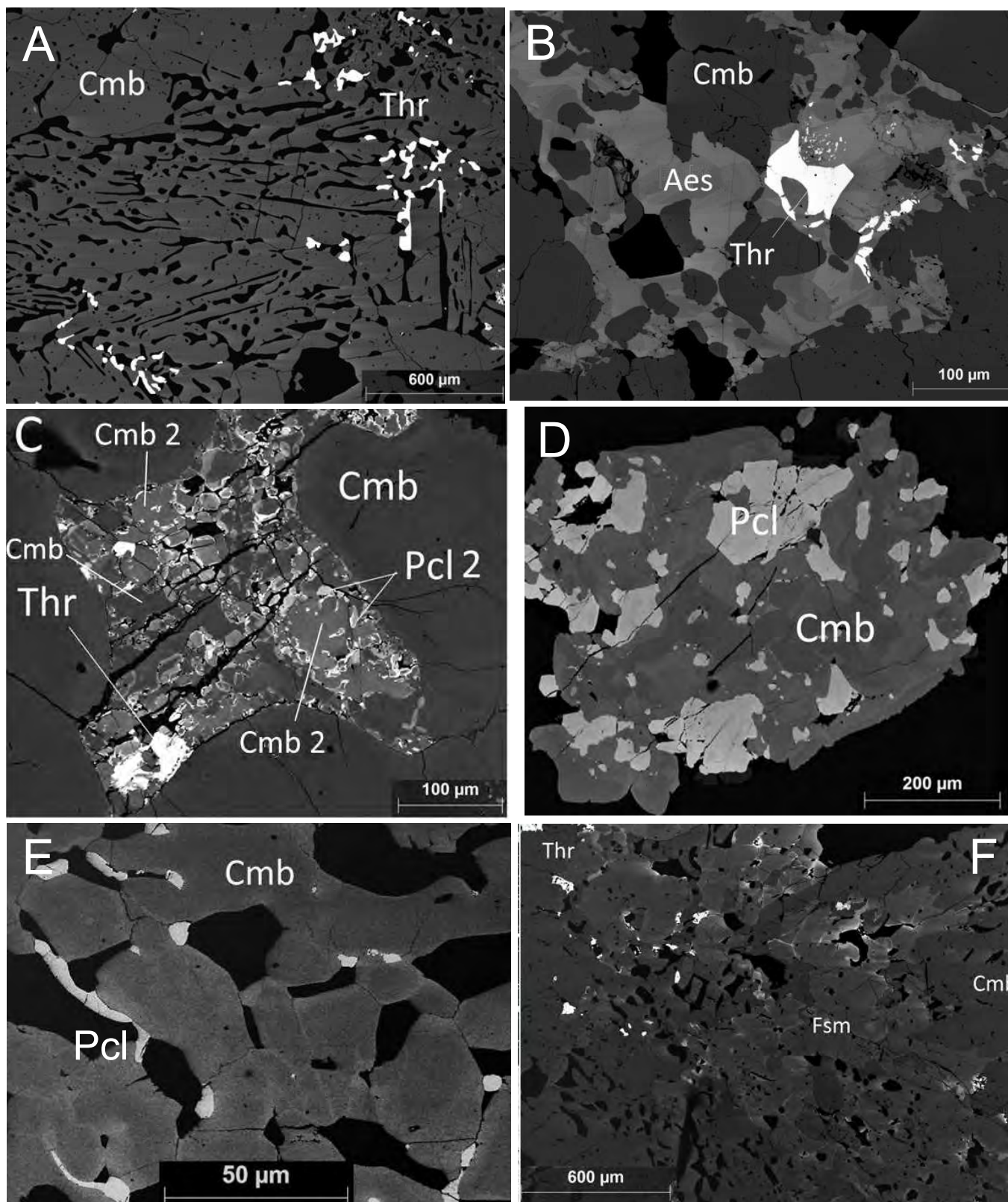


Fig. 20. Examples of paragenetic relationships of ferrocolumbite (Cmb) at Upper Fir (BSE images from Chudy, 2013). **a)** Poikilitic crystal with vermicular calcite and thorite (Thr) inclusions. **b)** Interstitial, zoned niobaeschnite-(Ce) (Aes) and thorite. **c)** Secondary ferrocolumbite (Cmb 2) with lower Nb/Ta ratio and high-Ta pyrochlore (Pcl 2) and thorite replacing primary ferrocolumbite (Cmb). **d)** Altered ferrocolumbite with abundant pyrochlore (Pcl) inclusions. **e)** Poikilitic ferrocolumbite with pyrochlore inclusions. Note brighter rims with lower Nb/Ta ratio than that of the darker cores. **f)** Fersmite (Fsm) replacing poikilitic ferrocolumbite with thorite inclusions.

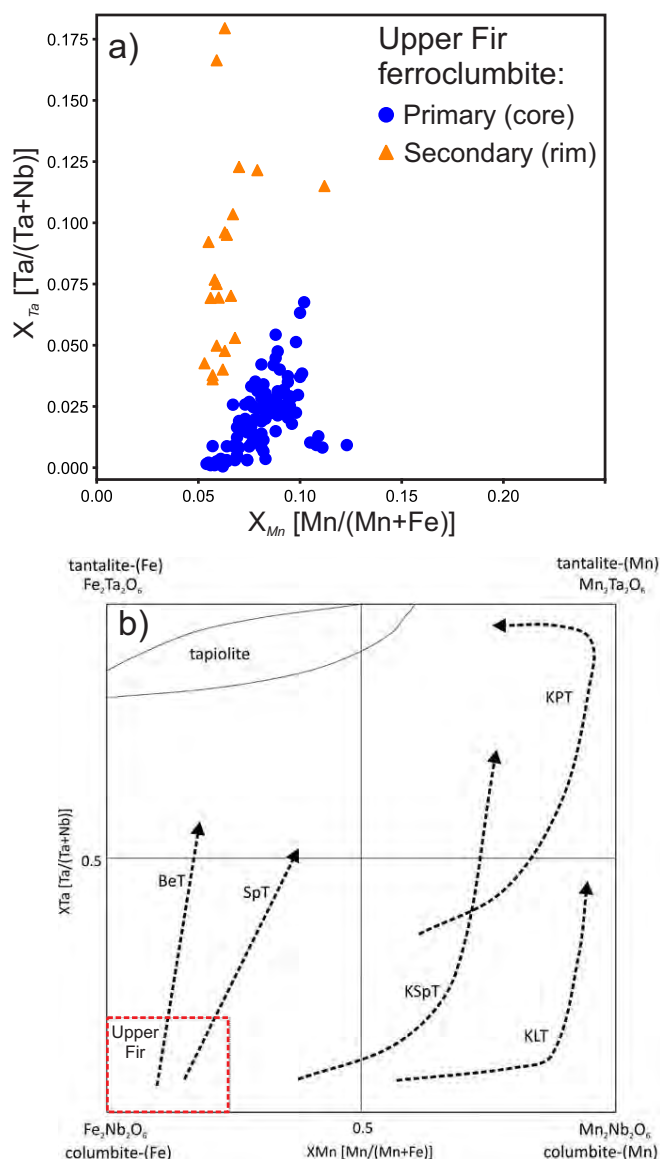


Fig. 21. Quadrilateral X_{Mn} [Mn/(Mn+Fe)] vs. X_{Ta} [Ta/(Ta+Nb)] (a.p.f.u.) diagram for columbite group. **a)** Compositions of ferroclumbite from the Upper Fir complex after Chudy (2013). **b)** Evolutionary trends for columbite group in rare metal pegmatites after Černý et al. (1986): BeT = beryl type, SpT = spodumene type, KSpT = complex spodumene type, KLT = complex lepidolite type, KPT = complex petalite type.

correlates with the main mineralogical facies described above (Appendices 1 and 3). To better assess the overall geochemical character of the Upper Fir carbonatites, the data from highly heterogeneous samples with large accumulations of non-carbonate minerals (i.e., >30 vol.% of compositional banding) were omitted from the following summary.

The three mineralogical facies of the magnesiocarbonatites have virtually identical average total Fe (7.82–8.12 wt% as Fe_2O_3), MgO (15.15–15.41 wt%), and CaO (29.93–30.27 wt%) contents but distinct minor- and trace-element contents (Figs. 25 and 26). The anchimonomineralic- and ferriwinchite-bearing carbonatites have similar average MnO (0.96 and 0.94 wt%),

P_2O_5 (3.21 and 3.51 wt%), Sr (5310 and 5000 ppm), and total REE (608 and 630 ppm) contents. Reflecting mainly different modal abundances of amphibole, the anchimonomineralic carbonatites have generally lower average SiO_2 (2.0 wt%) and Na_2O (0.08 wt%) concentrations but similar Na_2O/SiO_2 ratios (0.04) as the ferriwinchite-bearing carbonatites, which have 4.03 wt% SiO_2 , 0.2 wt% Na_2O , and Na_2O/SiO_2 ratios of 0.05 (Chudy, 2013). Likewise, the anchimonomineralic carbonatites have distinctly lower average Nb (791 ppm) and Ta (88 ppm) than those of the ferriwinchite facies, which have 1538 ppm Nb and 196 ppm Ta, but similar Nb/Ta ratios (8–9), consistent with the different modal abundances of ferroclumbite.

The ferrikatophorite-bearing dolomite carbonatites have slightly lower average MnO (0.8 wt%) and Sr (4225 ppm) but slightly higher P_2O_5 (4.22 wt%), Na_2O (0.4 wt%), and total REE (660 ppm) contents than those of the anchimonomineralic and ferriwinchite-bearing carbonatites. The average Na_2O/SiO_2 value (0.14) is also distinctly higher, and the Nb/Ta ratio (ca. 3) is distinctly lower in the ferrikatophorite-bearing dolomite carbonatite compared with those of the ferriwinchite-anchimonomineralic dolomite carbonatites (Fig. 26a).

The calcite carbonatite has higher average total Fe (16.5 wt% as Fe_2O_3), Na_2O (0.57 wt%), P_2O_5 (5.13 wt%), and total REE (951 ppm) concentrations than those of the dolomite carbonatites. The calcite carbonatite has lower average MnO (0.67 wt%) but similar Sr concentrations (5162 ppm) relative to those of the ferriwinchite-bearing dolomite carbonatites. The average Na_2O/SiO_2 ratio is very similar to that of the katophorite-bearing dolomite carbonatites, whereas the average Nb/Ta ratio of 2.4 is the lowest of all the carbonatites at Upper Fir (Figs. 25 and 26; Chudy, 2013).

Across the four carbonatite facies, the high-field strength elements (Ti, Nb, Ta, Zr, and Hf), U, and Th show systematic variations. Niobium decreases from the marginal facies (anchimonomineralic and ferriwinchite-bearing carbonatites) towards the center (calcite carbonatite), whereas Ta abruptly increases from the anchimonomineralic to the ferriwinchite- and ferrikatophorite-bearing dolomite carbonatites and calcite carbonatite, where it is at approximately the same level (195–204 ppm) resulting in a continuous decrease in the Nb/Ta ratio from ca. 10 to 2 (using average values). The Zr/Hf ratio shows the opposite behavior and increases from the marginal facies (26–30) towards the calcite carbonatite (59). A similar trend is observed for the U/Th ratio, which increases from ca. 1 to ca. 33 from the anchimonomineralic facies to the calcite carbonatite (Chudy, 2013). The calcite carbonatites also have much higher Y and slightly higher total REE contents than those of the dolomite carbonatites at Upper Fir (Fig. 26).

Compared to other carbonatites of the Blue River area, the Upper Fir carbonatites have distinctly higher MnO and Ta, lower median Cs, Rb, Ba, Hf, Zr, Ti, and REE, but generally similar median Th, K, and P contents, and similar slopes of chondrite-normalized REE patterns (Figs. 25–27). Some calcite carbonatites such as the Gum Creek occurrence immediately to the east of the Upper Fir have much higher Sr and total REE

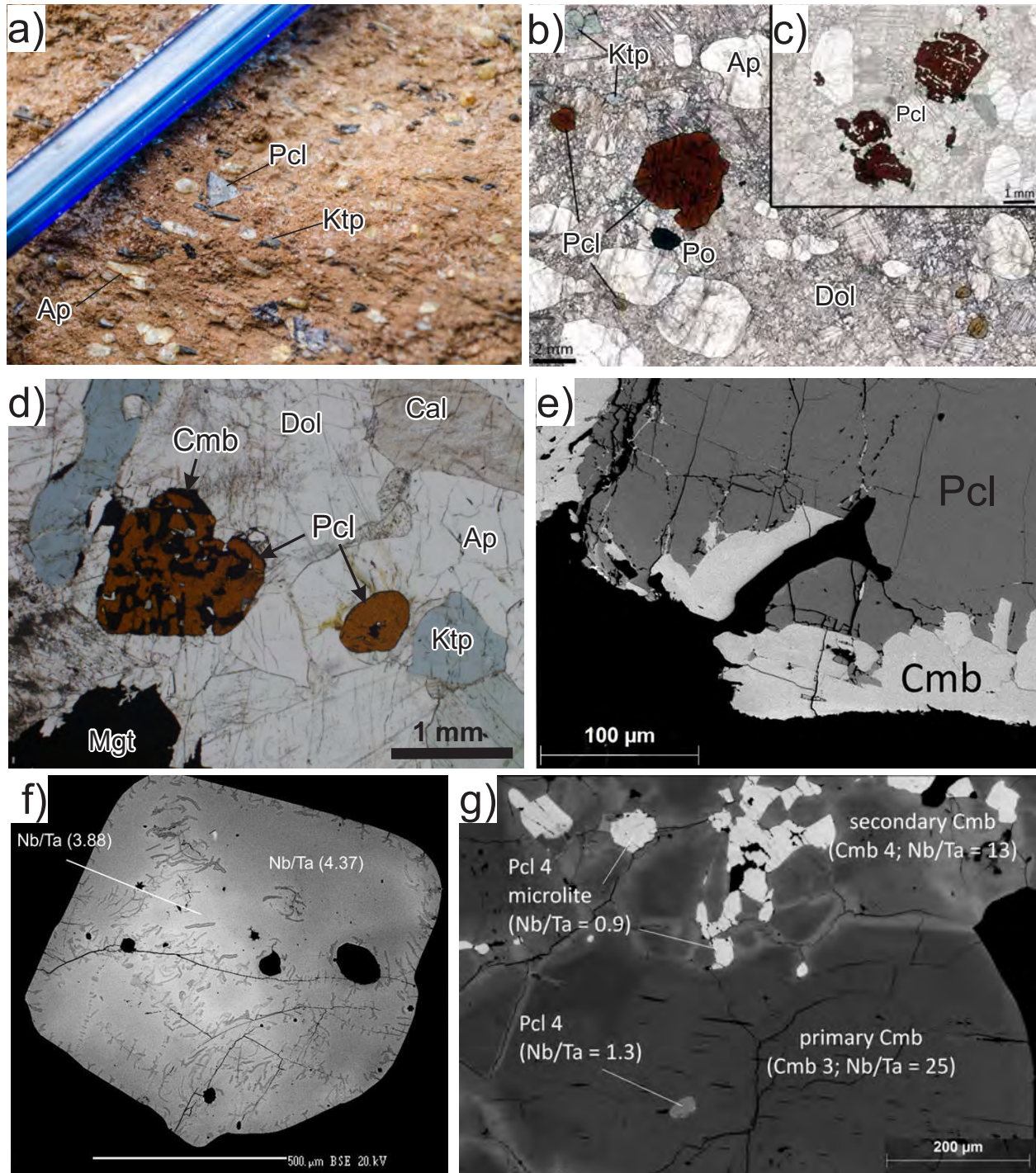


Fig. 22. Examples of paragenetic relationships of pyrochlore (Pcl) at Upper Fir (b, c, d plane-polarized light photomicrographs; e, f, g BSE images from Chudy, 2013). **a)** Euhedral U-Ta-rich pyrochlore crystal in weathered, porphyroclastic dolomite carbonatite containing fluorapatite (Ap) and ferrikataphorite (Ktp), BS-1 cut (Stop 4). Pen for scale. **b)** Dark-red pyrochlore coexisting with yellow pyrochlore in porphyroclastic dolomite carbonatite containing fluorapatite, ferrikataphorite, and pyrrhotite (Po). **c)** Primary pyrochlore inclusion in fluorapatite and poikilitic pyrochlore with dolomite and fluorapatite inclusions. **d)** Mg-Ta-rich ferrocolumbite (Cmb) replacing orange U-Ta-rich pyrochlore in granoblastic calcite-dolomite carbonatite containing fluorapatite, ferrikataphorite (transitional to richterite), Ti-bearing magnetite (Mgt) with exsolution lamellae of ilmenite, calcite (Cal) with sub- μm to coarse exsolution lamellae of dolomite, pyrrhotite, and accessory Fe^{3+} -rich ilmenite, Fe^{2+} -Na-rich phlogopite, Na-Ca-deficient and U-Fe-Ta-rich pyrochlore, zircon, and chalcopyrite (sample 16-ARU-101, Table 1). **e)** Ferrocolumbite forming a replacement rim on unzoned pyrochlore from a fluorapatite-rich layer in ferriwinchite-bearing dolomite carbonatite. **f)** Low-temperature alteration forming darker coloured dendritic features overprinting primary compositional zoning in a pyrochlore crystal with lower Nb/Ta ratio of the brighter coloured core compared to that of the darker coloured rim. **g)** Microlite associated with secondary ferrocolumbite (lighter grey) having lower Nb/Ta ratio relative to that of the primary ferrocolumbite (darker grey) with inclusions of Ta-rich pyrochlore (Pcl 4).

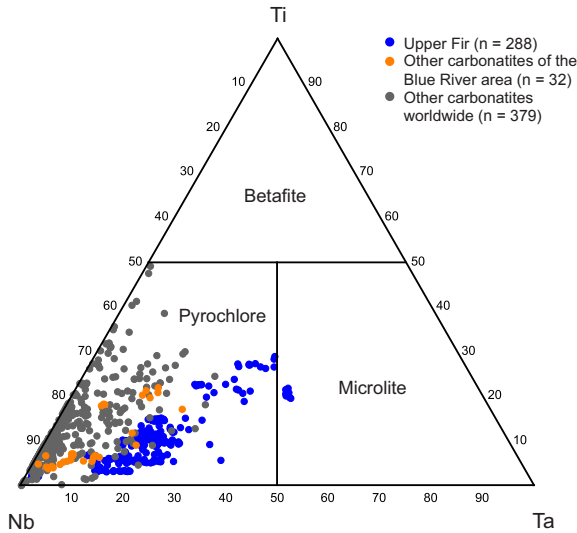


Fig. 23. Ternary Ti–Nb–Ta diagram (mol.%) after Atencio et al. (2010) for pyrochlore supergroup from the Blue River carbonatites compared with pyrochlore compositions from worldwide carbonatites. Data from Chakhmouradian (2006), Chakhmouradian et al. (2015), Mackay and Simandl (2015), Chudy (2013), and Rukhlov et al. (unpublished data from Blue River carbonatites).

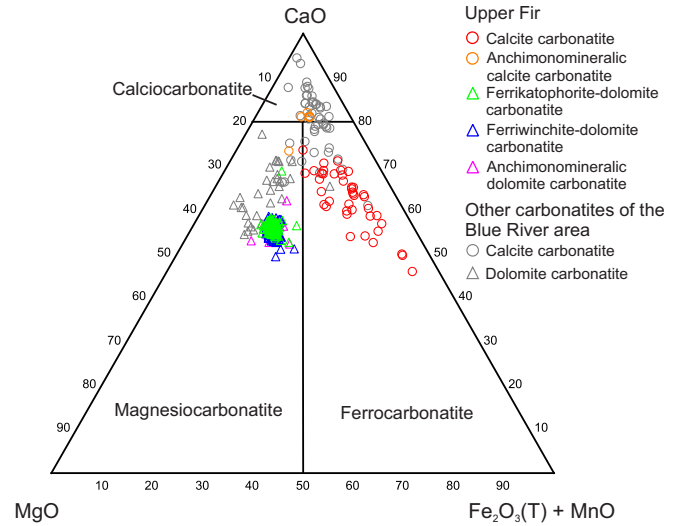


Fig. 24. Ternary CaO–MgO–[Fe₂O₃(T) + MnO] diagram (in wt.%) after Woolley and Kempe (1989) for the Blue River carbonatites with <20 wt% SiO₂. Note that magnetite-bearing calcite carbonatites plot into the ferrocarbonatite field. Data from Rukhlov and Gorham (2007), Gorham (2008), and Chudy (2013).

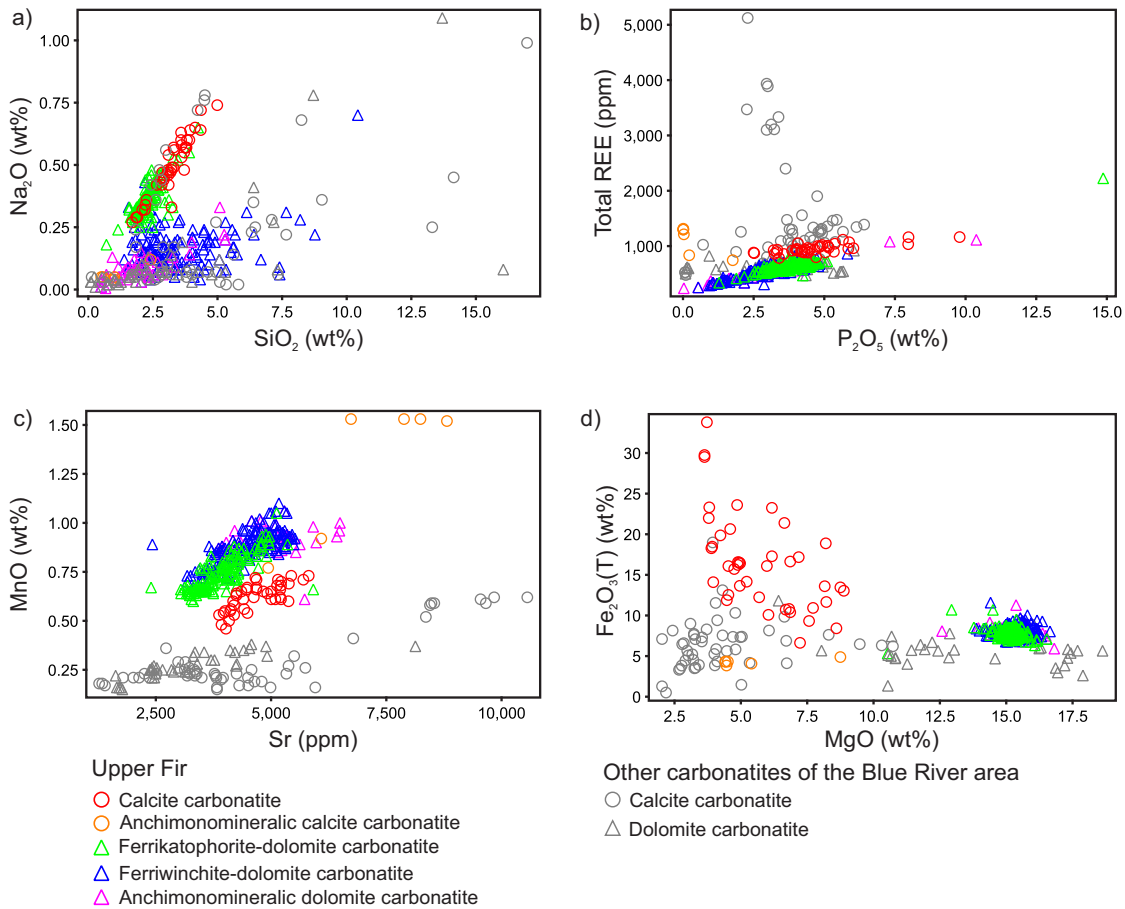


Fig. 25. Whole-rock geochemical variation plots for the Blue River carbonatites: **a)** SiO₂ (wt%) vs Na₂O (wt%). **b)** P₂O₅ (wt%) vs total REE (ppm). **c)** Sr (ppm) vs MnO (wt%). **d)** MgO (wt%) vs Fe₂O₃(T) (wt%). Data from Rukhlov and Gorham (2007), Gorham (2008), and Chudy (2013).

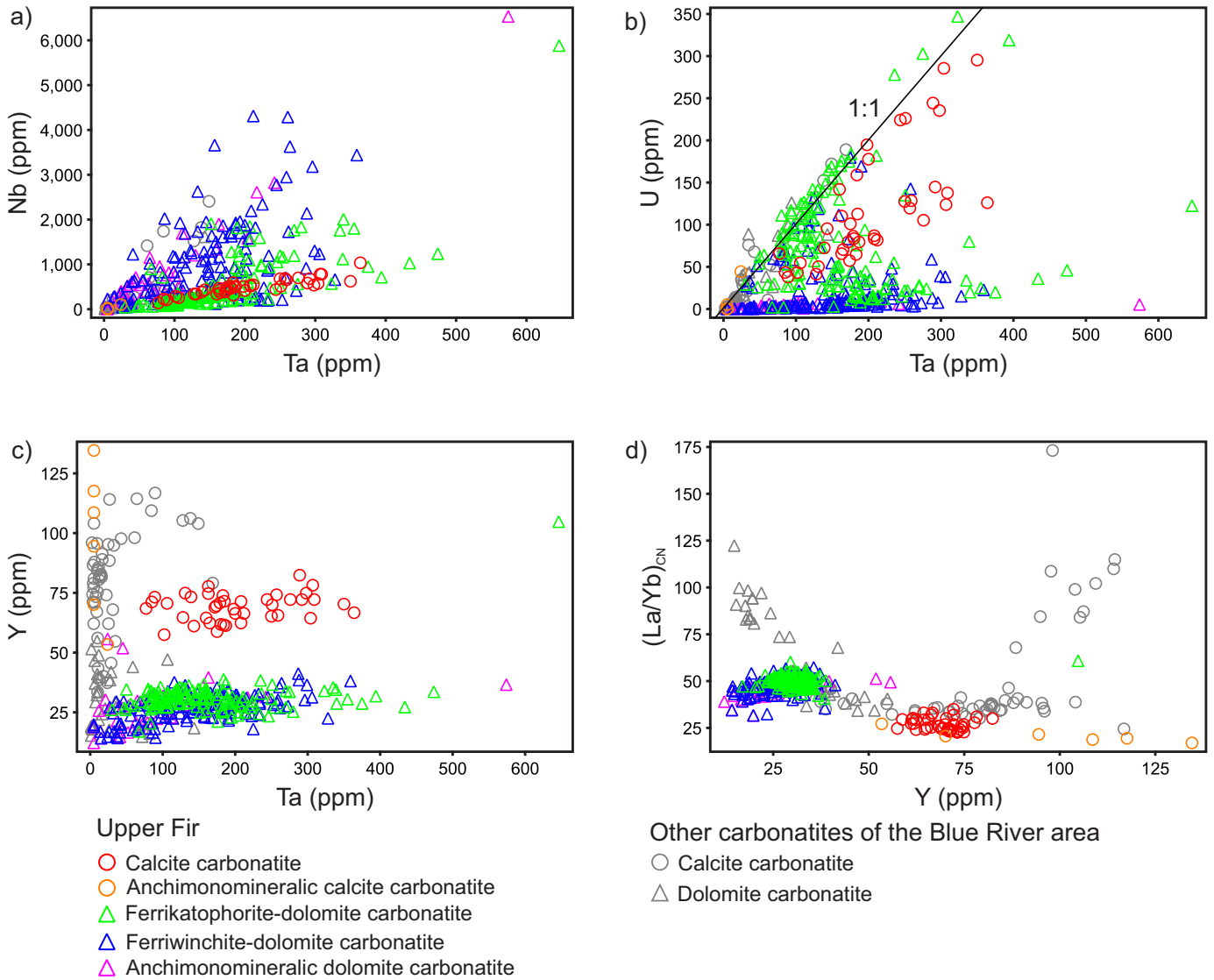


Fig. 26. Whole-rock geochemical variation plots for the Blue River carbonatites: **a)** Ta (ppm) vs Nb (ppm). **b)** Ta (ppm) vs U (ppm). **c)** Ta (ppm) vs Y (ppm). **d)** Y (ppm) vs $(La/Yb)_{CN}$, using chondrite normalization of Boynton (1984). Data from Rukhlov and Gorham (2007), Gorham (2008), and Chudy (2013).

contents, and higher $(La/Yb)_{CN}$ ratios compared to those of the Upper Fir carbonatites (Figs. 25 and 26). These geochemical characteristics directly reflect the mineralogical compositions of the Blue River carbonatites (Table 1), whereby K_2O , Na_2O and SiO_2 are controlled by the amphibole, pyroxene and mica species, MnO and Sr by the composition of the carbonates, REEs mainly by apatite (Mitchell et al., 2017), and the high-field strength elements and V by complex oxide phases such as pyrochlore, ferrocolumbite, aeschynite, zirconolite, ilmenite, magnetite, and baddeleyite, and by other accessory minerals such zircon and thorite.

The Blue River carbonatites have very similar primordial mantle-normalized patterns to those of the ca. 344 Ma Aley carbonatite, except for much higher Th and lower Ta contents in the latter (Fig. 27; Chakhmouradian et al., 2015). Nepheline syenites associated with the Paradise Lake and Howard Creek carbonatites have lower median P, Sr, Y, and REE contents,

lower $(La/Yb)_{CN}$ ratio, and higher median K, Cs, Rb, Ba, Zr, Hf, and Ti contents relative to those of the Blue River and Aley carbonatites (Fig. 27). The normalized REE and multi-element patterns for regional marbles in the Blue River differ completely from those of the carbonatites and related alkaline, silica-undersaturated rocks (Fig. 27).

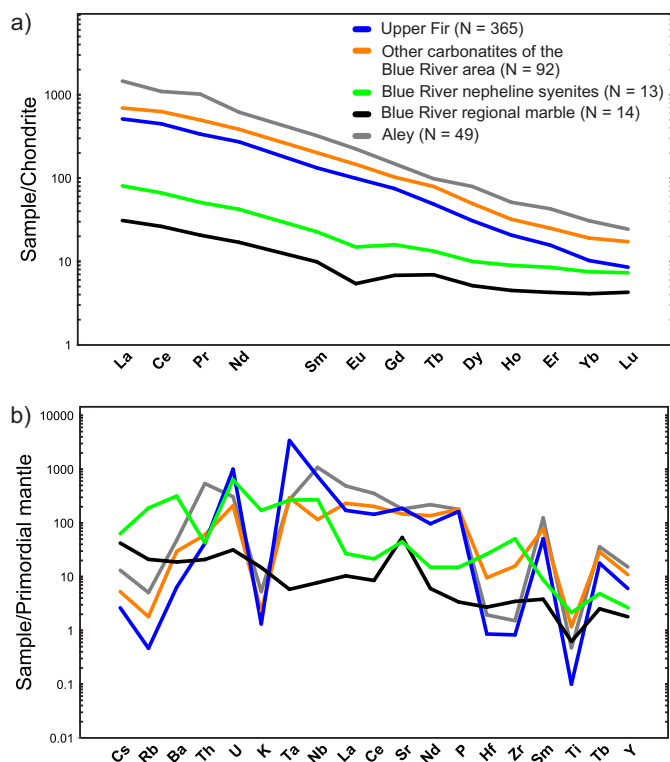


Fig. 27. Median compositions of the Blue River carbonatites, related nepheline syenites, and regional marbles: **a)** Chondrite-normalized rare earth element plot, using normalization of McDonough and Sun (1995). **b)** Primordial mantle-normalized spider diagram, using normalization of Wood et al. (1979). Data from Rukhlov and Gorham (2007), Gorham (2008), and Chudy (2013). Compositions of the Aley carbonatites from Chakhmouradian et al. (2015).

6.6 Geochronology and Sr-Pb-Nd isotopes

Summarizing radiometric dates from the Blue River carbonatites and related rocks, Pell (1994) interpreted that determinations of ca. 360 to ca. 325 Ma from the Verity and Mud Lake carbonatites and the Paradise Lake nepheline syenite represent magmatic crystallization ages. Similar dates were obtained by Rukhlov and Bell (2010) from the Verity dolomite carbonatite (ca. 350 Ma, $^{207}\text{Pb}/^{206}\text{Pb}$ zircon), and by Millonig et al. (2012, 2013) from the Serpentine Creek carbonatite (341 Ma, U-Th-Pb zircon). Millonig et al. (2012, 2013) also reported much older dates of ca. 498 Ma on zircon from the Felix carbonatite and ca. 496 Ma on baddeleyite from the Little Chicago carbonatite, which record the Cambrian pulse of carbonatite activity in western Laurentia (Millonig and Groat, 2013). Zircons from the Gum Creek and Howard Creek carbonatites have extremely low U and Th contents and failed to yield reliable U-Pb dates, but high Th-U zircons from the Felix carbonatite yielded a date of 524 ± 4 Ma (Mitchell et al., 2017), broadly consistent with the 498 ± 2 Ma age of Millonig et al. (2012). Titanites from the Howard Creek nepheline syenites also have very low U and a high common Pb resulting in variable U-Pb dates that indicate considerable disturbance of the U-Th-Pb systems (Mitchell et al., 2017). However, regressing a subset of the titanite data showing the least Pb loss, anchored to

a model common $^{207}\text{Pb}/^{206}\text{Pb}$ ratio (Stacey and Kramers, 1975), on the U-Pb concordia diagram still gives a date of 363 ± 9 Ma, in agreement with the Late Paleozoic Cordilleran carbonatite emplacement ages (Mitchell et al., 2017).

In contrast, much younger K/Ar dates on phlogopite and amphiboles and U-Th-Pb dates on pyrochlore, monazite, zirconolite, and zircon (ca. 205–49 Ma) from the Blue River carbonatites overlap K/Ar mica and hornblende cooling ages and U-Pb zircon, monazite and xenotime ages from the country metamorphic rocks and syntectonic granites (171–46 Ma; see Pell 1994; Rukhlov and Bell, 2010; Millonig et al. 2012, 2013; Gervais and Hynes, 2013; Mitchell et al., 2017). These data reflect open system behaviour and substantial resetting of the K/Ar and U-Th-Pb systems in primary carbonatite minerals during multiple episodes of metamorphism (e.g., Digel et al., 1998; Crowley et al., 2000; Ghent and Villeneuve, 2006; Gervais and Hynes, 2013). The young U-Th-Pb dates on zircon, pyrochlore, monazite, and zirconolite from the Blue River carbonatites are best explained by episodic Pb loss during amphibolite-facies metamorphism rather than by continuous diffusion (Rukhlov and Bell, 2010; Millonig et al., 2012, 2013; Mitchell et al., 2017).

Zircons from the Upper Fir carbonatite were analyzed in situ for U-Pb geochronology (Commerce Resources Corp. pers. comm.) using laser ablation, multi-collector inductively coupled plasma mass spectrometry (LA-MC-ICP-MS). Analyses (Table 2, Fig. 28) and data reduction were by A. Simonetti at the University of Alberta; the analytical method is described in Simonetti et al. (2005). Due to the relatively young age and the low Pb and U contents of the zircons, most analyses used a relatively large laser spot (~ 80 μm) instead of usual ~ 40 μm spot. Two results using a 40 μm spot are consistent with those obtained from the 80 μm analyses. The 21 analyses show variable degrees of Pb loss and yield a weighted average $^{207}\text{Pb}/^{206}\text{Pb}$ date of 332.5 ± 5.7 Ma (2σ), interpreted to establish the time of magmatic crystallization, and consistent with results from other Late Paleozoic carbonatites in the area.

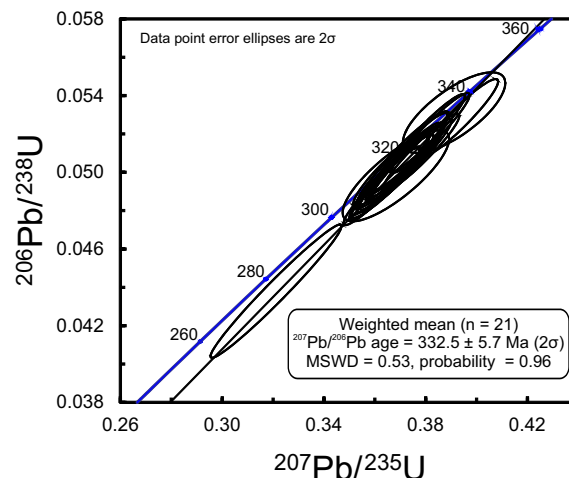


Fig. 28. Concordia $^{207}\text{Pb}/^{235}\text{U}$ vs. $^{206}\text{Pb}/^{238}\text{U}$ diagram for zircons from the Upper Fir carbonatite. The calculated weighted mean $^{207}\text{Pb}/^{206}\text{Pb}$ date of 332.5 ± 5.7 Ma (2σ) establishes the crystallization age.

Table 2. In situ U-Pb analyses on zircons from the Upper Fir carbonatite by laser ablation, multi-collector inductively coupled plasma mass spectrometry, obtained by A. Simonetti at the University of Alberta (Commerce Resource Corp., pers. comm.).

Grain	Spot size (µm)	^{206}Pb cps ⁻¹	$^{206}\text{Pb}/^{204}\text{Pb}$	$^{207}\text{Pb}/^{206}\text{Pb}$	2σ	$^{207}\text{Pb}/^{235}\text{U}$	2σ	$^{206}\text{Pb}/^{238}\text{U}$	2σ	rho	$^{207}\text{Pb}/^{206}\text{Pb}$		$^{206}\text{Pb}/^{238}\text{U}$		% discordance
											Age (Ma)	2σ	Age (Ma)	2σ	
1	40	83992	infinite	0.05315	0.00063	0.3671	0.0133	0.0498	0.0018	0.946	335	27	313	11	6.5
2	40	74043	infinite	0.05325	0.00067	0.3700	0.0140	0.0502	0.0019	0.943	340	29	316	12	7.0
3	80	266514	infinite	0.05362	0.00060	0.3932	0.0125	0.0528	0.0017	0.939	355	25	332	10	6.6
4	80	318560	6371	0.05329	0.00145	0.3683	0.0171	0.0498	0.0019	0.810	341	62	313	12	8.2
5	80	55691	11138	0.05347	0.00153	0.3912	0.0164	0.0531	0.0017	0.733	349	65	334	11	4.3
6	80	207733	infinite	0.05310	0.00058	0.3712	0.0121	0.0504	0.0016	0.943	333	25	317	10	4.8
7	80	136502	infinite	0.05276	0.00073	0.3212	0.0211	0.0438	0.0028	0.977	319	32	276	18	13.3
8	80	396317	infinite	0.05334	0.00057	0.3781	0.0124	0.0510	0.0017	0.946	343	24	321	10	6.6
9	80	154123	infinite	0.05304	0.00059	0.3672	0.0116	0.0502	0.0016	0.938	331	25	316	10	4.5
10	80	494479	infinite	0.05312	0.00056	0.3719	0.0120	0.0504	0.0016	0.948	334	24	317	10	5.0
11	80	162296	infinite	0.05281	0.00057	0.3658	0.0123	0.0498	0.0017	0.949	321	24	313	10	2.3
12	80	444894	infinite	0.05309	0.00056	0.3626	0.0122	0.0493	0.0016	0.950	333	24	310	10	6.9
13	80	180088	infinite	0.05296	0.00057	0.3720	0.0117	0.0506	0.0016	0.940	327	25	318	10	2.7
14	80	296279	infinite	0.05314	0.00057	0.3684	0.0119	0.0500	0.0016	0.944	335	24	315	10	6.0
15	80	292390	infinite	0.05308	0.00055	0.3820	0.0125	0.0521	0.0017	0.950	332	23	327	11	1.5
16	80	63212	infinite	0.05281	0.00075	0.3664	0.0123	0.0501	0.0016	0.907	321	32	315	10	1.8
17	80	499319	infinite	0.05306	0.00057	0.3642	0.0116	0.0494	0.0016	0.941	331	25	311	10	6.1
18	80	78756	infinite	0.05266	0.00068	0.3729	0.0132	0.0510	0.0018	0.932	314	29	321	11	-2.1
19	80	366099	infinite	0.05338	0.00057	0.3741	0.0131	0.0506	0.0018	0.953	345	24	318	11	7.7
20	80	478962	infinite	0.05303	0.00056	0.3738	0.0121	0.0511	0.0016	0.946	330	24	321	10	2.7
21	80	343648	infinite	0.05286	0.00055	0.3805	0.0122	0.0520	0.0017	0.947	323	24	327	10	-1.3

T counts per second.

The British Columbia alkaline province has only sparse Sr-Nd isotopic data (Rich and Gower, 1968; Mumford, 2009; Tappe and Simonetti, 2013; Mitchell et al., 2017). Rukhlov et al. (2018) analyzed separated calcite, dolomite, and apatite fractions from 21 carbonatite and related rocks that were sampled at nine 360-330 Ma complexes in the Blue River area for Pb, Sr, and Nd isotopic compositions. The analysis was performed at the University of British Columbia and used thermal ionization mass spectrometry for Sr and solution MC-ICP-MS for Pb and Nd. Concentrations of Rb, Sr, Nd, Sm, Pb, Th and U were determined by high-resolution ICP-MS on the same dissolution. In addition, molybdenite from a coarse-grained ferrikatophorite-apatite-dolomite carbonatite at the Upper Fir (sample 16-ARU-198; Table 1; Fig. 3) was analyzed for Pb isotopic composition by MC-ICP-MS, along with Pb, Th and U concentrations by ICP-MS, and for Re/Os model age determination by negative thermal ionization mass spectrometry at the University of Alberta. The molybdenite has 14 ppm ^{187}Re and 42 ppb ^{187}Os , shows no common Os above blank levels, and is probably strongly decoupled with respect to Re and Os (Rukhlov et al., unpublished).

Initial $^{87}\text{Sr}/^{86}\text{Sr}$ ratios (0.702875 - 0.704589) and the $\epsilon_{\text{Nd}}(\text{T})$ values (-0.7 to 6.3; Fig. 29) for calcite, dolomite, and apatite fractions from the Blue River carbonatites and related rocks overlap the in situ data from apatites from the Blue River carbonatites obtained by Mitchell et al. (2017). The Upper Fir carbonatites have the lowest initial $^{87}\text{Sr}/^{86}\text{Sr}$ ratios (0.702902 - 0.702963) and the highest $\epsilon_{\text{Nd}}(\text{T})$ values (5.64 to 6.28) compared to other carbonatites and related rocks in the Blue River area, indicating a depleted mantle source similar to FOZO. Calcite from the Gum Creek carbonatite has the lowest $\epsilon_{\text{Nd}}(\text{T})$ value of -0.7 and a higher initial $^{87}\text{Sr}/^{86}\text{Sr}$ ratio of 0.704084 relative to most of the data from the Blue River carbonatites and related rocks. The data define a mixing array between the depleted end-member (FOZO) and the enriched end-member (EM1) in the Sr-Nd isotopic correlation diagram, similar to the mixing trends for the 370 Ma Kola alkaline province, East African carbonatites and most other <200 Ma carbonatites worldwide (Fig. 29). However, calcites from the Paradise Lake nepheline syenite and from the Switch Creek silicocarbonatite (containing abundant olivine, phlogopite, and zirconolite) have slightly higher initial $^{87}\text{Sr}/^{86}\text{Sr}$ ratios (0.704357 - 0.704589) at $\epsilon_{\text{Nd}}(\text{T})$ values of ca. +4, indicating involvement of a third mantle component with relatively high time-integrated Rb/Sr and moderately superchondritic (depleted) time-integrated Sm/Nd.

Despite the very low U/Pb ratios (<0.08) in all samples, the Pb isotopic compositions of apatites, carbonates, and molybdenite from the Blue River carbonatites and related rocks show an extreme range of values ($^{206}\text{Pb}/^{204}\text{Pb}_{\text{initial}} = 19.24\text{--}238.57$, $^{207}\text{Pb}/^{204}\text{Pb}_{\text{initial}} = 15.65\text{--}24.42$, $^{208}\text{Pb}/^{204}\text{Pb}_{\text{initial}} = 34.39\text{--}114.23$). They define a line on the $^{206}\text{Pb}/^{204}\text{Pb}$ vs. $^{207}\text{Pb}/^{204}\text{Pb}$ diagram, yielding a Pb-Pb isochron date (using robust regression) of 324 ± 40 Ma (Fig. 29a) consistent with the emplacement ages of the Upper Fir and other late Paleozoic carbonatites in the Blue

River area. The extremely radiogenic Pb isotopic compositions of the low-U molybdenite, carbonates and apatite from the

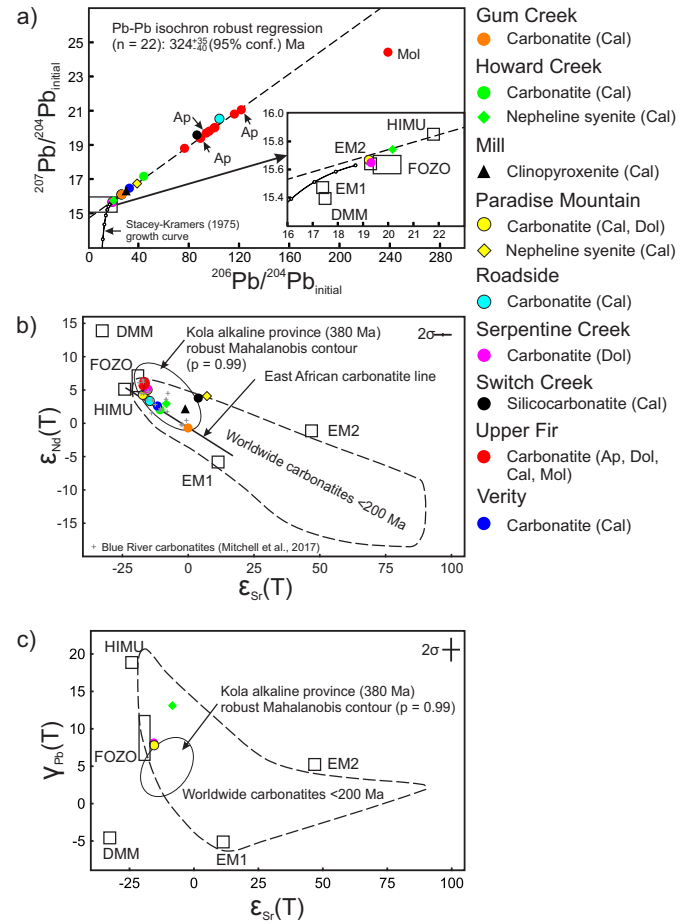


Fig. 29. Sr-Pb-Nd isotope correlation diagrams for the 360-330 Ma carbonatites and related rocks of the Blue River area (after Rukhlov et al., 2018). **a)** Initial $^{206}\text{Pb}/^{204}\text{Pb}$ vs. initial $^{207}\text{Pb}/^{204}\text{Pb}$ for separated calcite (Cal), dolomite (Dol), apatite (Ap) and molybdenite (Mol) fractions (U/Pb < 0.08 in all samples); 2σ error bars are less than the symbol size. **b)** $\epsilon_{\text{Nd}}(\text{T})$ vs. $\epsilon_{\text{Sr}}(\text{T})$ for separated calcite, dolomite, and apatite fractions. East African carbonatite line after Bell and Blenkinsop (1987b). Compiled data from the Blue River carbonatites from Mitchell et al. (2017). **c)** $\epsilon_{\text{Sr}}(\text{T})$ vs. $\gamma_{\text{Pb}}(\text{T})$ for separated calcite and dolomite fractions with the lowest initial $^{206}\text{Pb}/^{204}\text{Pb}$ ratios. $\epsilon_{\text{Sr}}(\text{T}) = [(^{87}\text{Sr}/^{86}\text{Sr}_{\text{sample}} / ^{87}\text{Sr}/^{86}\text{Sr}_{\text{BE}}) - 1] \cdot 10^4$, where $^{87}\text{Sr}/^{86}\text{Sr}_{\text{sample}}$ is the initial ratio in the sample and $^{87}\text{Sr}/^{86}\text{Sr}_{\text{BE}}$ is the ratio in the bulk Earth (after DePaolo and Wasserburg, 1976) at that time; $\gamma_{\text{Pb}}(\text{T}) = [(^{206}\text{Pb}/^{204}\text{Pb}_{\text{sample}} / ^{206}\text{Pb}/^{204}\text{Pb}_{\text{BSE}}) - 1] \cdot 10^2$, where $^{206}\text{Pb}/^{204}\text{Pb}_{\text{sample}}$ is the initial ratio in the sample and $^{206}\text{Pb}/^{204}\text{Pb}_{\text{BSE}}$ is the ratio in the bulk silicate Earth (BSE; after Allègre and Lewin, 1989) at that time; $\epsilon_{\text{Nd}}(\text{T}) = [(^{143}\text{Nd}/^{144}\text{Nd}_{\text{sample}} / ^{143}\text{Nd}/^{144}\text{Nd}_{\text{CHUR}}) - 1] \cdot 10^4$, where $^{143}\text{Nd}/^{144}\text{Nd}_{\text{sample}}$ is the initial ratio in the sample and $^{143}\text{Nd}/^{144}\text{Nd}_{\text{CHUR}}$ is the ratio in the chondritic uniform reservoir (CHUR; after Jacobsen and Wasserburg, 1980; Hamilton et al., 1983) at that time. Depleted MORB mantle (DMM), enriched mantle 1 and 2 (EM1 and EM2), 'FOCUS ZONE' (FOZO), and high- $^{238}\text{U}/^{204}\text{Pb}$ or μ (HIMU) mantle components after Hart et al. (1992), Stracke et al. (2005), and Stracke (2012). Fields for the Kola alkaline province and the <200 Ma worldwide carbonatites from Rukhlov et al. (2015) and references therein.

Upper Fir carbonatites reflect various proportions of radiogenic Pb sequestered from coexisting U-rich pyrochlore during metamorphism, constrained by the molybdenite Re/Os model age of 175.2 ± 0.8 (2 σ) Ma (Rukhlov et al., 2018).

In the Sr-Pb-Nd isotopic correlation diagrams using the lowest initial $^{206}\text{Pb}/^{204}\text{Pb}$, the Blue River carbonatites and related rocks follow the mixing trend involving FOZO and EM1 mantle end-members found in oceanic island basalts, young (<200 Ma) carbonatites worldwide, and the plume-related Kola alkaline province (370 Ma; for an overview, see Rukhlov et al., 2015 and references therein). Thus, despite protracted deformation and upper amphibolite-facies metamorphism, the Blue River carbonatites are isotopically indistinguishable from worldwide carbonatites generated by deep-mantle plumes (Mitchell et al., 2017; Rukhlov et al., 2018).

6.7 Stable isotopes

The C and O isotopic compositions of separated calcite and dolomite fractions ($\delta^{13}\text{C} = -5.5$ to -2.2 ‰ VPDB, $\delta^{18}\text{O} = 4.0$ to 9.3 ‰ VSMOW) are within the range of mantle values (e.g., Deines, 1989, 2002), scattering from the field of ‘primary (unaltered) carbonatite’ of Taylor et al. (1967) towards lighter $\delta^{13}\text{C}$ and $\delta^{18}\text{O}$ values. Regional marbles in the Blue River area have much heavier $\delta^{13}\text{C}_{\text{VSMOW}}$ values (-0.15 to 6.55) and $\delta^{18}\text{O}_{\text{VSMOW}}$ values (14.52 to 20.47), typical of continental crust. We do not think that the scattering of the C-O data from the Blue River carbonatites and alkaline rocks reflects seawater influence. Instead, the scatter possibly indicates a ^{13}C -heterogeneous mantle source coupled with high-temperature alteration during metamorphism (Fig. 30a). Most of the coexisting dolomite-calcite pairs indicate isotopic disequilibrium for both $\delta^{13}\text{C}$ and

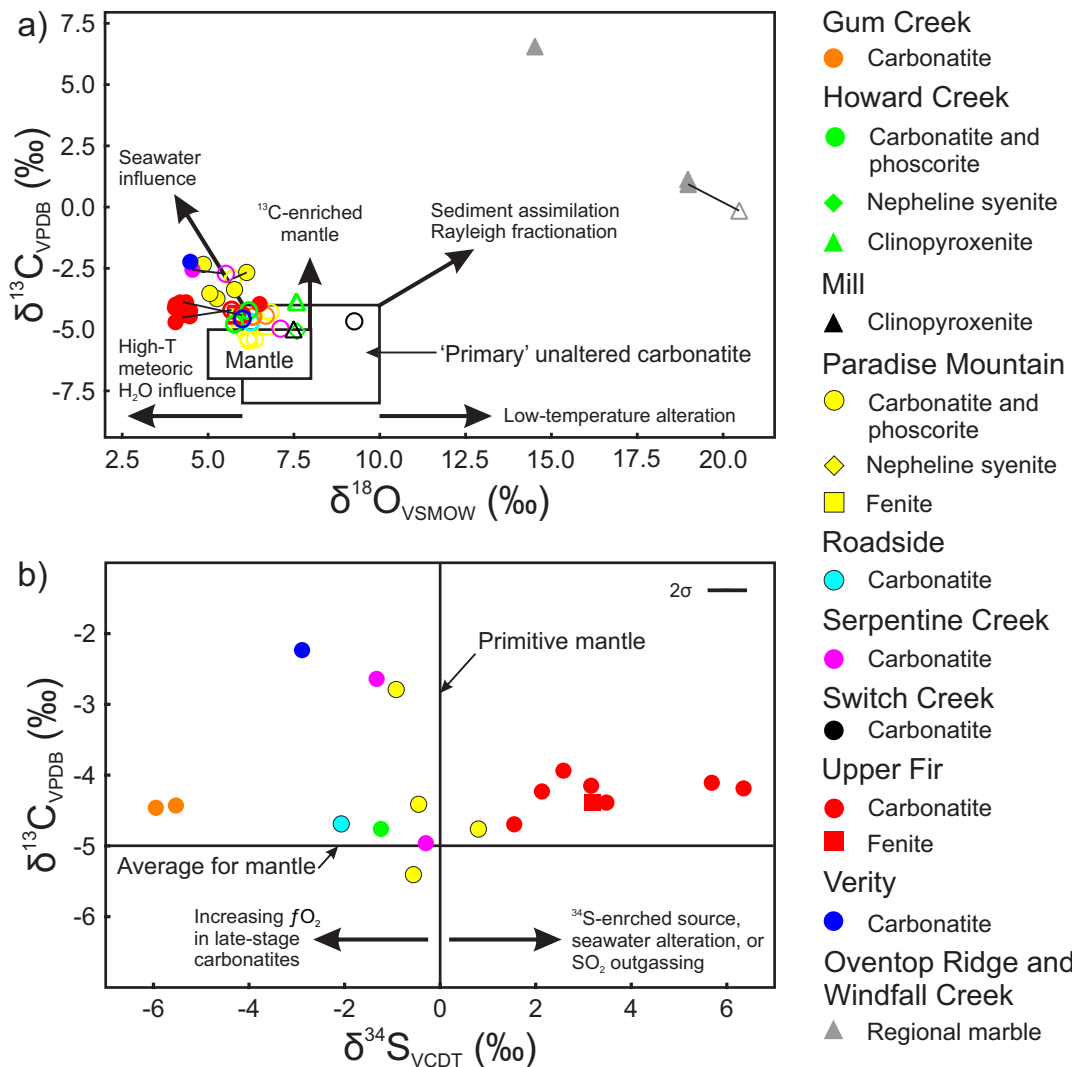


Fig. 30. Stable isotope diagrams for the Blue River carbonatites, related rocks, and regional marbles (after Rukhlov et al., 2018). **a)** $\delta^{18}\text{O}_{\text{VSMOW}}$ (‰) vs $\delta^{13}\text{C}_{\text{VPDB}}$ (‰) for separated calcite (open symbols) and dolomite (filled symbols) fractions, with ties shown for coexisting phases; 2 σ error bars are less than the symbol size. Arrows indicate processes causing shifts in $\delta^{18}\text{O}$ and $\delta^{13}\text{C}$ (after Demény et al., 2004 and references therein). ‘Primary’ unaltered carbonatite field after Taylor et al. (1967) and mantle field after Deines (1989). **b)** $\delta^{34}\text{S}_{\text{VCDT}}$ (‰) vs $\delta^{13}\text{C}_{\text{VPDB}}$ (‰) for separated, coexisting pyrrhotite and molybdenite ($\delta^{34}\text{S}$ data) and calcite and/or dolomite ($\delta^{13}\text{C}$ data). Arrows indicate processes causing shifts in $\delta^{34}\text{S}$ after Deines (1989) and Rollinson (1993). Average $\delta^{13}\text{C}$ value for mantle after (Deines, 2002) and assumed $\delta^{34}\text{S}$ value for primitive mantle after Hoefs (2009).

$\delta^{18}\text{O}$, consistent with recrystallization and consequent open-system behaviour during metamorphism as recorded by the Pb isotopic data. The C-O isotopic data from the Blue River carbonatite show little fractionation of the parental carbonatite magmas and clearly rule out any assimilation of crustal materials, consistent with the Sr-Nd-Pb isotopic evidence discussed above. In contrast to the whole-rock geochemical composition, the C-O isotopic compositions from the Upper Fir carbonatites do not show systematic variations related to the mineralogical facies (Chudy, unpublished).

The range of S isotopic compositions of separated pyrrhotite and molybdenite fractions from the Blue River carbonatites and related rocks ($\delta^{34}\text{S} = -6.0$ to 6.5 ‰ CDT) encompasses both heavier and lighter values than that of assumed primitive mantle (e.g., Hoefs, 2009), similar to the range of $\delta^{34}\text{S}$ values in carbonatites from the Canadian Shield (Farrell et al., 2010) and from the Kola alkaline province (Bell et al., 2015). All $\delta^{34}\text{S}$ values for pyrrhotite and molybdenite from the Upper Fir are heavier than assumed primitive mantle (1.55–6.47 ‰ CDT), with the molybdenite having $\delta^{34}\text{S}_{\text{CDT}}$ value of 2.41, slightly heavier than that of the coexisting pyrrhotite (1.55). Considering their depleted Sr and Nd isotopic compositions, crustal contamination is an unlikely cause for the heavy S isotopic composition of the Ta-rich Upper Fir carbonatites, which instead perhaps reflect ^{34}S -enriched source or SO_2 degassing during their emplacement. On the other hand, the very light S isotopic compositions ($\delta^{34}\text{S}$) of pyrrhotite from the Sr- and REE-rich Gum Creek calcite carbonatites (–6.00 to –5.40 ‰ CDT), probably reflect fractionation of the carbonatite magma accompanied by the increasing $f\text{O}_2$ (Deines, 1989; Rollinson, 1993; Farrell et al., 2010; Bell et al., 2015).

The stable isotope data indicate that the Blue River carbonatites and related silica-undersaturated rocks retained their primary mantle signature despite high-grade metamorphism and retrograde shearing, which contrasts with data from many carbonatites worldwide (e.g., Demény et al., 2004), including Cordilleran carbonatites such as the Aley (Chakhmouradian et al., 2015) and the Wiccheeda Lake (Trofanenko et al., 2016).

7. Petrogenetic summary

7.1 Geothermobarometry

The Blue River carbonatites and related rocks show a range of temperatures inferred from chemical or oxygen isotope equilibrium between coexisting minerals (Figs. 31 and 32). Chudy (2013) used the calcite-dolomite solvus in the ternary CaCO_3 – MgCO_3 – FeCO_3 system after Anovitz and Essene (1987) to estimate crystallization temperatures of the Upper Fir carbonatites. The highest temperatures preserved by calcite, considered to represent magmatic crystallization temperature, were at least 50°C above those reached during metamorphism in the Blue River area (up to $\sim 700^\circ\text{C}$; e.g., Digel et al., 1998; Ghent and Villeneuve, 2006). Distinctly lower temperatures (below 450°C) were attributed to retrograde overprint (Chudy, 2013). New calcite-dolomite equilibrium data from 9 carbonatite complexes in the Blue River area obtained by Rukhlov et al. (2018) are consistent with these findings (Fig. 31). The carbonate solvus data generally show more restricted range of temperatures compared with those based on Fe-Ti equilibrium between coexisting magnetite – ilmenite solid solution series after Andersen and Lindsley (1985). Calcite from regional marble in this study yielded equilibrium temperatures of 561 – 626°C or 667 – 709°C with reintegrated 5 vol.% dolomite

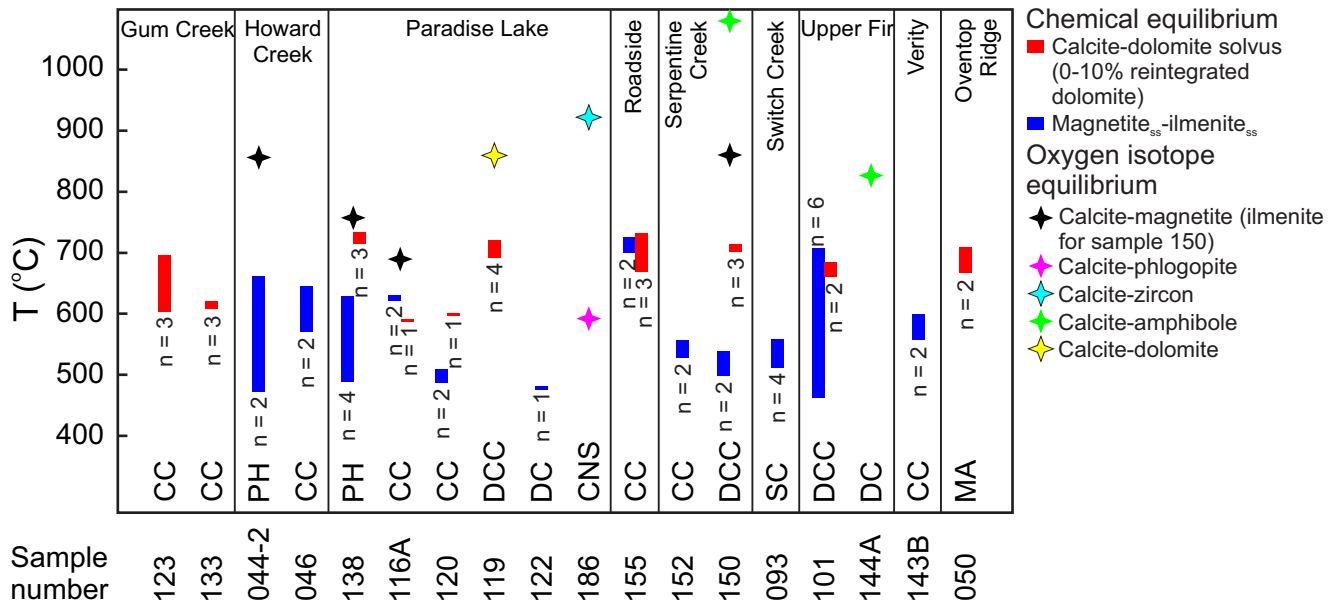


Fig. 31. Summary of the geothermometry for the Blue River carbonatites, related rocks, and regional marbles (after Rukhlov et al., 2018), based on calcite-dolomite solvus, assuming 0–10 vol % reintegrated dolomite (after Anovitz and Essene, 1987), magnetite-ilmenite solid solutions (after Andersen and Lindsley, 1985), and oxygen isotope equilibrium between the co-existing mineral pairs (after Chacko et al., 2001; Valley, 2003). Abbreviations: CC = calcite-carbonatite, CNS = calcite-nepheline syenite, DC = dolomite-carbonatite, DCC = dolomite-calcite carbonatite, MA = regional marble, PH = phoscorite, SC = silicocarbonatite.

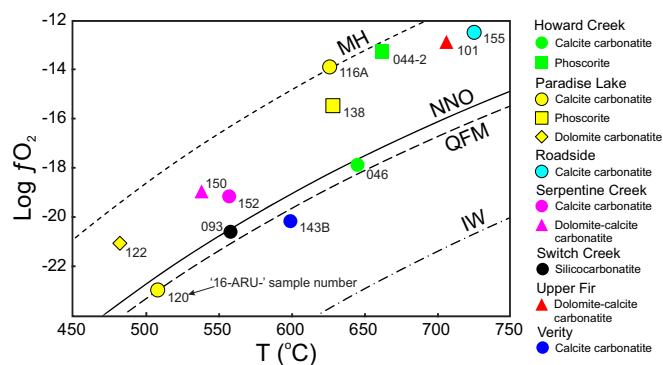


Fig. 32. Summary of the maximum T (°C) vs Log fO_2 estimates for the Blue River carbonatites and phoscorites (after Rukhlov et al., 2018), based on the magnetite-ilmenite geothermobarometer after Andersen and Lindsley (1985). Solid buffers after Frost (1991).

exsolution lamellae, which straddle the maximum calcite-dolomite and magnetite-ilmenite temperature estimates from the Blue River carbonatites (Fig. 31). In contrast, the oxygen isotope equilibrium temperatures for dolomite, magnetite, ilmenite, zircon, and amphiboles coexisting with calcite, using fractionation factors after Chacko et al. (2001) and Valley (2003) yield values between 689–1079 °C, which are clearly much higher than the regional metamorphic temperatures and hence reflect crystallization temperatures of relatively hot, oxidized ($\Delta QFM = -0.5$ to $+5$) magmas (Figs. 31 and 32). The oxygen isotope equilibrium temperature for coexisting calcite-phlogopite pair from the Paradise Lake nepheline syenite (592 °C) is 330 °C lower than that for coexisting zircon-calcite pair from the same sample, and thus records metamorphism.

7.2 Parental magmas and magmatic evolution

Most carbonatites in the Blue River area lack silica-undersaturated rocks such as calcite-rich nepheline syenites, ultramafic, and phoscoritic rocks that are intimately associated with carbonatites at Howard Creek and Paradise Lake (Rich and Gower, 1968; Mariano, 1982; White, 1985; Pell, 1994). This suggests that the Blue River carbonatites could have formed from primary carbonatitic magmas with only a small proportion of silicate, or that rocks that could represent their unevaluated parental magmas (e.g., melilitites to kamafugites) are not exposed (Mitchell, 2015; Mitchell et al., 2017). Although the disaggregated masses of heterogeneous phlogopite-titanite-amphibole-pyroxene ultramafic and phoscorite-like, apatite-olivine-magnetite rocks at Howard Creek could represent cumulates, the magnetite-rich rocks at Upper Fir might have formed from a late-stage ferrocarnatite magma that crystallized at higher temperatures (>700 °C) than that of ankerite or siderite stability (<500 °C; Chudy, 2013; Mitchell et al., 2017).

Primary minerals in the Blue River carbonatites generally crystallized in the following order: Nb-Ta-Zr oxides \pm zircon \pm ilmenite-amphibole-apatite-olivine-pyroxene-magnetite \pm pyrrhotite \pm chalcopyrite \pm molybdenite \pm pyrite \pm phlogopite-dolomite \pm calcite. However, phlogopite could also have

crystallized relatively early, and magnetite, apatite and Nb oxides could have been the last phases to form (Mitchell et al., 2017; Rukhlov et al., 2018). Compositions of amphiboles from the Upper Fir carbonatites show a magmatic evolutionary trend from the Al- and Ti-rich Ca end member towards the Na-Ca and Na end member, which is commonly observed in carbonatites elsewhere (e.g., Hogarth, 1989), but the high F contents distinguish the Upper Fir from most occurrences (Chudy, 2013). The crystallization of magnesio-arfvedsonite and K-richrichterite in some carbonatites of the Blue River area reflects alkali-rich, late-stage fluids that altered earlier amphibole species and were responsible for the fenitization of the country rocks. Compositions of amphiboles in the exocontact fenites are distinct from those of regional amphibolites (Chudy, 2013).

The abundant ferrocolumbite and its paragenesis with pyrochlore supergroup minerals in carbonatites at Upper Fir (Figs. 20 and 22) are the hallmark of this complex (Chudy, 2013; Mitchell, 2015). The Nb/Ta, U, and Ti increase from the early U-Ta-rich pyrochlore towards the later pyrochlore, consistent with the uranpyrochlore evolutionary trend observed in carbonatites elsewhere (e.g., Hogarth, 1989; Lee et al., 2006; Chakhmouradian et al., 2015). However, microlite is clearly related to the metasomatic alteration of the primary ferrocolumbite at Upper Fir (Fig. 22g). Chudy (2013) proposed that such metasomatic alteration could result from recharge of a more evolved (high Nb/Ta, low Na, and possibly high OH/F) carbonatite magma, precipitating ferriwinchite with ferrocolumbite, by the more primitive magma (low Nb/Ta, high Na) crystallizing ferrikatophorite transitional to magnesio-arfvedsonite with the pyrochlore supergroup.

The lack of siderite and hydrothermal Na-, Sr- and REE-bearing (fluoro)carbonates in the Blue River carbonatites suggests that they formed from relatively unevaluated parental magmas, which could be a consequence of their emplacement as small bodies such as sills as opposed to large zoned complexes made up of predominantly alkaline, silica-undersaturated rocks with highly differentiated, late-stage carbonatites (Mitchell et al., 2017). Based on the whole-rock geochemical and the mineralogical evidence, the Upper Fir carbonatites likely formed from a weakly fractionated, primary magnesiocarnatite magma with high Ta, (sub)chondritic Ti, Zr, Hf contents and Nb/Ta ratio, and low REE, Ba and Sr contents, hence the geochemical attributes of its mantle source rather than protracted magmatic evolution (Chudy, 2013).

The distinct mineralogy, whole-rock geochemistry, Sr-Nd-Pb isotopic and trace-element signatures of minerals from individual carbonatite occurrences in the Blue River area rule out their origin from a single parental magma (Mitchell et al., 2017; Rukhlov et al., 2018). Instead, each complex likely represents weakly fractionated, low-volume, low-degree partial melt from isotopically heterogeneous, carbonated mantle peridotite (e.g., Harmer and Gittins, 1998; Wyllie and Lee, 1998; Lee and Wyllie, 2000).

7.3 Isotopic constraints on the mantle source and tectonic implications

The Sr, Nd and Pb isotopic compositions from the ca. 500 Ma and 360-330 Ma carbonatites in the Blue River area (Mitchell et al., 2017; Rukhlov et al., 2018) fit the evolutionary model for the depleted component in the sources of carbonatites worldwide with the present-day Sr-Pb-Nd-Hf isotopic attributes of FOZO, also found in OIBs and considered to represent ancient (>4 Ga), depleted, deep mantle (for an overview, see Rukhlov et al., 2015 and references therein).

Mitchell et al. (2017) noted that the Blue River carbonatites tapped a sub-lithospheric mantle source that is isotopically similar to that of carbonatites from cratonic interiors such as the Canadian Shield (e.g., Bell et al., 1982). Mitchell et al. (2017) also recognized that the compositional similarity of rocks in the British Columbia alkaline province implies partial melting of the same type of depleted mantle during a period of ca. 480 Ma, and suggested that lithospheric extension provided pathways for the low-degree, sub-lithospheric partial melts along reactivated, detachment faults resulting in sill-like intrusions distributed along the length of the continental margin. However, Mitchell et al. (2017) considered that the rocks were unlikely to record a mantle plume because associated flood basalts and large volumes of undersaturated silicate rocks are lacking, because the multiple episodes of carbonatite emplacement span ca. 480 Ma (ca. 810-700 Ma, ca. 500 Ma, ca. 360-330 Ma), and because the geometry of the British Columbia alkaline province defines a long (at least 1,000 km), narrow (ca. 200 km) orogen-parallel belt (Fig. 1), rather than one that could reflect plume-related regional doming.

Here we build on the Mitchell et al.'s (2017) findings and emphasize that the isotopic and elemental compositions of minerals from Blue River carbonatites and related rocks are indistinguishable from worldwide carbonatites generated by deep-mantle plumes (Fig. 29). The Late Paleozoic Cordilleran examples formed along the western margin of Laurentia while subduction was taking place immediately to the west. Lithospheric extension related to this Late Paleozoic subduction is considered responsible for rifting the continental margin and initiating the Slide Mountain ocean as a back-arc basin (e.g., Nelson et al., 2013). We suggest that this same back-arc extension triggered the most prolific pulse of alkaline magmatism in the Cordillera, including emplacement of the Blue River carbonatites, which were derived from a long-lived, deep-level mantle plume that was tapped episodically since the Neoproterozoic. Such a continuous lower-mantle source beneath western Laurentia is in keeping with Cambrian-Ordovician lamprophyres and alkaline rocks (Fig. 1; Pell, 1994; Millonig and Groat, 2013) and with the ca. 780 Ma Gunbarrel LIP, the ca. 725-690 Ma Franklin-Thule and Gataga-Edwardsburg LIPs, and the ca. 570-500 Ma Hamill-Gog and Wichita LIPs (e.g., Ernst, 2014). Interestingly, paleogeographic reconstructions place both Laurentia and Baltica, and hence the plume-generated, 370-330 Ma Kola and Cordilleran alkaline provinces, above the equatorial Jason large low shear wave

velocity province that is considered to be a long-lived plume-generation zone at the core-mantle boundary for hundreds of m.y. (Torsvik et al. 2006; Burke, 2011), with only a few degrees of northward drift during the Paleozoic (e.g., Nelson et al., 2013).

Acknowledgements

This field trip was sponsored by the Mineralogical Association of Canada. Jody Dahrouge, Chris Grove, Mike Hodge, and Jenna Hardy (Commerce Resources Corp.) provided drill-core samples, confidential data, and assistance in the field. We are grateful to G. Fortin (British Columbia Geological Survey) for assisting during the 2017 fieldwork and during the field trip, and to L.J. Millonig for providing photographs and details for some of the carbonatites. We thank L.B. Aspler (British Columbia Geological Survey) for insightful discussions and critical review of an early draft, and for offering that the unusual active-margin setting for the Late Paleozoic carbonatites might be explained in terms of back arc-extension stretching the inboard continental lithosphere and thus triggering carbonatite magmatism by tapping a long-lived mantle plume. We also thank J.R. Chiarenzelli (St. Lawrence University) and S.P. Regan (United States Geological Survey and University of Alaska Fairbanks) for perceptive reviews.

References cited

- Aquist, B.E., 1981. Report on diamond drilling on the AZ-1 claim group, Kamloops Mining Division, N.T.S. 83D/6E. British Columbia Ministry of Energy, Mines and Petroleum Resources, British Columbia Geological Survey, Assessment Report 9923, 7 p., 4 appendices.
- Aquist, B.E., 1982a. Exploration assessment report for 1981 on the carbonatites north of Blue River, British Columbia, N.T.S. 83D/6E. British Columbia Ministry of Energy, Mines and Petroleum Resources, British Columbia Geological Survey, Assessment Report 10274, 30 p., 5 maps (1:100, 1:1,000, 1:4,000 and 1:50,000 scale), 13 cross sections (1:100, 1:400 and 1:500 scale), 6 appendices.
- Aquist, B.E., 1982b. Exploration assessment report for 1982 on three claims north of Blue River, British Columbia, N.T.S. 83D/6E. British Columbia Ministry of Energy, Mines and Petroleum Resources, British Columbia Geological Survey, Assessment Report 10955, 5 p., 2 maps (1:4,000 and 1:200,000 scale), 2 appendices.
- Aquist, B.E., 1982c. Exploration assessment report for 1982 on the carbonatites north of Blue River, British Columbia, N.T.S. 83D/6E. British Columbia Ministry of Energy, Mines and Petroleum Resources, British Columbia Geological Survey, Assessment Report 11130, 15 p., 4 maps (1:4,000, 1:10,000 and 1:200,000 scale), 8 appendices.
- Ahroon, T.A., 1979. Airborne helicopter magnetometer-spectrometer survey on the Blue River carbonatite project, British Columbia, Canada. British Columbia Ministry of Energy, Mines and Petroleum Resources, British Columbia Geological Survey, Assessment Report 8216, 11 p., 6 maps (1:20,000 scale), 1 appendix.
- Ahroon, T.A., 1980. Geologic report on the Blue River project, British Columbia, Canada. British Columbia Ministry of Energy, Mines and Petroleum Resources, British Columbia Geological

- Survey, Assessment Report 9566, 13 p., 5 maps (1:10,000 and 1:20,000 scale), 3 cross sections (1:500 and 1:1,000 scale), 4 appendices.
- Allègre, C.J. and Lewin, E., 1989. Chemical structure and history of the Earth, evidence from global non-linear inversion of isotopic data in a three-box model. *Earth and Planetary Science Letters*, 96, 61-88.
- Andersen, D.J. and Lindsley, D.H., 1985. New (and final!) models for the Ti-magnetite/ilmenite geothermometer and oxygen barometer. In: AGU 1985 spring meeting, Baltimore, United States. American Geophysical Union, Eos Transactions, 66 (18), p. 416.
- Anovitz, L.M. and Essene, E.J., 1987. Phase equilibria in the system $\text{CaCO}_3\text{-MgCO}_3\text{-FeCO}_3$. *Journal of Petrology*, 28, 389-415.
- Atencio, D., Andrade, M.B., Christy, A.G., Gieré, R., and Kartashov, P.M., 2010. The pyrochlore supergroup of minerals: Nomenclature. *Canadian Mineralogist*, 48, 673-698.
- Bakes, J.M., Jeffery, P.G., and Sandor, J., 1964. Pyrochlore minerals as a potential source of reactor-grade niobium. *Nature*, 204, 867-868.
- Bally, A.W., Gordy P.L., and Stewart, G.A., 1966. Structure, seismic data, and orogenic evolution of southern Canadian rocky mountains. *Bulletin of Canadian Petroleum Geology*, 14, 337-381.
- Bell, K., ed., 1989. *Carbonatites: Genesis and Evolution*. Unwin Hyman, London, 618 p.
- Bell, K., 1998. Radiogenic isotope constraints on relationships between carbonatites and associated silicate rocks — a brief review. *Journal of Petrology*, 39, 1987-1996.
- Bell, K., 2001. Carbonatites: Relationships to mantle-plume activity. In: Ernst, R.E. and Buchan, K.L., (Eds.), *Mantle Plumes: Their Identification Through Time*. Geological Society of America, Special Paper 352, pp. 267-290.
- Bell, K., and Blenkinsop, J., 1987a. Neodymium and strontium isotope geochemistry of carbonatites. In: Bell, K. (Ed.), *Carbonatites: Genesis and Evolution*. Unwin Hyman, London, pp. 278-299.
- Bell, K., and Blenkinsop, J., 1987b. Nd and Sr isotopic compositions of East African carbonatites: implications for mantle heterogeneity. *Geology*, 15, 99-102.
- Bell, K. and Keller, J., eds., 1995. *Carbonatite Volcanism: Oldoinyo Lengai and the Petrogenesis of Natrocarbonatites*. IAVECI Proceeding in Volcanology 4, 210 p.
- Bell, K., and Rukhlov, A.S., 2004. Carbonatites from the Kola Alkaline Province: origin, evolution and source characteristics. In: Wall, F., and Zaitsev, A.N., (Eds.), *Phoscorites and Carbonatites from Mantle to Mine: The Key Example of the Kola Alkaline Province*. Mineralogical Society Series, 10, The Mineralogical Society, London, United Kingdom, pp. 433-468.
- Bell, K. and Simonetti, A., 1996. Carbonatite magmatism and plume activity: implications from the Nd, Pb and Sr isotope systematics of Oldoinyo Lengai. *Journal of Petrology*, 37, 1321-1339.
- Bell, K. and Simonetti, A., 2010. Source of parental melts to carbonatites – critical isotope constraints. *Mineralogy and Petrology*, 98, 77-89.
- Bell, K. and Tilton, G.R., 2001. Nd, Pb and Sr isotopic compositions of East African carbonatites: evidence for mantle mixing and plume inhomogeneity. *Journal of Petrology*, 42, 1927-1945.
- Bell, K., and Tilton, G.R., 2002. Probing the mantle: the story from carbonatites. *American Geophysical Union, Eos Transactions*, 83 (273), 276-277.
- Bell, K., Blenkinsop, J., Cole, T.S.J., and Menagh, D.P., 1982. Evidence from Sr isotopes for longlived heterogeneities in the upper mantle. *Nature*, 298, 251-253.
- Bell, K., Kjarsgaard, B.A., and Simonetti, A., 1998. Carbonatites—into the twenty-first century. *Journal of Petrology*, 39 (11-12), 1839-1845.
- Bell, K., Zaitsev, A.N., Spratt, J., Fröjdo, S., and Rukhlov, A.S., 2015. Elemental, lead and sulfur isotopic compositions of galena from Kola carbonatites, Russia: implications for melt and mantle evolution. *Mineralogical Magazine*, 79, 219-241.
- Biondi, J.C., 2005. Brazilian mineral deposits associated with alkaline and alkaline-carbonatite complexes. In: Comin-Chiaromonti, P. and Gomes, C.B., (Eds.), *Mesozoic to Cenozoic Alkaline Magmatism in the Brazilian Platform*. Editora da Universidade de São Paulo: Fapesp, São Paulo, pp. 707-750.
- Bizzarro, M., Simonetti, A., Stevenson, R.K., and David, J., 2002. Hf isotope evidence for a hidden mantle reservoir. *Geology*, 30, 771-774.
- Bond, G.C. and Kominz, M.A., 1984. Construction of tectonic subsidence curves for the Early Paleozoic miogeocline, southern Canadian Rocky Mountains: implications for subsidence mechanisms, age of breakup, and crustal thinning. *The Geological Society of America Bulletin*, 95 (2), 155-173.
- Bowen, N.L., 1924. The Fen area in Telemark, Norway. *American Journal of Science*, 8, 1-11.
- Boynton, W.V., 1984. Geochemistry of the rare earth elements: Meteorite studies. In: Henderson, P., (Ed.), *Rare Earth Element Geochemistry*. Elsevier, New York, pp. 63-114.
- Brøgger, W.C., 1921. *Die Eruptivgesteine des Kristianiagebietes*. IV. Das Fengebiet in Telemark, Norwegen. Norsk Videnskapselskapets Skrifter, I. Matematisk-naturvidenskabelig klasse, 1920, 9, 408 p.
- Burke, K., 2011. Plate tectonics, the Wilson cycle, and mantle plumes: Geodynamics from the top. *The Annual Review of Earth and Planetary Sciences*, 39, 1-29.
- Burt, D.M., 1989. Compositional and phase relations among rare earth element minerals, Chapter 10. In: Lipin, B.R., and McKay, G.A. (Eds.), *Geochemistry and Mineralogy of Rare Earth Elements*. Mineralogical Society of America, Reviews in Mineralogy, 21, pp. 259-307.
- Campbell, R.B., 1968. *Geology, Canoe River, British Columbia*. Geological Survey of Canada, Preliminary Map 15-1967, 1:253,400 scale.
- Campbell, I.H. and O'Neill, H.St.C., 2012. Evidence against a chondritic Earth. *Nature*, 483, 553-558.
- Cannings, S., Nelson, J.L., and Cannings, R., 2011. *Geology of British Columbia, A Journey through Time* (new edition). Greystone Books Ltd., Vancouver, Berkley, 154 p.
- Carr, S.D., 1992. Tectonic setting and U-Pb geochronology of the early Tertiary Ladybird leucogranite suite, Thor-Odin-Pinnacles area, southern Omineca belt, British Columbia. *Tectonics* 11, 258-278.
- Cecile, M.P., Morrow, D.W. and Williams, G.K., 1997. Early Paleozoic (Cambrian to Early Devonian) tectonic framework, Canadian Cordillera. *Bulletin of Canadian Petroleum Geology*, 45, 54-74.
- Černý P. and Ercit, T.S., 2005. The classification of granitic pegmatites revisited. *The Canadian Mineralogist*, 43, 2005-2026.
- Černý P., Goad, B.E., Hawthorne, F.C., and Chapman, R., 1986. Fractionation trends of the Nb- and Ta-bearing oxide minerals in the Greer Lake pegmatitic granite and its pegmatite aureole, southeastern Manitoba. *American Mineralogist*, 71, 501-517.
- Chakhmouradian, A.R., 2006. High-field-strength elements in

- carbonatitic rocks: geochemistry, crystal chemistry and significance for constraining the sources of carbonatites. *Chemical Geology*, 235, 138-160.
- Chakhmouradian, A.R., and Zaitsev, A.N., 2012. Rare earth mineralization in igneous rocks: sources and processes. *Elements*, 8, 347-353.
- Chakhmouradian, A.R., Reguir, E.P., Kressall, R.D., Crozier, J., Pisiak, L.K., Sidhu, R., and Yang, P., 2015. Carbonatite-hosted niobium deposit at Aley, northern British Columbia (Canada): Mineralogy, geochemistry and petrogenesis. *Ore Geology Reviews*, 64, 642-666.
- Chakhmouradian, A.R., Reguir, E.P., and Zaitsev, A.N., 2016a. Calcite and dolomite in intrusive carbonatites. I. Textural variations. *Mineralogy and Petrology*, 110, 333-360.
- Chakhmouradian, A.R., Reguir, E.P., Couëslan, C., and Yang, P., 2016b. Calcite and dolomite in intrusive carbonatites. II. Trace-element variations. *Mineralogy and Petrology*, 110, 361-377.
- Chakhmouradian, A.R., Reguir, E.P., Zaitsev, A.N., Couëslan, C., Xu, C., Kynický, J., Mumin, A., and Yang, P., 2017. Apatite in carbonatitic rocks: Compositional variation, zoning, element partitioning and petrogenetic significance. *Lithos*, 274-275, 188-213.
- Chacko, T., Cole, D.R., and Horita, J., 2001. Equilibrium oxygen, hydrogen and carbon isotope fractionation factors applicable to geologic systems. In: Valley, J.W. and Cole, D., (Eds.), *Stable Isotope Geochemistry*. Mineralogical Society of America, Geochemical Society, Reviews in Mineralogy and Geochemistry, 43, pp. 1-82.
- Chen, W. and Simonetti, A., 2015. Isotopic (Pb, Sr, Nd, C, O) evidence for plume-related sampling of an ancient, depleted mantle reservoir. *Lithos*, 216-217, 81-92.
- Chudy, T.C., 2013. The petrogenesis of the Ta-bearing Fir carbonatite system, east-central British Columbia, Canada. Unpublished Ph.D. thesis, University of British Columbia, Canada, 316 p., 7 appendices.
- Colpron, M., Logan, J.M., and Mortensen, J.K., 2002. U-Pb zircon age constraint for late Neoproterozoic rifting and initiation of the lower Paleozoic passive margin of western Laurentia. *Canadian Journal of Earth Sciences*, 39, 133-143.
- Crowley, J.L., Ghent, E.D., Carr, S.D., Simony, P.S., and Hamilton, M.A., 2000. Multiple thermotectonic events in a continuous metamorphic sequence, Mica Creek area, southeastern Canadian Cordillera. *Geological Materials Research*, 2, 1-45.
- Currie, K.L. 1975. The geology and petrology of the Ice River Alkaline Complex, British Columbia. *Geological Survey of Canada, Bulletin* 245, 68 p.
- Currie, K.L., 1976. The alkaline rocks of Canada. *Geological Survey of Canada, Bulletin* 239, 228 p.
- Dahrouge, J., 2001a. Commerce Resources Corp. 2000 geologic mapping and sampling on the Fir property, north of Blue River, British Columbia. British Columbia Ministry of Energy and Mines, British Columbia Geological Survey, Assessment Report 26549, 10 p., 1 map (1:10,000 scale), 4 appendices.
- Dahrouge, J., 2001b. Commerce Resources Corp. 2000 geologic mapping and sampling on the Verity property, north of Blue River, British Columbia. British Columbia Ministry of Energy and Mines, British Columbia Geological Survey, Assessment Report 26550, 10 p., 1 map (1:10,000 scale), 4 appendices.
- Dahrouge, J., 2002. The Fir carbonatite: a potential tantalum-niobium resource. In: *Exploration and Mining in British Columbia – 2001, Part B*. British Columbia Ministry of Energy and Mines, pp. 83-88.
- Dahrouge, J. and Reeder, J., 2001. Commerce Resources Corp. 2001 geologic mapping, sampling and geophysical surveys on the Mara property, north of Blue River, British Columbia. British Columbia Ministry of Energy and Mines, British Columbia Geological Survey, Assessment Report 26733, 19 p., 3 maps (1:7,500 scale), 6 appendices.
- Dahrouge, J. and Wolbaum, R., 2004. Commerce Resources Corp. 2003 exploration at the Blue River property, north of Blue River, British Columbia. British Columbia Ministry of Energy and Mines, British Columbia Geological Survey, Assessment Report 27412, 16 p., 6 appendices.
- Daly, R.A., 1933. *Igneous Rocks and the Depths of the Earth*. McGraw-Hill, New York, N.Y., 598 p.
- Dauphas, N., and Marty, B., 1999. Heavy nitrogen in carbonatites of the Kola Peninsula: a possible signature of the deep mantle. *Science*, 286, 2488-2490.
- Davis, C., 2005. Commerce Resources Corp. 2005 diamond drilling and exploration at the Blue River property, north of Blue River, British Columbia. British Columbia Ministry of Energy, Mines and Petroleum Resources, British Columbia Geological Survey, Assessment Report 28104, 13 p., 5 appendices.
- Dawson, G.M. 1886. *Geological and Natural History Survey of Canada, Annual Report* 1, 122B-124B.
- de Ignacio, C., Muñoz, M., Sagredo, J., Fernández-Santín, S., and Johansson, Å., 2006. Isotope geochemistry and FOZO mantle component of the alkaline-carbonatitic association of Fuerteventura, Canary Islands, Spain. *Chemical Geology*, 232, 99-113.
- Deines, P., 1989. Stable isotope variations in carbonatites. In: Bell, K., (Ed.), *Carbonatites – Genesis and Evolution*. Unwin Hyman, London, pp. 301-359.
- Deines, P., 2002. The carbon isotope geochemistry of mantle xenoliths. *Earth-Science Reviews*, 58, 247-278.
- Demény, A., Sitnikova, M.A., and Karchevsky, P.I., 2004. Stable C and O isotope compositions of carbonatite complexes of the Kola alkaline province: phoscorite-carbonatite relationships and source compositions. In: Wall, F. and Zaitsev, A.N., (Eds.), *Phoscorites and Carbonatites from Mantle to Mine: The Key Example of the Kola Alkaline Province*. Mineralogical Society Series, 10, The Mineralogical Society, London, United Kingdom, pp. 407-431.
- DePaolo, D.J., and Wasserburg, G.J., 1976. Inferences about magma sources and mantle structure from variations of $^{143}\text{Nd}/^{144}\text{Nd}$. *Geophysical Research Letters*, 3, 743-746.
- Digel, S.G., Ghent, E.D., and Simony, P.S., 1989. Metamorphism and structure of the Mount Cheadle area, Monashee Mountains, British Columbia. In: *Current Research, Part E*, Geological Survey of Canada, Paper 89-1E, pp. 95-100.
- Digel, S.G., Ghent, E.D., Carr, S.D., and Simony, P.S., 1998. Early Cretaceous kyanite-sillimanite metamorphism and Paleocene sillimanite overprint near Mount Cheadle, southeastern British Columbia: geometry, geochronology, and metamorphic implications. *Canadian Journal of Earth Sciences*, 35, 1070-1087.
- Ernst, R. E., ed., 2014. *Large Igneous Provinces*. Cambridge University Press, Cambridge, England, 653 p.
- Ernst, R.E., and Bell, K., 2010. Large igneous provinces (LIPs) and carbonatites. *Mineralogy and Petrology*, 98, 55-76.
- Evenchick, C.A., McMechan, M.E., McNicoll, V.J., and Carr, S.D., 2007. A synthesis of the Jurassic-Cretaceous tectonic evolution of the central and southeastern Canadian Cordillera: exploring links across the orogen. In: Sears, J.W., Harms, T.A., and Evenchick, C.A., (Eds.), *Whence the Mountains? Inquiries into the Evolution*

- of Orogenic Systems: a Volume in Honor of Raymond A. Price. The Geological Society of America, Special Paper 433, pp. 117-145.
- Fajber, R., Simandl, G.J., and Luck, P., 2015. Exploration for carbonatite-hosted niobium-tantalum deposits using biogeochemical methods (orientation survey), Blue River area, British Columbia, Canada. In: Z. Lasemi, (Ed.), Proceedings of the 47th Forum on the Geology of Industrial Minerals, May 15–17, 2011, Champaign, Illinois. Illinois State Geological Survey, Circular 587, pp. 1-18.
- Farrell, S., Bell, K. and Clark, I., 2010. Sulphur isotopes in carbonatites and associated silicate rocks from the Superior Province, Canada. *Mineralogy and Petrology*, 98, 209-226.
- Gerlach, D.C., Cliff, R.A., Davies, G.R., Norry, M., and Hodgson, N., 1988. Magma sources of the Cape Verdes archipelago: isotopic and trace element constraints. *Geochimica et Cosmochimica Acta*, 52, 2979-2992.
- Gervais, F. and Hynes, A., 2013. Linking metamorphic textures to U–Pb monazite in-situ geochronology to determine the age and nature of aluminosilicate-forming reactions in the northern Monashee Mountains, British Columbia. *Lithos*, 160-161, 250-267.
- Ghent, E. and Villeneuve, M., 2006. ⁴⁰Ar/³⁹Ar dates on hornblende, muscovite, and biotite from the Mica Creek area, British Columbia: regional metamorphic and tectonic implications. *Canadian Journal of Earth Sciences*, 43, 83-100.
- Ghent, E.D., Simony, P.S., Mitchell, W., Perry, J., Robbins, D., and Wagner, J., 1977. Structure and metamorphism in the southeast Canoe River area, British Columbia. In: Report of Activities, Part C, Geological Survey of Canada, Paper 77–1C, pp. 13-17.
- Ghent, E.D., Simony, P.S., Knitter, C.C., 1980. Geometry and pressure-temperature significance of the kyanite–sillimanite isograd in the Mica Creek Area, British Columbia. *Contributions to Mineralogy and Petrology*, 74, 67-73.
- Ghent, E.D., Stout, M.Z., Raeside, R.P., 1983. Plagioclase–clinopyroxene–garnet–quartz equilibria and the geobarometry and geothermometry of garnet amphibolites from Mica Creek, British Columbia. *Canadian Journal of Earth Sciences*, 20, 699-706.
- Gittins, J. and Harmer, R.E., 2003. Myth and reality in the carbonatite – silicate rock “association”. *Periodico di Mineralogia*, 72, 19-26.
- Goodfellow, W.D., Cecile, M.P., and Leybourne, M.I., 1995. Geochemistry, petrogenesis, and tectonic setting of lower Paleozoic alkalic and potassic volcanic rocks, Northern Canadian Cordilleran Miogeocline. *Canadian Journal of Earth Sciences*, 32(8), 1236-1254.
- Gorham, J., 2008. Commerce Resources Corp. 2007 diamond drilling and exploration at the Blue River Property, north of Blue River, British Columbia. British Columbia Ministry of Energy, Mines and Natural Gas, British Columbia Geological Survey, Assessment Report 30011, 48 p., 20 appendices.
- Gorham, J., Ulry, B., and Brown, J., 2009. Commerce Resources Corp. 2008 diamond drilling and exploration at the Blue River property, north of Blue River, British Columbia. British Columbia Ministry of Energy, Mines and Petroleum Resources, British Columbia Geological Survey, Assessment Report 31174, 149 p., 21 appendices.
- Gorham, J., Ulry, B., Brown, J., and Carter, M., 2011a. Commerce Resources Corp. 2009 diamond drilling and exploration at the Blue River property, north of Blue River, British Columbia. British Columbia Ministry of Energy and Mines, British Columbia Geological Survey, Assessment Report 31948, 62 p., 14 appendices.
- Gorham, J., Ulry, B., and Brown, J., 2011b. Commerce Resources Corp. 2010 diamond drilling and exploration at the Blue River Property, north of Blue River, British Columbia. British Columbia Ministry of Energy and Mines, British Columbia Geological Survey, Assessment Report 32424, 55 p., 15 appendices.
- Gorham, J., Ulry, B., and Brown, J., 2013. Commerce Resources Corp. 2012 exploration at the Blue River Property, north of Blue River, British Columbia. British Columbia Ministry of Energy, Mines and Natural Gas, British Columbia Geological Survey, Assessment Report 33906, 37 p., 6 maps (1:2,000, 1:5,000, 1:10,000, 1:20,000, and 1:150,000 scale), 5 appendices.
- Grywul, R., and Reeder, J., 2003. Reconnaissance geochemistry of the Mud Lake property, Cbt claim group, Niobi 1 thru 4 and Cbt 1 thru 12 claims, east-central British Columbia. British Columbia. British Columbia Ministry of Energy and Mines, British Columbia Geological Survey, Assessment Report 27103, 11 p., 8 appendices, 3 maps (1:50,000, 1:25,000, and 1:2,500 scale).
- Frost, B.R., 1991. Introduction to oxygen fugacity and its petrologic importance, Chapter 1. In: Donald H. Lindsley, D.H., (Ed.), *Oxide Minerals: Petrologic and Magnetic Significance*. Mineralogical Society of America, Reviews in Mineralogy and Geochemistry, 25, pp. 1-9.
- Hamilton, P.J., O’Nions, R.K., Bridgwater, D., and Nutman, A., 1983. Sm–Nd studies of Archaean metasediments and metavolcanics from West Greenland and their implications for the Earth’s early history. *Earth and Planetary Science Letters*, 62, 263-272.
- Harmer, R.E. and Gittins, J., 1998. The case for primary, mantle-derived carbonatite magma. *Journal of Petrology*, 39 (11-12), 1895-1903.
- Hart, S.R., Hauri, E.H., Oschmann, L.A., and Whitehead, J.A., 1992. Mantle plumes and entrainment: isotopic evidence. *Science*, 256, 517-520.
- Hauri, E.H., Whitehead, J.A., and Hart, S.R., 1994. Fluid dynamic and geochemical aspects of entrainment in mantle plumes. *Journal of Geophysical Research*, 99(B12), 24275-24300.
- Heinrich, W. Wm., 1966. The Geology of Carbonatites. Rand McNally and Company, Chicago, 555 p.
- Hickin, A.S., Ward, B.C., Plouffe, A., and Nelson, J., 2017. Introduction to the geology, physiography, and glacial history of the Canadian Cordillera in British Columbia and Yukon In: Ferbey, T., Plouffe, A., and Hickin, A.S., (Eds.), *Indicator Minerals in Till and Stream Sediments of the Canadian Cordillera*. Geological Association of Canada Special Paper Volume 50 and Mineralogical Association of Canada Topics in Mineral Sciences Volume 47, pp. 27-51.
- Hickson, C.J. and Vigouroux, N., 2014. Volcanism and glacial interaction in the Wells Gray–Clearwater volcanic field, east-central British Columbia. In: Dashtgard, S. and Ward, B. (Eds.), *Trials and Tribulations of Life on an Active Subduction Zone: Field Trips in and around Vancouver, Canada*. Geological Society of America, Field Guide 38, pp. 169-191.
- Hoefs, J., 2009. *Stable Isotope Geochemistry*. 6th Edition, Springer-Verlag, Berlin Heidelberg, 286 p.
- Hoernle, K.A., and Tilton, G.R., 1991. Sr–Nd–Pb isotope data for Fuerteventura (Canary Islands) basal complex and subaerial volcanics: applications to magma genesis and evolution. *Schweizerische Mineralogische und Petrographische Mitteilungen*, 71, 3-18.
- Hofmann, A.W., 2014. Sampling mantle heterogeneity through

- oceanic basalts: isotopes and trace elements. In: Carlson, R.W., (Ed.), *Treatise on Geochemistry* (Second Edition), Volume 3: The Mantle and Core. Elsevier, Oxford, United Kingdom, pp. 67-101.
- Hogarth, D.D., 1989. Pyrochlore, apatite and amphibole: distinctive minerals in carbonatite, Chapter 6. In: Bell, K., (Ed.), *Carbonatites: Genesis and Evolution*. Unwin Hyman, London, United Kingdom, pp. 105-148.
- Hogarth, D.D., Williams, C.T., and Jones, P., 2000. Primary zoning in pyrochlore group minerals from carbonatites. *Mineralogical Magazine*, 64, 683-697.
- Högbom, A.G., 1895. Über das Nephelinsyenitgebiet auf der Insel Alnö. *Geologiska Föreningen i Stockholm Förhandlingar*, 17, 100-160.
- Höy, T., 1988. Geology of the Cottonbelt lead-zinc-magnetite layer, carbonatites and alkaline rocks in the Mount Grace area, Frenchman Cap dome, southeastern British Columbia. British Columbia Ministry of Energy, Mines and Petroleum Resources, British Columbia Geological Survey, Bulletin 80, 99 p, 1:25,000 scale map.
- Hulett, S.R.W., Simonetii, A., Rasbury, E.T. and Hemming, N.G., 2016. Recycling of subducted crustal components into carbonatite melts revealed by boron isotopes. *Nature Geoscience*, 9, 904-909.
- Jacobsen, S.B., and Wasserburg, G.J., 1980. Sm-Nd isotopic evolution of chondrites. *Earth and Planetary Science Letters*, 50, 139-155.
- Johannsen, A., 1938. *A Descriptive Petrography of the Igneous Rocks IV*. University of Chicago Press, Chicago, Illinois, 523 p.
- Johnston, G., Jalbert, R., and Johnston, M., 1990a. Assessment report on the prospecting, geological, geochemical and geophysical work done on the Orion claim, Kamloops Mining Division, N.T.S. 83D/3E. British Columbia. British Columbia Ministry of Energy, Mines and Petroleum Resources, British Columbia Geological Survey, Assessment Report 20501, 20 p., 5 appendices, 3 maps 1:2,000 scale.
- Johnston, G., Jalbert, R., and Johnston, M., 1990b. Assessment report on the prospecting, geological, geochemical and geophysical work done on the Pleiades claim, Kamloops Mining Division, N.T.S. 83D/3E. British Columbia. British Columbia Ministry of Energy, Mines and Petroleum Resources, British Columbia Geological Survey, Assessment Report 20572, 16 p., 5 appendices, 3 maps 1:2,000 scale.
- Kresten, P., 1983. Carbonatite nomenclature. *Geologische Rundschau*, 72 (1), 389-395.
- Kogarko, L.N., Kononova, V.A., Orlova, M.A., and Woolley, A.R., 1995. *The Alkaline Rocks and Carbonatites of the World: Part 2, Former USSR*. Chapman and Hall, London, United Kingdom, 226 p.
- Kogarko, L.N., Lahaye, Y., and Brey, G.P., 2010. Plume-related mantle source of super-large rare metal deposits from the Lovozero and Khibina massifs on the Kola Peninsula, eastern part of the Baltic Shield: Sr, Nd and Hf isotope systematics. *Mineralogy and Petrology*, 98, 197-208.
- Kraft, J.L., 2011. Structural geology of the Upper Fir carbonatite deposit, Blue River, British Columbia: Report and addendum for Dahrouge Geological Consulting Ltd. and Commerce Resources Corp. In: Gorham, J., Ulry, B., and Brown, J. (compilers), *Commerce Resources Corp. 2010 Diamond Drilling and Exploration at the Blue River Property*, British Columbia Ministry of Forests, Mines and Lands, British Columbia Geological Survey, Assessment Report 32424, pp. 3225-3258.
- Krasnova, N.I., Petrov, T.G., Balaganskaya, E.G., Garcia, D., Moutte, J., Zaitsev, A.N., Wall, F., 2004. Introduction to phoscorites: occurrence, composition, nomenclature and petrogenesis. In: Wall, F., and Zaitsev, A.N. (Eds.), *Phoscorites and Carbonatites from Mantle to Mine: The Key Example of the Kola Alkaline Province*. Mineralogical Society Series 10, Mineralogical Society, London, United Kingdom, pp. 45-74.
- Kulla, G., and Hardy, J., 2015. Commerce Resources Corp. Blue River tantalum–niobium project, British Columbia, Canada, project update report. NI 43-101 Technical Report, 138 p.
- Kynicky, J., Smith, M. P., and Xu, C., 2012. Diversity of rare earth deposits: The key example of China, *Elements*, 8, 361-367.
- Le Bas, M.J., 1977. *Carbonatite–Nephelinite Volcanism: an African Case History*. John Wiley & Sons. London, United Kingdom, 347 p.
- Le Maitre, R.W., compiler, 2002. *Igneous Rocks: a Classification and Glossary of Terms*, 2nd Edition. Cambridge University Press, Cambridge, United Kingdom, 236 p.
- Lee, W.-J. and Wyllie, P.J., 2000. The system CaO-MgO-SiO₂-CO₂ at 1 GPa, metasomatic wehrlites, and primary carbonatite magmas. *Contributions to Mineralogy and Petrology*, 138 (3), 214-228.
- Lee, M.J., Lee, J.I., Garcia, D., Moutte, J.A., Williams, C.T., Wall, F.R., and Kim, Y., 2006. Pyrochlore chemistry from the Sokli phoscorite-carbonatite complex, Finland: Implications for the genesis of phoscorite and carbonatite association. *Geochemical Journal*, 40 (1), 1-13.
- Logan, J.M., 2013. Porphyry systems of central and southern BC: Overview and field trip road log. In: Logan, J.M. and Schroeter, T.G., (Eds.), *Porphyry Systems of Central and Southern British Columbia: Tour of central British Columbia Porphyry Deposits from Prince George to Princeton*. Society of Economic Geologists, Inc. Field Trip Guidebook Series 43, pp. 1-45.
- Mackay, D.A.R. and Simandl, G.J. 2014. Geology, market, and supply chain of niobium and tantalum – A review. *Mineralium Deposita*, 49, 1025-1047.
- Mackay, D.A.R., and Simandl, G.J., 2015. Pyrochlore and columbite–tantalite as indicator minerals for specialty metal deposits. *Geochemistry: Exploration, Environment, Analysis*, 15, 167-178.
- Mao, M., Rukhlov, A.S., Rowins, S.M., Spence, J., and Coogan, L.A., 2016. Apatite trace-element compositions: A robust new tool for mineral exploration. *Economic Geology*, 111, 1187-1222.
- Mariano, A.N., 1979. Report on Nb-Ta-U Mineralization in the Blue River carbonatites. Confidential report for Anschutz (Canada) Mining Ltd., 360 p.
- Mariano, A.N., 1982. Petrology, mineralogy and geochemistry of the Blue River carbonatites. Confidential report for Anschutz (Canada) Mining Ltd., 130 p.
- Mariano, A.N., 1989. Nature of economic mineralization in carbonatites and related rocks, Chapter 7. In: Bell, K., (Ed.), *Carbonatites: Genesis and Evolution*. Unwin Hyman, London, United Kingdom, pp. 149-176.
- Marty, B., Tolstikhin, I., Kamensky, I.L., Nivin, V., Balaganskaya, E., and Zimmermann, J.-L., 1998. Plume-derived rare gases in 380 Ma carbonatites from the Kola region (Russia) and the argon isotopic composition in the deep mantle. *Earth and Planetary Science Letters*, 164, 179-192.
- Mathews, W.H., 1986. Physiographic map of the Canadian Cordillera. Geological Survey of Canada, Map 1701A, scale 1:5,000,000.
- Mathews, B. and Monger, J., 2005. *Roadside Geology of Southern British Columbia*, Mountain Press Publishing Company, Missoula,








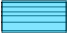

- Montana, 404 p.
- McCammon, J.W., 1951. Vermiculite. In: British Columbia for the Year Ended 31st December 1950, British Columbia Department of Mines, pp. A229-A230.
- McCammon, J.W., 1953. Lempriere. In: British Columbia Minister of Mines Annual Report for the Year Ended 31st December 1952, British Columbia Department of Mines, pp. A115-A119.
- McCammon, J.W., 1955. Lempriere. In: British Columbia Minister of Mines Annual Report for the Year Ended 31st December 1954, British Columbia Department of Mines, p. A111.
- McDonough, M.R. and Murphy, D.C., 1990. Geology, Valemout (830/14) map area, British Columbia. Geological Survey of Canada, Open File 2259, scale 1:50,000.
- McDonough, M.R., Simony, P.S., 1988. Structural evolution of basement gneisses and Hadrynian cover, Bulldog Creek area, Rocky Mountains, British Columbia. *Canadian Journal of Earth Sciences*, 25, 1687-1702.
- McDonough, W.F., and Sun, S.-s., 1995. The composition of the Earth. *Chemical Geology*, 120, 223-253.
- McDonough, M.R., Morrison, M.L., Currie, L.D., Walker, R.T., Pell, J., and Murphy, D.C., 1991a. Canoe Mountain, British Columbia; Geological Survey of Canada, Open File 2511, scale 1:50,000.
- McDonough, M.R., Simony, P.S., Morrison, M.L., Oke, C., Sevigny, J.H., Robbins, D.B., Seigel, S.G., and Grasby, S.E., 1991b. Howard Creek, British Columbia; Geological Survey of Canada, Open File 2411, scale 1:50,000.
- McDonough, M.R., Simony, P.S., Sevigny, J.H., Robbins, D.B., Raeside, R., Doucet, P., Pell, J., and Dechesne, R.G., 1992. Geology of Nagle Creek and Blue River, British Columbia (83d/2 and 83d/3). Geological Survey of Canada, Open File 2512, scale 1:50,000.
- Meyers, E., 1977. Reconnaissance geological, magnetometer and scintillometer survey, Verity #1, AR # 1, 2 claims, Paradise Creek, uranium-columbium prospect, Kamloops Mining Division, Blue River. British Columbia. British Columbia Ministry of Energy, Mines and Petroleum Resources, British Columbia Geological Survey, Assessment Report 6741, 22 p., 2 appendices.
- Mihalynuk, M.G., Nelson, J., and Diakow, L.J., 1994. Cache Creek terrane entrapment: oroclinal paradox within the Canadian Cordillera. *Tectonics*, 13, 575-595.
- Millonig, L.J. and Groat, L.A., 2013. Carbonatites in western North America—occurrences and metallogeny. In: Colpron, M., Bissig, T., Rusk, B.G., and Thompson, F.H. (Eds.), *Tectonics, Metallogeny, and Discovery: The North American Cordillera and Similar Accretionary Settings*. Society of Economic Geologists, Inc., Special Publication 17, pp. 245-264.
- Millonig, L.J., Gerdes, A., and Groat, L.A., 2012. U–Th–Pb geochronology of meta-carbonatites and meta-alkaline rocks in the southern Canadian Cordillera: a geodynamic perspective. *Lithos*, 152, 202-217.
- Millonig, L.J., Gerdes, A., and Groat, L.A., 2013. The effect of amphibolite facies metamorphism on the U–Th–Pb geochronology of accessory minerals from meta-carbonatites and associated meta-alkaline rocks. *Chemical Geology*, 353, 199-209.
- Mitchell, R.H., 2005. Carbonatites and carbonatites and carbonatites. *Canadian Mineralogist*, 43, 2049-2068.
- Mitchell, R.H., 2015. Primary and secondary niobium mineral deposits associated with carbonatites. *Ore Geology Reviews*, 64, 626-641.
- Mitchell, R., Chudy, T., McFarlane, C.R.M., and Wu, F.-Y., 2017. Trace element and isotopic composition of apatite in carbonatites from the Blue River area (British Columbia, Canada) and mineralogy of associated silicate rocks. *Lithos*, 286-287, 75-91.
- Monger, J.W.H., 2014. Seeking the suture: The Coast-Cascade conundrum. *Geoscience Canada*, 41, 379-398.
- Monger, J.W.H. and Hutchison, W.W., 1971. Metamorphic map of the Canadian cordillera. Geological Survey of Canada, Paper 70-33, 71 p.
- Monger, J.W.H. and Price, R.A. 1979. Geodynamic evolution of the Canadian Cordillera - progress and problems. *Canadian Journal of Earth Sciences*, 16, 770-791.
- Monger, J.W.H., Price, R.A., and Tempelman-Kluit, D.J., 1982. Tectonic accretion and the origin of two major metamorphic and plutonic belts in the Canadian Cordillera: *Geology*, 10, 70-75.
- Morrison, M.L., 1982. Structure and petrology of the Malton gneiss complex, British Columbia. Unpublished Ph.D. thesis, University of Calgary, Canada, 314 p.
- Morton, J., 1979. Prospecting report on AEG #1 & #2 and JTM #1 & #2 claims. British Columbia Ministry of Energy, Mines and Petroleum Resources, British Columbia Geological Survey, Assessment Report 7783, 21 p.
- Mumford, T., 2009. Dykes of the Moose Creek Valley, Ice River alkaline complex, southeastern BC. Unpublished M.Sc. thesis, The University of New Brunswick, Canada, 230 p.
- Murphy, D.C., compiler, 2007. Geology, Canoe River, British Columbia-Alberta. Geological Survey of Canada, Map 2110A, scale 1:250,000.
- Nelson, D.R., Chivas, A.R., Chappell, B.W., and McCulloch, M.T., 1988. Geochemical and isotopic systematics in carbonatites and implications for the evolution of ocean-island sources. *Geochimica et Cosmochimica Acta*, 52, 1-17.
- Nelson, J.L., Colpron, M., and Israel, S., 2013. The Cordillera of British Columbia, Yukon and Alaska: tectonics and metallogeny. In: Colpron, M., Bissig, T., Rusk, B.G., and Thompson, F.H., (Eds.), *Tectonics, Metallogeny, and Discovery: The North American Cordillera and Similar Accretionary Settings*. Society of Economic Geologists, Inc. Special Publication 17, pp. 53-109.
- Pană, D.I., and van der Pluijm, B.A., 2015. Orogenic pulses in the Alberta Rocky Mountains: Radiometric dating of major faults and comparison with the regional tectonostratigraphic record. *Geological Society of America Bulletin*, 127, 480-502.
- Paradis, S., Bailey, S.L., Creaser, R.A., Piercey, S.J., Schiarizza, P.A., 2006. Paleozoic Magmatism and Syngenetic Massive Sulphide Deposits of the Eagle Bay Assemblage, Kootenay Terrane, Southern British Columbia. In: Colpron, M. and Nelson, J., (Eds.), *Paleozoic Evolution and Metallogeny of Pericratonic Terranes at the Ancient Pacific Margin of North America*, Canadian and Alaskan Cordillera. Geological Association of Canada, Special Paper 45, pp. 383-414.
- Parrish, R.R. and Scammell, R.J., 1988. The age of the Mount Copeland syenite gneiss and its metamorphic zircons, Monashee complex, southeastern British Columbia. In: *Radiogenic Age and Isotopic Studies: Report 2*, Geological Survey of Canada, Paper 88-2, pp. 21-28.
- Parrish, R.R., Carr, S.D., and Parkinson, D.L., 1988. Eocene extensional tectonics and geochronology of the southern Omineca Belt, British Columbia and Washington. *Tectonics*, 7, 181-212.
- Pell, J., 1985. Carbonatites and related rocks in British Columbia. In: *Geological Fieldwork 1984*, British Columbia Ministry of Energy, Mines and Petroleum Resources, British Columbia Geological Survey, Paper 1985-1, pp. 85-94.
- Pell, J., 1987. Alkaline ultrabasic rocks in British Columbia:

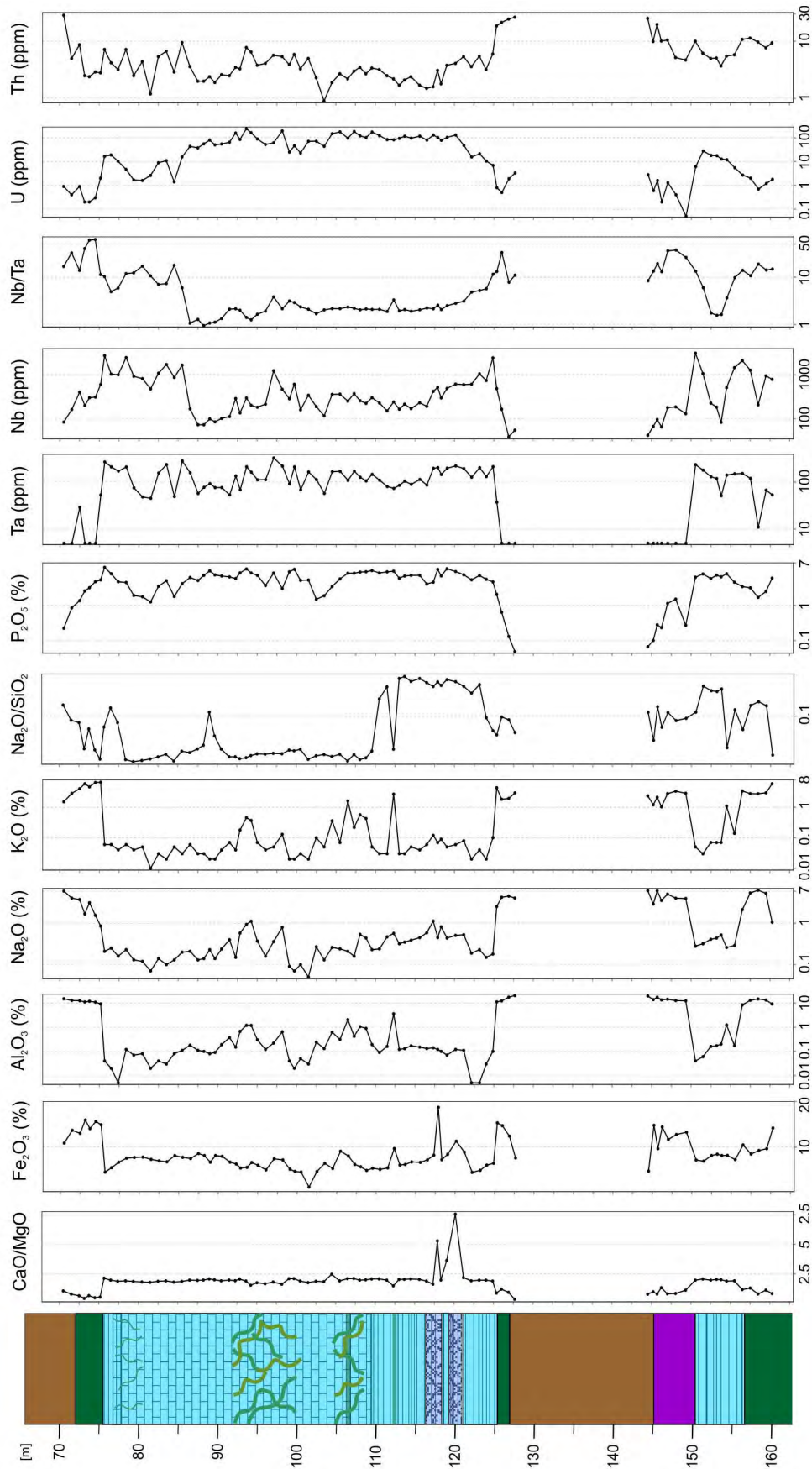
- carbonatites, nepheline syenites, kimberlites and related rocks. British Columbia Ministry of Energy, Mines and Petroleum Resources, British Columbia Geological Survey, Open File 1987-17, 109 p.
- Pell, J., 1994. Carbonatites, nepheline syenites, kimberlites and related rocks in B.C. British Columbia Ministry of Energy, Mines and Petroleum Resources, British Columbia Geological Survey, Bulletin 88, 136 p.
- Pell, J.A., 1996. Mineral deposits associated with carbonatites and related alkaline igneous rocks. In: Mitchell, R.H., (Ed.), *Undersaturated Alkaline Rocks: Mineralogy, Petrogenesis, and Economic Potential*. Mineralogical Association of Canada, Short Course Handbook 24, pp. 271-310.
- Pell, J. and Höy, T., 1989. Carbonatites in a continental margin environment - the Canadian Cordillera. In: Bell, K. (Ed.), *Carbonatites: Genesis and Evolution*. Unwin Hyman, London, United Kingdom, pp. 200-220.
- Pell, J. and Simony, P., 1981. Stratigraphy, structure and metamorphism in the southern Cariboo Mountains, British Columbia. In: *Current Research, Part A. Geological Survey of Canada, Paper 81-1A*, pp. 227-230.
- Pell, J. and Simony, P.S., 1987. New correlations of Hadrynian strata, south-central British Columbia. *Canadian Journal of Earth Sciences*, 24, 302-313.
- Peterson, T.D., and Currie, K.L. 1994. The Ice River Complex, British Columbia. In: *Current Research, Part A. Geological Survey of Canada, Paper 1994-A*, pp. 185-192.
- Price, R.A. and Mountjoy, E.W., 1970. Geological structure of the Canadian Rocky Mountains between Bow and Athabasca rivers, a progress report. In: Wheeler, O.J., (Ed.), *Structure of the Southern Canadian Cordillera*. Geological Association of Canada, Special Publication 6, pp. 7-25.
- Pozharitskaya, L.K. and Samoylov, V.S., 1972. *Petrologiya, Mineralogiya i Geokhimiya Karbonatitov Vostochnoi Sibiri* [Petrology, mineralogy and geochemistry of carbonatites of eastern Siberia]. Nauka, Moscow, 268 p. (in Russian).
- Raeseide, R.P. and Simony, P.S., 1983. Stratigraphy and deformational history of the Scrip Nappe, Monashee Mountains, British Columbia. *Canadian Journal of Earth Sciences*, 20, 639-650.
- Rankin, A.H., 2005. Carbonatite-associated rare metal deposits: composition and evolution of ore-forming fluids - the fluid inclusion evidence. In: Linnen, R. L. and Samson, L.M., (Eds.), *Rare Earth Geochemistry and Mineral Deposits*. Geological Association of Canada, Short Course Notes 17, pp. 299-314.
- Read, P.B. and Brown, R.L., 1981. Columbia River fault zone: southeastern margin of the Shuswap and Monashee complexes, southern British Columbia. *Canadian Journal of Earth Sciences*, 18(7), 1127-1145.
- Read, P.B., Woodsworth, G.J., Greenwood, H.J., Ghent, E.D., and Evenchick, C.A., 1991. Metamorphic map of the Canadian Cordillera. Geological Survey of Canada, Map 1714A, scale 1:2,000,000.
- Reeder, J. and Dahrouge, J., 2002. Commerce Resources Corp. 2001 geologic mapping, sampling, and geophysical surveys on the Fir property, north of Blue River, British Columbia. British Columbia Ministry of Energy and Mines, British Columbia Geological Survey, Assessment Report 26781, 13 p., 3 maps (1:5,000 and 1:10,000 scale), 5 appendices.
- Reeder, J., and Grywul, R., 2002. Reconnaissance geochemistry of the Mud Lake property, Niobi 5, 8, 9, 10, and 11 claims, east-central British Columbia. British Columbia Ministry of Energy and Mines, British Columbia Geological Survey, Assessment Report 26936, 8 p., 6 appendices, 3 maps (1:50,000, 1:31,680, and 1:10,000 scale).
- Reguir, E.P., Chakhmouradian, A.R., Pisiak, L., Halden, Yang, P., Xu, C., Kynický, J., Couëslan, C.G., 2012. Trace-element composition and zoning in clinopyroxene- and amphibole-group minerals: implications for element partitioning and evolution of carbonatites. *Lithos*, 128-131, 27-45.
- Rich, A. and Gower, J.A., 1968. Geological report on the Paradise group, about 4 miles southeast of Lempriere. British Columbia Ministry of Energy, Mines and Petroleum Resources, British Columbia Geological Survey, Assessment Report 1630, 13 p., 1 map 1:1,417 scale.
- Richardson, D.G., and Birkett, T.C. 1996. Carbonatite-associated deposits. In: Eckstrand, O.R., Sinclair, W.D., and Thorpe, R.I., (Eds.), *Geology of Canadian Mineral Deposit Types*. Geological Survey of Canada, *Geology of Canada* 8, pp. 541-558.
- Roback, R.C., Sevigny, J.H., and Walker, N.W. 1994. Tectonic setting of the Slide Mountain terrane, southern British Columbia. *Tectonics*, 13, 1242-1258.
- Rollinson, H.R., 1993. *Using Geochemical Data: Evaluation, Presentation, Interpretation*. Addison-Wesley Longman Ltd., United Kingdom, 384 p.
- Ross, G.M., 1991. Tectonic setting of the Windermere Supergroup revisited. *Geology*, 19, 1125-1128.
- Rowe, R.P., 1958. Niobium (columbium) deposits of Canada. Geological Survey of Canada, *Economic Geology Series*, 18, 108 p.
- Rukhlov, A.S. and Bell, K., 2010. Geochronology of carbonatites from the Canadian and Baltic Shields, and the Canadian Cordillera: clues to mantle evolution. *Mineralogy and Petrology*, 98, 11-54.
- Rukhlov, A.S. and Gorham, J., 2007. Commerce Resources Corp. 2006 diamond drilling and exploration at the Blue River Property, north of Blue River, British Columbia. British Columbia Ministry of Energy, Mines and Petroleum Resources, British Columbia Geological Survey, Assessment Report 29024, 41 p., 16 appendices.
- Rukhlov, A.S., Bell, K., and Amelin, Y., 2015. Carbonatites, isotopes and evolution of the subcontinental mantle: An overview. In: Simandl, G.J. and Neetz, M., (Eds.), *Symposium on Strategic and Critical Materials Proceedings*, November 13-14, 2015, Victoria. British Columbia, British Columbia Ministry of Energy and Mines, British Columbia Geological Survey, Paper 2015-3, pp. 39-64.
- Rukhlov, A.S., Mao, M., Aspler, L.B., Spence, J., Creaser, R.A., Czech, E., and Gabites, J., 2018. Mineral chemistry and isotopic systematics of carbonatites and related rocks from the Blue River area. British Columbia Ministry of Energy, Mines and Petroleum Resources, British Columbia Geological Survey GeoFile 2018-1.
- Russell, H.D., Hiemstra, S.A., Groenveld, D., 1954. The mineralogy and petrology of the carbonatite at Loolekop, Eastern Transvaal. *Transactions Geological Society of South Africa*, 57, 197-208.
- Sasada, T., Hiyagon, H., Bell, K., and Ebihara, M., 1997. Mantle derived noble gases in carbonatites. *Geochimica et Cosmochimica Acta*, 61, 4219-4228.
- Scammell, R.J., 1987. Stratigraphy, structure and metamorphism of the north flank of the Monashee complex, southeastern British Columbia: a record of Proterozoic extension and Phanerozoic crustal thickening. Unpublished M.Sc. thesis, Carleton University, Ottawa, Canada, 205 p.
- Scammell, R.J., 1993. Mid-Cretaceous to Tertiary thermotectonic history of former mid-crustal rocks, southern Omineca belt,

- Canadian Cordillera. Unpublished Ph.D. thesis, Queens University, Kingston, Ontario, 576 p.
- Scammell, R.J. and Brown, R.L., 1990. Cover gneisses of the Monashee terrane: a record of synsedimentary rifting in the North American Cordillera. *Canadian Journal of Earth Sciences*, 27, 712-726.
- Sevigny, J. and Simony, P.S., 1989. Geometric relationship between the Scrip Nappe and metamorphic isograds in the northern Adams River area, Monashee Mountains, British Columbia. *Canadian Journal of Earth Sciences*, 26, 606-610.
- Sevigny, J.H., Parrish, R.R., Ghent, E.D., 1989. Petrogenesis of peraluminous granites, Monashee Mountains, southeastern Canadian Cordillera. *Journal of Petrology*, 30, 557-581.
- Sevigny, J.H., Parrish, R.R., Donelick, R.A., Ghent, E.D., 1990. Northern Monashee mountains, Omineca crystalline belt, British Columbia: timing of metamorphism, anatexis, and tectonic denudation. *Geology*, 18, 103-106.
- Shand, S.J., 1943. Eruptive Rocks: Their Genesis, Composition, Classification and their Relation to Ore Deposits with a Chapter on Meteorites, Second Edition. Thomas Murby, London, 444 p.
- Sigloch, K. and Mihalynuk, M.G., 2017. Mantle and geological evidence for a Late Jurassic–cretaceous suture spanning North America. *The Geological Society of America Bulletin*, 129 (11/12), 1489-1520.
- Simandl, G.J., Jones, P.C., and Rotella, M., 2002. Blue river carbonatites, British Columbia–primary exploration targets for tantalum. In: *Exploration and Mining in British Columbia – 2001, Part B*, British Columbia Ministry of Energy and Mines, pp. 73-82.
- Simandl, G.J., Paradis, S., Simandl, L., and Dahrouge, J., 2010. Vermiculite in the Blue River area, east-central British Columbia, Canada (NTS 083D/06). In: *Geological Fieldwork 2009*, British Columbia Ministry of Forests, Mines and Lands, British Columbia Geological Survey, Paper 2010-1, pp. 83-91.
- Simonetti, A., Bell, K., and Viladkar, S.G., 1995. Isotopic data from the Amba Dongar carbonatite complex, west-central India: evidence for an enriched mantle source. *Chemical Geology*, 122, 185-198.
- Simonetti, A., Goldstein, S.L., Schmidberger, S.S., and Viladkar, S.G., 1998. Geochemical and Nd, Pb, and Sr isotope data from Deccan alkaline complexes: inferences for mantle sources and plume-lithosphere interaction. *Journal of Petrology*, 39, 1847-1864.
- Simonetti, A., Heaman, L.M., Hartlaub, R.P., Creaser, R.A., MacHattie, T.G., and Böhm, C., 2005. U–Pb zircon dating by laser ablation-MC-ICP-MS using a new multiple ion counting Faraday collector array. *Journal of Analytical Atomic Spectrometry*, 20, 677-686.
- Simony, P.S. and Carr, S.D., 2011. Cretaceous to Eocene evolution of the southeastern Canadian Cordillera: Continuity of Rocky Mountain thrust systems with zones of “in-sequence” mid-crustal flow. *Journal of Structural Geology*, 33, 1417-1434.
- Simony, P.S., Ghent, E.D., Craw, D., and Mitchell, W., 1980. Structural and metamorphic evolution of the northeast flank of the Shuswap complex, southern Canoe River area, British Columbia. In: Crittenden, M.D., Coney, P.J., and Davis, G.H. (Eds.), *Cordilleran Metamorphic Core Complexes*. Geological Society of America Memoir 153, pp. 445-461.
- Smith, M. and Dahrouge, J., 2002a. Commerce Resources Corp. 2001 diamond drilling on the Fir property, north of Blue River, British Columbia. British Columbia Ministry of Energy and Mines, British Columbia Geological Survey, Assessment Report 26911, 19 p., 5 appendices.
- Smith, M. and Dahrouge, J., 2002b. International Arimex Resources Inc. 2002 exploration of the Gum Creek property, north of Blue River, British Columbia. British Columbia Ministry of Energy and Mines, British Columbia Geological Survey, Assessment Report 26990, 13 p., 4 appendices.
- Smith, M. and Dahrouge, J., 2003. Commerce Resources Corp. 2002 diamond drilling and exploration on the Blue River property, north of Blue River, British Columbia. British Columbia Ministry of Energy and Mines, British Columbia Geological Survey, Assessment Report 27131, 31 p., 6 appendices.
- Soellner, J., 1927. Zur petrographie und geologie des Kaiserstuhlgebirges im Breisgau. *Neues Jahrbuch für Mineralogie, Geologie und Paläontologie, Beilage-bänd. Abt. A.*, 55, 299-318.
- Song, W.L., Xu, C., Veksler, I.V., and Kynicky, J., 2016. Experimental study of REE, Ba, Sr, Mo and W partitioning between carbonatitic melt and aqueous fluid with implications for rare metal mineralization. *Contributions to Mineralogy and Petrology*, 171, 1-12.
- Stacey, J.S., and Kramers, J.D., 1975. Approximation of terrestrial lead isotopic evolution by a two-stage model. *Earth and Planetary Science Letters*, 26, 207-221.
- Stracke, A., 2012. Earth’s heterogeneous mantle: a product of convection-driven interaction between crust and mantle. *Chemical Geology*, 330-331, 274-299.
- Stracke, A., Hofmann, A.W., and Hart, S.R., 2005. FOZO, HIMU, and the rest of the mantle zoo. *Geochemistry, Geophysics, Geosystems*, 6 (5), Q05007, DOI: 10.1029/2004GC000824.
- Tappe, S. and Simonetti, A., 2012. Combined U–Pb geochronology and Sr–Nd isotope analysis of the Ice River perovskite standard, with implications for kimberlite and alkaline rock petrogenesis. *Chemical Geology*, 304-305, 10-17.
- Taylor, H.P., Frechen, J., and Degens, E.T., 1967. Oxygen and carbon isotope studies of carbonatites from the Laacher See district, West Germany and the Alnö district, Sweden. *Geochimica et Cosmochimica Acta*, 31, 407-430.
- Thom, J., 2013. Geophysical survey and petrographic study on the Blue River project. British Columbia Ministry of Energy, Mines and Natural Gas, British Columbia Geological Survey, Assessment Report 34289, 20 p., 3 appendices.
- Tinkham, D.K. and Ghent, E.D., 2005. Estimating P–T conditions of garnet growth with isochemical phase-diagram sections and the problem of effective bulk-composition. *The Canadian Mineralogist*, 43, 35-50.
- Tolstikhin, I.N., Kamensky, I.L., Marty, B., Nivin, V.A., Vetrin, V.R., Balaganskaya, E.G., Ikorsky, S.V., Gannibal, M.A., Weiss, D., Verhulst, A., and Demaiffe, D., 2002. Rare gas isotopes and parent trace elements in ultrabasic-alkaline-carbonatite complexes, Kola Peninsula: identification of lower mantle plume component. *Geochimica et Cosmochimica Acta*, 66, 881-901.
- Torsvik TH, Smethurst MA, Burke K, Steinberger B. 2006. Large igneous provinces generated from the margins of the large low-velocity provinces in the deep mantle. *Geophysical Journal International*, 167, 1447-1460.
- Trofanenko, J., Williams-Jones, A.E., Simandl, G.J., and Migdisov, A.A., 2016. The nature and origin of the REE mineralization in the Wicheeda carbonatite, British Columbia, Canada. *Economic Geology*, 111(1), 199-223.
- Tuttle, O.F. and Gittins, J., eds., 1966. Carbonatites. Interscience Publishers, John Wiley & Sons, Inc., New York, 592 p.
- Valley, J.W., 2003. Oxygen isotopes in zircon. In: Hanchar, J.M. and Hoskin, P.W.O. (Eds.), *Zircon*. Mineralogical Society of America,

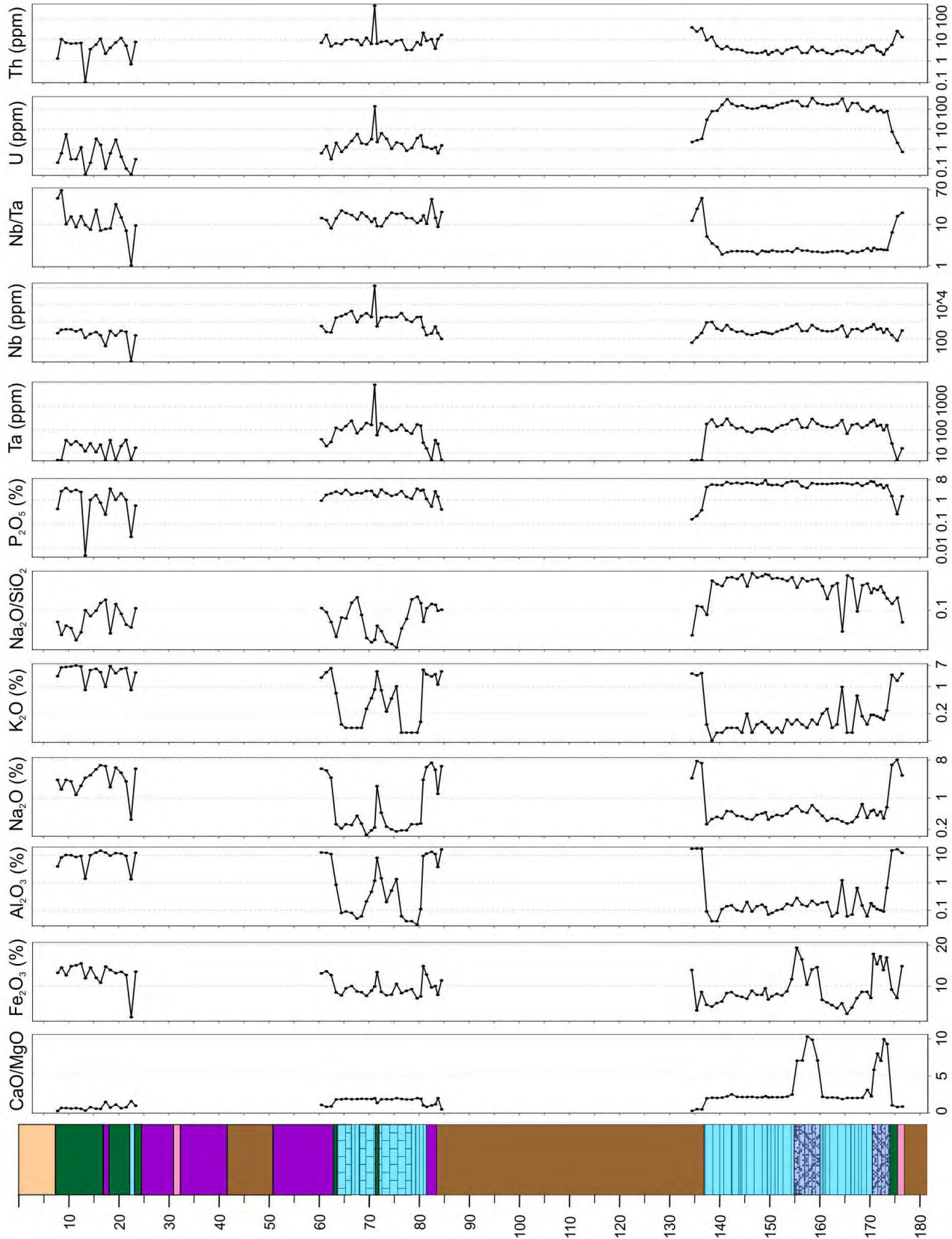
- Geochemical Society, *Reviews in Mineralogy and Geochemistry*, 53 (1), pp. 343-385.
- Veen, A.H., van der, 1963. A study of pyrochlore. *Verhandelingen van het Koninklijk Nederlands Geologisch Mijnbouwkundig Genootschap, Geologische Serie*, 22, 188 p.
- Wall, F., and Zaitsev, A.N., eds., 2004. *Phoscorites and Carbonatites from Mantle to Mine: The Key Example of the Kola Alkaline Province*. Mineralogical Society Series, 10, The Mineralogical Society, London, United Kingdom, 503 p.
- White, G.P.E., 1980. Potential carbonatite localities. In: *Geological Fieldwork 1979*, British Columbia Ministry of Energy, Mines and Petroleum Resources, British Columbia Geological Survey, Paper 1980-1, pp. 118-119.
- White, G.P.E., 1981. Further potential carbonatite localities (83D/6E). In: *Geological Fieldwork 1980*. British Columbia Ministry of Energy, Mines and Petroleum Resources, British Columbia Geological Survey, Paper 1981-1, p. 111.
- White, G.P.E., 1982. Notes on carbonatites in central British Columbia. In: *Geological Fieldwork 1981*. British Columbia Ministry of Energy, Mines and Petroleum Resources, British Columbia Geological Survey, Paper 1982-1, pp. 68-69.
- White, G.P.E., 1985. Further notes on carbonatites in central British Columbia (83D/6E, 7W). In: *Geological Fieldwork 1984*. British Columbia Ministry of Energy, Mines and Petroleum Resources, British Columbia Geological Survey, Paper 1985-1, pp. 95-100.
- Wood, D.A., Joron, J.L., Treuil, M., Norry, M., and Tarney, J., 1979. Elemental and Sr isotope variations in basic lavas from Iceland and the surrounding ocean floor. *Contributions to Mineralogy and Petrology*, 70, 3219-3239.
- Woolley, A.R., 1987. *The Alkaline Rocks and Carbonatites of the World. Part 1: North and South America*. British Museum (Natural History) and University of Texas Press, 216 p.
- Woolley, A.R., 2001. *Alkaline Rocks and Carbonatites of the World. Part 3: Africa*. Geological Society, London, 372 p.
- Woolley, A.R., 2003. Igneous silicate rocks associated with carbonatites: Their diversity, relative abundances and implications for carbonatite genesis. *Periodico di Mineralogia*, 72, 9-17.
- Woolley, A.R., and Bailey, D.K., 2012. The crucial role of lithospheric structure in the generation and release of carbonatites: geological evidence. In: Downes, H., Wall, F., Demény, A., and Szabo, C., (Eds.), *Continuing the Carbonatite Controversy*. *Mineralogical Magazine*, 76, 259-270.
- Woolley, A.R. and Kempe, D.R.C., 1989. Carbonatites: nomenclature, average chemical compositions, and element distribution. In: Bell, K. (Ed.), *Carbonatites: Genesis and Evolution*. Unwin Hyman, London, United Kingdom, pp. 1-14.
- Woolley, A.R., and Kjarsgaard, B.A., 2008a. Carbonatite occurrences of the world: map and database. Geological Survey of Canada, Open File 5796, 1 CD-ROM plus 1 map.
- Woolley, A.R., and Kjarsgaard, B.A., 2008b. Paragenetic types of carbonatite as indicated by the diversity and relative abundances of associated silicate rocks: evidence from a global database. *The Canadian Mineralogist*, 46, 741-752.
- Wyllie, P.J., 1989. Origin of carbonatites: evidence from phase equilibrium studies. In: Bell, K. (Ed.), *Carbonatites: Genesis and Evolution*. Unwin Hyman, London, pp. 500-545.
- Wyllie, P.J. and Lee, W.-J., 1998. Model system controls on conditions for formation of magnesiocarbonatite and calciocarbonatite magmas from the mantle. *Journal of Petrology*, 39 (11-12), 1885-1893.
- Xu, C., Kynicky, J., Chakhmouradian, A.R., Qi, L., and Song, W., 2010. A unique Mo deposit associated with carbonatites in the Qinling orogenic belt, central China. *Lithos*, 118, 50-60.

Appendix 1. Downhole lithological and geochemical profiles for selected elements and elemental ratios at Upper Fir

-  Overburden
-  Regional gneiss and schist
-  Regional amphibolite
-  Calcite-pyroxene amphibolite (Na-fenite)
-  Glimmerite (phlogopite fenite)
-  Dolomite carbonatite (granoblastic or gneissic fabric)
-  Dolomite carbonatite (granoblastic or gneissic fabric with calc-silicate veins)
-  Dolomite carbonatite (foliated porphyroclastic fabric)
-  Calcite carbonatite



Appendix 1 a) Diamond drill hole F10-198 (72.33-129.56 m; collar NAD83 UTM zone 11 coordinates: 352813 m E, 5796902 m N; elevation: 1201 m; plunge: 60° E).



Appendix 1 b) Diamond drill hole F10-208 (7.32-230.19 m; NAD83 UTM zone 11 coordinates: 352967 m E, 5796622 m N, 1268 m, 75° E).

Appendix 2. Road log

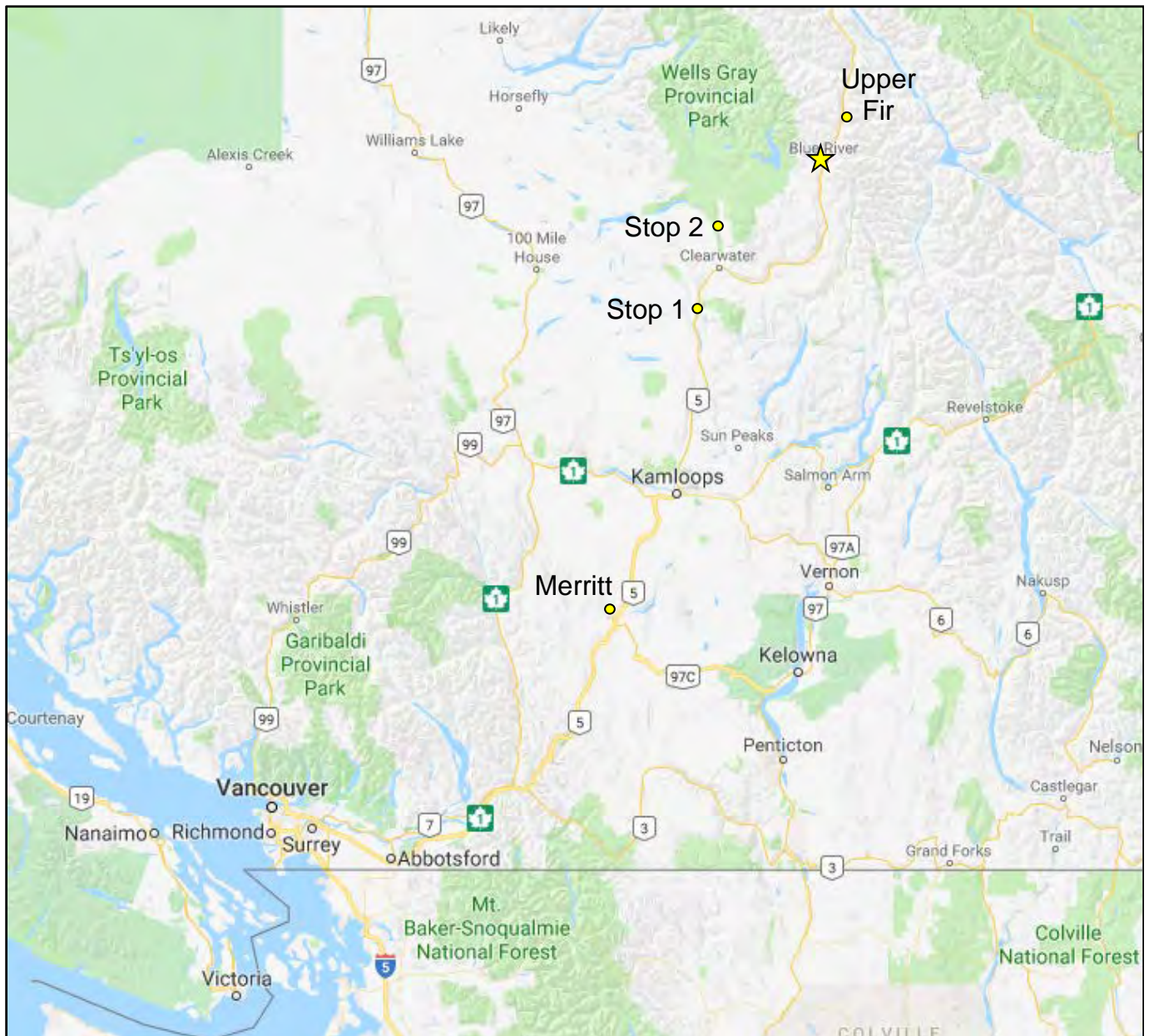


Fig. A2.1. Field trip stops and route (Highway 1 and Highway 5) from Vancouver to Blue River, east-central British Columbia.

Day 1. Vancouver to Blue River (Fig. A2.1)

0.0 km. Assemble at the front entrance to Vancouver Convention Centre West (Burrard St at Canada Pl) at **7:30 AM**. We leave at **8:00 AM**.

Travel east from Vancouver Convention Centre to get on Trans-Canada Hwy (BC-1E)

35.5 km. Hwy 17/15 overpass. Continue southeast on Trans-Canada Hwy (BC-1E) for about 36 km to the Hwy BC-17/15 overpass.

0.0 km. Reset odometre at the merging immediately past the overpass.

40.0 km. Coast belt. Heading northeast, our route follows the Fraser River valley, which is filled with unconsolidated deltaic, fluvial, and glacial deposits. The valley separates the rugged Coast Mountains to the north and the Cascade Mountains to the southeast (Fig. 2b). These mountains form a chain 100-200 km-wide and 1600 km-long along the mainland coast from the Yukon Plateau near latitude 60° to the North Cascades near latitude 48°30' and coincide with the core of the Pacific or Coast-Cascade orogen (Monger, 2014). Their rugged topography reflects differential uplift of up to 4 km and glacial-fluvial erosion in the past 10 million years.

For the next 135 km, we pass through uplifted and dissected Middle Devonian to Miocene rocks comprising: 1) remnants of island arcs and oceanic lithosphere accreted to, and displaced along, the margin of the Ancestral North America, and 2) overlap basins and younger continental arcs built on older rocks due to convergence between the North American and Pacific plates. The core of the Coast-Cascade orogen straddles the Coast morphogeological belt between the Insular (western) and Intermontane (interior) belts of accreted offshore crust (Figs. 1 and 2a). The Coast Belt is a tectonic 'welt' resulting from Mesozoic collision of the Insular arcs with the Intermontane terranes and subsequent crustal thickening, plutonism, and differential uplift, related to eastward subduction, orthogonal shortening, northwest-southeast transcurrent displacement, and late transtension and extension. Middle Jurassic to Eocene granitoid plutons make up about 80% of the Coast Belt and, together with the high-grade metamorphic rocks (Fig. 2c), comprise the Coast Plutonic Complex, which developed as the Insular island arcs above west-dipping subduction during their accretion and collision with the Intermontane terranes at the leading edge of Ancestral North America, and subsequent continental front arcs above the east-dipping Farallon slab since ca. 155 Ma (Sigloch and Mihalynuk, 2017). Younger granitic plutons and volcanic rocks (34-0 Ma) of the Coast Belt south of latitude 51° mark the northern end of the Cascade magmatic arc, which extends to northern California above the currently subducting Juan de Fuca and Gorda plates. The syntectonic plutons 'stitch' the accreted Insular superterrane to the west and the Intermontane superterrane to the east, along with several small terranes and overlapping basins wedged between the two superterranes in the southern Coast belt. These small terranes

comprise remnants of Middle Devonian to Late Jurassic island arcs (Nooksack-Harrison and Chilliwack terranes) and Mississippian to Middle Jurassic ocean (Bridge River, Methow and Cadwallader terranes; Fig. 1). Late Jurassic to Early Cretaceous marine siliciclastic rocks of the Tyaughton-Methow basin overlap all three oceanic terranes.

88.3 km. Cascade magmatic arc. The western margin of a Miocene, quartz monzonite-granodiorite-tonalite pluton (Mount Barr batholith; 208 km²), related to the Cascade magmatic arc, is exposed alongside the highway southwest of the Harrison Lake. The pluton intrudes marine siliciclastic strata and arc-related volcanic rocks of the Gambier Group (Early Cretaceous) and 'stitches' the north-south Fraser fault, which accommodated ca. 140 km of dextral displacement in the Eocene.

138.8 km. Oceanic terranes. We pass by Mississippian to Middle Jurassic rocks of the Bridge River, Cadwallader and Methow terranes, made up of disrupted oceanic crust, lenses of serpentinized mantle and Late Triassic blueschist, argillite, radiolarian chert, and local arc-related volcanic and siliciclastic strata (Monger, 2014). These ocean floor remnants overlying Late Jurassic to earliest Cretaceous marine clastic rocks of the Tyaughton-Methow basin comprise an accretionary complex wedged between the Insular and Intermontane superterranes in the southern Coast belt (Sigloch and Mihalynuk, 2017). Synorogenic (ca. 95 to 45 Ma) granitic plutons related to eastward subduction of the Pacific plates under North America cut all three oceanic terranes and the overlapping siliciclastic strata.

161.0 km. Coquihala Pass. At the Coquihala Summit recreational area, an Eocene granodiorite pluton (208 km²) intrudes Permian ophiolite that is overlain by Late Triassic to Middle Jurassic arc-related volcanic and siliciclastic rocks of the Cadwallader terrane. These rocks are thrust over Late Jurassic to Early Cretaceous marine siliciclastic strata of the Tyaughton-Methow basin, and overlain by Eocene conglomerates and sandstones. The view from the rest area features Zopkios Peak to the north and Markhor and Needle peaks to the south.

165.0 km. Coast belt boundary. Heading northeast, our route passes through a northwest-southeast belt of Middle Jurassic to mid-Cretaceous granitic plutons marking the transition from the Coast belt to the Intermontane morphogeological belt, which occupies the central part of the Canadian Cordillera (Fig. 2a). As we leave the rugged Cascade Mountains behind, this transition corresponds with the physiographic change to the more subdued, gently rolling topography of the Interior Plateau (Fig. 2b).

179.1 km. Intermontane Belt. We pass through volcano-sedimentary rocks of the Nicola Group (Late Triassic) at the leading edge of the Intermontane arc superterrane. Continuing northeast for the next 210 km, our route (Hwy 5) passes through Late Devonian to Middle Jurassic volcanic and sedimentary rocks that are cut by numerous Late Triassic to Early Jurassic granitic plutons of the Quesnel island arc

terrane, which underlies much of the Intermontane Belt. Younger, Middle Jurassic to Eocene granitic plutons and thick Early Cretaceous to Eocene volcanoclastic deposits overlapping the older Quesnel rocks record collisions of the offshore Insular arc terranes with the post-accretionary western margin of Ancestral North America, and continental magmatic arcs resulted from protracted subduction of the Pacific plates under North America. Extensive Miocene to Holocene alkali basalt lava flows and shield volcanoes, formed over a mantle hot spot, blanket vast areas of the Intermontane belt.

Unlike the flanking Coast and Omineca tectonic welts, the Intermontane Belt is underlain mainly by subgreenschist facies grade rocks (Fig. 2c; Monger, 2014). The Slide Mountain, Yukon-Tanana, Stikine, Quesnel, and Cache Creek terranes (collectively the Intermontane superterrane; Fig. 1) comprise remnants of ocean basins, microcontinents, island arcs, and forearc accretionary complexes that evolved outboard of the western margin of Ancestral North America in a setting perhaps similar to the modern western Pacific margin before they finally accreted onto the western edge of Laurentia by the Middle Jurassic (ca. 174 Ma). Middle to Late Devonian subduction along the western Laurentian margin was overprinted by Late Devonian to Mississippian widespread, plume-related carbonatite and alkaline magmatism and coeval rifting that led to the Slide Mountain ocean (up to 3000 km wide) between the continental margin and continental fragments (Yukon-Tanana terrane) detached from Laurentia by the Early Permian (e.g., Nelson et al., 2013; Monger, 2014). Juvenile intra-oceanic arcs (Quesnel and Stikine terranes) and those superimposed on pericratonic terranes formed above east-dipping subduction zones by westward drifting of the frontal arcs into the proto-Pacific ocean (Panthalassa) in the Mississippian through the Early Permian. The Slide Mountain ocean collapsed by west-dipping subduction by the end of the Permian, and the North American plate drifting westward from spreading of the new Atlantic ocean was colliding with the Intermontane arc terranes throughout the Triassic and Early Jurassic (Nelson et al., 2013).

These arc-continent collisions trapped an oceanic accretionary complex (Cache Creek terrane) between the Stikine and Quesnel arc terranes, which form an oroclinal fold hinged in the Yukon-Tanana terrane (Mihalynuk et al., 1994). The Cache Creek accretionary complex contains slivers of blueschist, abundant Pennsylvanian to Late Triassic carbonate reef caps on seamounts or oceanic plateaus, widespread remnants of an extinct, Permian-Triassic arc (locally recognized as Kutcho terrane), and exotic Permian to Middle Triassic faunas that originated far out in Panthalassa and probably in Paleotethys ocean (e.g., Monger, 2014). The ocean-continent suture is marked by discontinuous slivers of the Slide Mountain terrane thrust against rocks of the ancestral continental margin underlying the Omineca belt to the east.

Late Triassic to Early Jurassic magmatic arcs superimposed on the Paleozoic basement of the Stikine and Quesnel terranes produced some of the largest porphyry Cu-Mo-Au deposits in the Canadian Cordillera (e.g., Copper Mountain,

Highland Valley, Mount Polley; e.g., Logan, 2013). Since the Middle Jurassic, rocks of the Intermontane superterrane were displaced along the North American margin by oblique collisions with the Insular arc terranes and an oceanic plateau. This was followed by westward extension in the Eocene, and overprinting by continental magmatic arcs that resulted from protracted subduction of the Pacific plates under North America. Examples of important post-accretionary deposits of the Intermontane Belt include Late Jurassic porphyry Mo (Endako), Late Cretaceous porphyry Cu-Mo (Huckleberry), epithermal Au-Ag (Blackwater), and Eocene porphyry Cu-Mo-Au (Granisle) and orogenic gold veins (Engineer, Blackdome; Nelson et al., 2013).

193.1 km. Spences Bridge Group. We pass by mainly intermediate to felsic volcanic rocks of the Spences Bridge Group (Early Cretaceous).

235.5 km. Exit 290 to Merritt. Take exit 290 toward Merritt City centre. Turn left on Princeton-Kamloops Hwy (BC-5A N)/Voght Street (signs to Merritt). Continue 600 m and turn right onto Belshaw St, turn right again at next intersection (50 m) onto De Wolf Way. Park on the left side at gas stations and fast food restaurants.

236.9 km. Fast food lunch stop (45 minutes). After lunch, return to Highway 5 by turning left on Belshaw St, then left on Princeton-Kamloops Hwy/Voght St/BC-5A and continue east for about 550 m. Slight right to ramp on Hwy BC-5 North/Yellowhead Hwy. Continue north.

302.6 km. Iron Mask batholith. The view ahead is of the Iron Mask monzonite-diorite-syenite batholith (Late Triassic to Early Jurassic).

312.9 km. Kamloops basin. The hills on the left (north) are underlain by Eocene volcanic and sedimentary rocks deposited in the Kamloops basin, which is bounded by northwest-trending normal faults.

321.5 km. Take exit 374 to Yellowhead Hwy 5 North (Sun Peaks Jasper).

337.1 km. Quesnel basement. We drive by deep-water sedimentary rocks interbedded with mafic to felsic volcanoclastic rocks and minor carbonate rocks of the Harper Ranch Group (Devonian to Permian; possible Paleozoic basement to Quesnel terrane; Mathews and Monger, 2005), that are overlain by rocks that may be part of the Nicola Group (Triassic) and are cut by Late Triassic to Early Jurassic monzonitic to syenitic plutons.

386.7 km. Slide Mountain terrane. Dark grey cliffs seen alongside the highway (to the east) immediately north of the town of Barriere are underlain mainly by pillow basalts, diabase, gabbro, and local chert with basal siliciclastic rocks of the Fennell Formation (Mississippian to Permian). They represent the Slide Mountain terrane that makes up discontinuous slivers along the eastern edge of the Quesnel and Yukon-Tanana arc terranes thrust over the continental margin (e.g., Roback et al., 1994; Paradis et al., 2006). This

oceanic suture marks the boundary between the accreted Intermontane superterrane to the west and the margin of Ancestral North America to the east. Continuing north, our route follows along the eastern edge of the Quesnel terrane and passes through the Slide Mountain terrane just south of the town of Clearwater. We will stop to look at basaltic rocks of the Fennell Formation.

420.4 km. Stop 1. Fennell Formation. 51°28'8.30"N, 120°10'40.18"W. Park on the right side of the highway.

Pillow and massive basalts of the Fennell Formation (Fig A2.2). Chloritization gives the lavas a mottled, maroon to light green colour. Minor phlogopite is present. Pillows (24 x 17 cm) are brecciated and are crosscut by dark grey, fine-grained to aphanitic diabase dikes (0.5 m wide; 285°/47° NE) and quartz veins (1 cm wide). An aplitic dike (1-4 cm) with quartz veinlets cores a subvertical shear zone (up to 12 cm wide) striking 75°-83° NE. The rocks are also cut by subvertical cleavage (041°/70° SE) and fractures (003°/43° SW and 296°/60° NE). These ophiolitic rocks represent remnants of the floor of a 3000 km-wide ocean that initiated with rifting along the active margin of Ancestral North America (then Laurentia) and coeval, widespread carbonatite and alkaline magmatism in the Late Devonian to Mississippian. The Slide Mountain ocean has been interpreted as a back-arc basin formed by lithospheric extension during east-dipping subduction of the Proto-Pacific plate under the western margin of Laurentia (e.g., Nelson et al., 2013).

The carbonatites of the Blue River area that we will see on this field trip have isotopic signatures identical to those of worldwide carbonatites formed by deep-mantle plumes (Mitchell et al., 2017; Rukhlov et al., 2018). We suggest that Slide Mountain ocean back-arc extension also triggered emplacement of the Blue River carbonatites, and that these rocks were sourced from a deep-level mantle plume that was tapped episodically since the Neoproterozoic (at ca. 810-700, 500, and 360-330 Ma).

445.1 km. Proceed north on the Yellowhead Highway 5. At roundabout turn left (third exit) and proceed northwest on the Clearwater Valley Rd.

Laurentian margin. As we continue north, our route leaves behind the Intermontane terranes and enters the Shuswap Highland and then the high Cariboo and Monashee mountains of the Omineca belt, the inner tectonic welt of the Cordillera, which is separated from the Foreland belt to the east by the Rocky Mountain Trench (Monger et al., 1982). Both the Omineca and Foreland belts are underlain by Proterozoic to Paleozoic successions formed in intracratonic basins before the breakup of the supercontinent Rodinia and as passive margin deposits on the flank of Laurentia after breakup (Goodfellow et al., 1995; Cecile et al., 1997; Colpron et al., 2002; Mathews and Monger, 2005). Mostly distal shelf to deep-water strata in the Omineca belt have undergone predominantly ductile deformation and greenschist- to upper amphibolitic-grade metamorphism from the Early Jurassic



Fig. A2.2. Pillow basalt of the Fennell Formation (Mississippian to Permian), Slide Mountain terrane.

through to the Paleocene, whereas the equivalent platform and shelf facies of the Foreland belt were deformed by thin-skinned folding and thrusting with little metamorphism mainly in the Cretaceous through the Paleocene (e.g., Bally et al., 1966; Price and Mountjoy, 1970; Evenchik et al., 2007; Simony and Carr, 2011; Pană and van der Pluijm, 2014). Synorogenic intrusions and local volcanic rocks are widespread in the Omineca belt, which was close to the collision zone between the offshore terranes and the Laurentian craton in the Early Jurassic. Crustal thickening, transpression, and uplift in the Omineca belt continued from the Middle Jurassic to the Paleocene. This was followed by transtension and uplift in the Eocene, which exhumed mid-crustal assemblages and, locally, crystalline cratonic basement in the southern Omineca belt (Parrish et al., 1988; Simony and Carr, 2011).

455.3 km. Turn left at Y intersection about 100 m past the bridge across Spahats Creek and drive 90 m. Turn left again and drive 130 m. Proceed right at Y intersection for 170 m to the Spahats Falls parking lot. **Stop 2: 51°44'9.92"N; 120°0'39.30"W.** Clearwater Valley/Spahats Falls.



Fig. A2.3. Spahats Falls cascading from alkali basaltic lava flows of the Clearwater unit (~400 Ky), underlain by unconsolidated sands and gravels near the base of the falls (courtesy of G. Fortin).

Walk along a trail to the viewing platform to see Spahats Falls (73 m high), which cascade from alkali basaltic lava flows of the Clearwater unit (~400 Ky) that overlie unconsolidated sands and gravels seen near the base of the falls (Fig. A2.3; Hickson and Vigouroux, 2014). The lack of erosion or soil development between successive lava flows suggests rapid filling of the paleo-Clearwater valley by the lava. The volcanic activity of the Wells Gray field spans from about 3.5 Ma to recent times (Cannings et al., 2011). Along with the vast outpourings of basaltic lava across the Interior Plateau since the Miocene, it is attributed to a mantle hot spot below western North America (Cannings et al., 2011). At Wells Gray, basaltic magma probably used crustal-scale dextral faults along the eastern edge of the Quesnel terrane (Hickson and Vigouroux, 2014). Stop for **45 min**.

Return east 290 m from Spahats Falls parking lot. Turn right and continue southeast 86 m, turn right on the Clearwater Valley Rd heading south. Drive 10.2 km back to Clearwater. At roundabout, take the 3rd exit to rejoin Yellowhead Hwy 5 heading north.

Drive to Blue River. We continue past Devonian to Mississippian volcanic rocks and Neoproterozoic to Paleozoic metamorphic rocks (Eagle Bay assemblage, Snowshoe Group and Mica Creek succession) formed on the Laurentian margin and intruded by syntectonic Jurassic to Paleocene granitic plutons (Mathews and Monger, 2005).

573.8 km. Arrive at Blue River. Turn right (SE) on Harrwood Dr. and proceed 71 m, turn left (NE) on Harrison Rd. and proceed 78 m to the Mike Wiegale Helicopter Skiing main lodge.

We will check in at the front desk and get some rest before dinner at the Saddle Mountain restaurant across the highway at **7:00 PM**.

Day 2. Blue River to Upper Fir deposit and back to Blue River.

7:30 AM: breakfast at Saddle Mountain restaurant 150 m from Mike Wiegale Helicopter Skiing main lodge across the Hwy 5 (about 5 min walk).

8:45 AM: assemble by the vehicles in front of the main lodge. We depart at **9:00 AM**.

0.0 km. From the main lodge, turn right and drive northwest for 71 m. Turn right and proceed northeast on Yellowhead Hwy 5.

19.2 km. Turn right (to the southeast) onto Bone Creek Forestry Service Rd, and cross the bridge across the North Thompson River (Fig. A2.4).

21.1 km. Proceed southeast on Bone Creek Forestry Service Rd; keep left at Y-junction to continue northeast on Gum Creek Forestry Service Rd.

21.7 km. Continue NE on Gum Creek Forestry Service Rd (keep straight/left) at Y-junction with forestry permit 1830 Rd.

23.5 km. Turn right turn at Y-junction and proceed northeast on forestry permit L600 Rd.

25.9 km. This is an alternate landing site ($52^{\circ}17'49.38''N$, $52^{\circ}17'49.38''N$); turn right (NE) to continue upslope on L600 Rd (see Fig 12).

25.98 km. Go left (NE) on L600 Rd at Y-jct with Shortcut Rd.

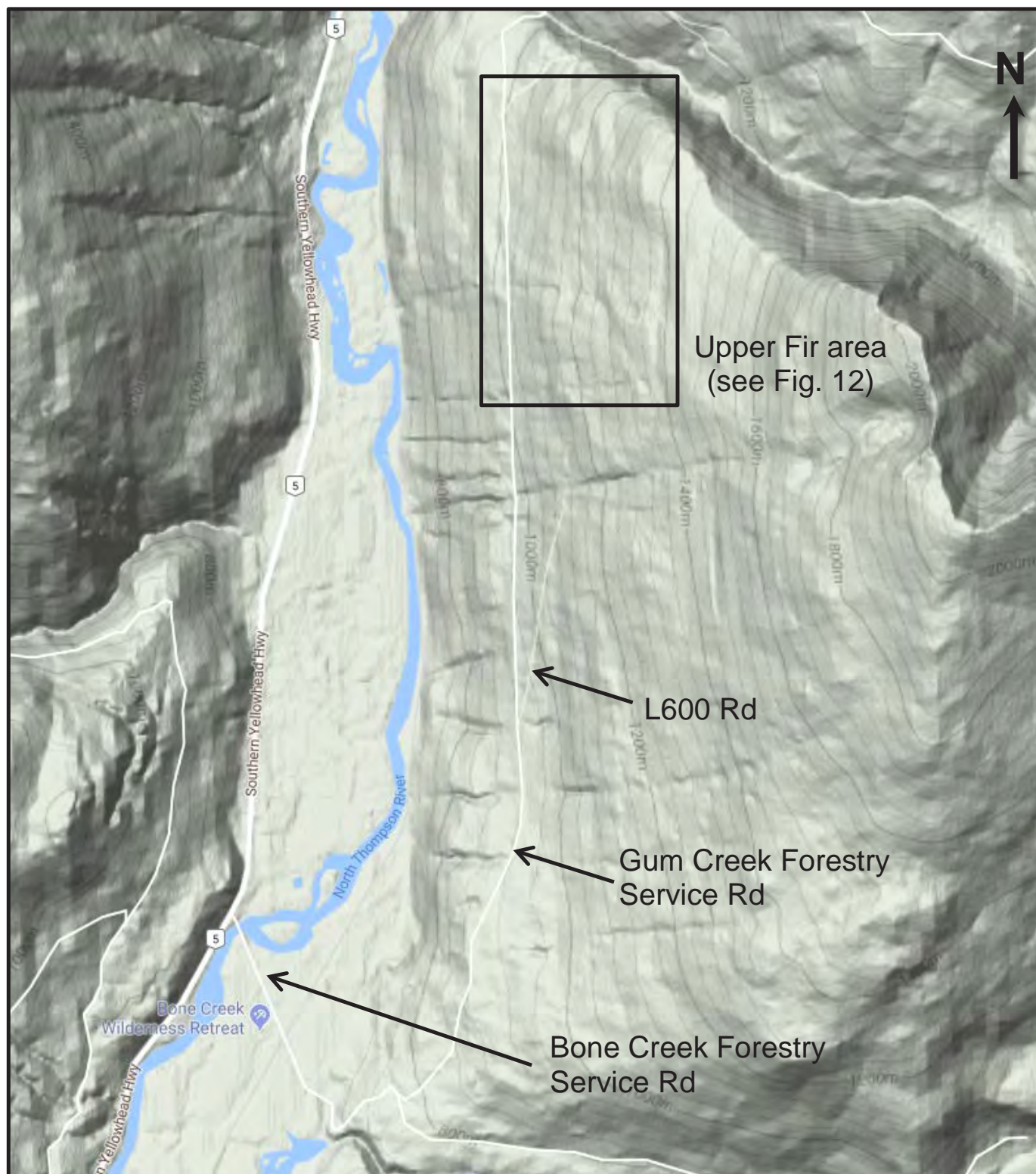


Fig. A2.4. Forestry service roads from Highway to Upper Fir, north of Blue River, east-central British Columbia.

26.06 km. Turn left (NE) on Upper Bulk Sample Rd. at Y-jct with 2900 Connector Rd.

26.33 km. Turn right on a connector road heading gently upslope to the northeast.

26.45 km. Continue straight (NE) on the connector road at Y-jct with 2900 Rd South Spur.

26.50 km. Turn right (NE) at Y-jct with 2900 Rd North and continue upslope on the connector road.

26.53 km. Arrive at Landing site (52°18'9.22"N, 119°9'27.03"W).

This is the start and end point of the Upper Fir hiking loop. We will leave vehicles here and hike to stops along deactivated trails and at excavation site BS-1 (Fig. 12). Take everything you will need during the day with you, i.e. backpacks, warm and waterproof clothing, footwear with ankle support, hard hats (to be worn at excavated sites), personal gear, lunch, snacks, water.

0.04 km. Walk southwest (downslope) on the connector road from Landing site. Turn right (north) on the deactivated 2900 Rd North. Proceed northeast on 2900 Rd North.

0.20 km. Stop 1 52°18'13.94"N, 119°09'26.88"W.
Contact between dolomite carbonatite and biotite gneiss (S_2 foliation = 323°/34° NE) cut by a pegmatite vein. Note abundant reddish-brown weathered carbonatite clasts in colluvium and grey till at the top of the road cut (Fig. A2.5). Stop for **25 min.**



Fig. A2.5. Stop 1. Weathered dolomite carbonatite clasts in colluvium.

As we continue walking north to Stop 2, note biotite gneiss offset by a local-scale, chloritized plane (005°/60° W) with slickenfibres (214° SW) about 15 m from the Stop 1 (Fig. A2.6). This late brittle structure is probably related to Eocene extension marked by the steep, west-side down North Thompson normal fault, which is traced by the valley immediately to the west (Digel et al., 1998).



Fig. A2.6. Late brittle fault surface with chlorite slickenfibres in biotite gneiss. The now-eroded block moved down dip, to lower right.

0.27 km. Stop 2: 52°18'16.24"N, 119°09'27.09"W.
Sheared glimmerite (phlogopite fenite) with dm vermiculite books separating porphyroclastic apatite-dolomite carbonatite below from amphibolite-biotite±garnet gneiss above. Banded, migmatitic semipelite (S_2 foliation: 65°/46° SE to 290°/6° NE) forms a 12 m-long recumbent isoclinal fold (F_3 hinges: 99°/26° to 104°/14°), cut by syntectonic pegmatite (10 cm wide) subparallel to axial surface (Fig. A2.7). Stop for **20 min.**



Fig. A2.7. Stop 2. Deformed and fenitized country rocks. **a)** Migmatitic amphibolite-biotite±garnet gneiss of the Mica Creek assemblage in a recumbent isoclinal fold, with coarse-grained glimmerite separating dolomite carbonatite (below) from country rocks (looking east). **b)** Dm vermiculite books from the hinge zone.

Proceed north from the end of 2900 Rd North to the upper bench of BS-1 cut. Watch your step and look out for falling rocks. Do not rush, and do not climb cliffs at the excavation site.

0.30 km. Stop 3: 52°18'17.49"N, 119°09'27.23"W.

Upper contact of a 20 m-thick carbonatite body mantled by calcite-bearing glimmerite (phlogopite fenite) interfingering with fenitized migmatitic amphibolite and biotite±garnet augen gneiss (S_2 foliation: 342°/18° NE) forming a mesoscopic recumbent isoclinal fold with parasitic cm- to dm-size isoclinal leucosome folds (Fig. A2.8; F_3 hinges: 124°/11° to 136°/5°). Garnet porphyroblasts are up to 3 cm in diameter (Fig. A2.9). Note a series of carbonatite 'eyes' (10 cm wide by 20-30 cm long lenses), mantled by the inner diopside, intermediate coarse-grained amphibole, and outer apatite-calcite glimmerite zones, which are widest along the principal axis, in the fenitized country rocks. Stop for **20 min**.



Fig. A2.8. Stop 3. Carbonatite-country rock relationships, BS-1 cut, Upper Fir. **a)** Highly strained, migmatitic semipelite with crumbly layers of carbonate-rich glimmerite above a 20 m-thick carbonatite body (looking north). Note readily oxidized Fe-rich dolomite in the carbonatite under a person and hinges of dm-scale isoclinal folds (closing south) gently plunging (5-11°) southeast. **b)** Close-up of the fenitized country rocks with coarse-grained, dolomite carbonatite 'eyes' (immediately above the hammer) in the isoclinal folds (looking east).



Fig. A2.9. Stop 3. Garnet-biotite-muscovite schist of the Mica Creek assemblage, BS-1 cut, Upper Fir.

0.38 km. Continue north (down) on ramp road past backslope outcrop of the dolomite carbonatite and a pile of carbonatite blocks, some of which contain segregations of very coarse-grained fluorapatite megacrysts (up to 3.0 x 5.5 cm) set in recrystallized ferroan dolomite matrix that readily oxidizes brown-red. Note aligned dark-green ferrikatophorite prisms locally forming segregation layers (Fig. A2.10). At the end of the ramp, turn left. Continue southwest on the BS-1 Rd.

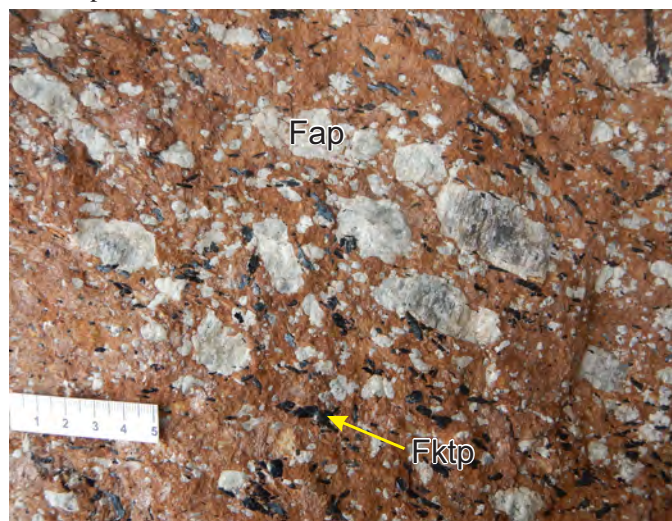


Fig. A2.10. Very coarse-grained fluorapatite (Fap) megacrysts in recrystallized, ferrikatophorite (Fktp)-bearing dolomite carbonatite, BS-1 cut, Upper Fir. Ferroan dolomite readily oxidizes reddish-brown on the surface (compare with fresh dolomite in Fig. 17).

0.41 km. Turn left at Y jct. Continue south on the lower ramp road past calcite carbonatite in the backslope outcrop from the northern end of a side ditch (Fig. A2.11). Note undulating subhorizontal fractures and gravelly weathering of the calcite carbonatite lens (3 m thick), which pinches out about 6 m to the south. It contains 5-10% anhedral magnetite clumps (up to 8 x 6 cm), 15-20% dark-green ferrikatophorite prisms (2-3 mm), and 5-10% fluorapatite. In contrast, more competent dolomite carbonatite underneath has strongly aligned (117°/4°) ovoid apatite porphyroclasts (3 x 10 mm; 20%) and light-green richterite (15%), with accessory black pyrochlore octahedra (2 mm) set in a dark-grey, fine-grained, recrystallized matrix. Segregation layer (298°/55° NE) of aligned (135°/17°) amphibole (50%) and apatite (25%) contains magnetite porphyroclasts (2 x 0.7 cm) and euhedral brown-red pyrochlore crystals (5 mm).



Fig. A2.11. Gravelly weathered, foliated calcite carbonatite above more competent dolomite carbonatite.

0.46 km Stop 4: 52°18'17.18"N, 119°9'29.65"W. (Lunch, 90 minutes).

Approximate lower contact of the carbonatite and subhorizontal pegmatite vein with biotite crystals up to 2 x 15 cm, underlain by country gneiss.

The pegmatite can be traced for at least 13 m from north to south. Note massive garnetiferous amphibolite with folded black amphibole segregations and late clinopyroxene-amphibole veins (Fig. A2.12). Sodium-rich amphibolites associated with carbonatites at Upper Fir contain abundant titanite, Mg-Fe³⁺-Na-rich hedenbergite, calcic to sodic-calcic amphibole, calcite, albite, and minor K-feldspar and fluorapatite (see Figs. 5i and 16). They represent Na-fenites

on the outer metasomatic envelop around the inner glimmerite (phlogopite fenite) mantle of the carbonatite bodies. Examine various dolomite carbonatites exposed in BS-1 (Figs. 9, 10a, A2.13), with fresh olive-green ferroan dolomite porphyroclasts, aligned amphibole (70%; up to 2 x 4 cm) and common segregation bands (342°/32° NE) with abundant ovoid fluorapatite (116°/20°, 119°/26°, 120°/16°) ± pyrochlore ± ferrocolumbite, S₂ foliation (25°/41° SE, 15°/42° SE, 0°/23° E) overprinted by high-strain zones (35°/50° SE), coarse-grained calc-silicate skarn veins (55°/40° NW), pyrrhotite veins (3-13 mm), and strained magnetite porphyroclasts (1.5 x 5 cm).

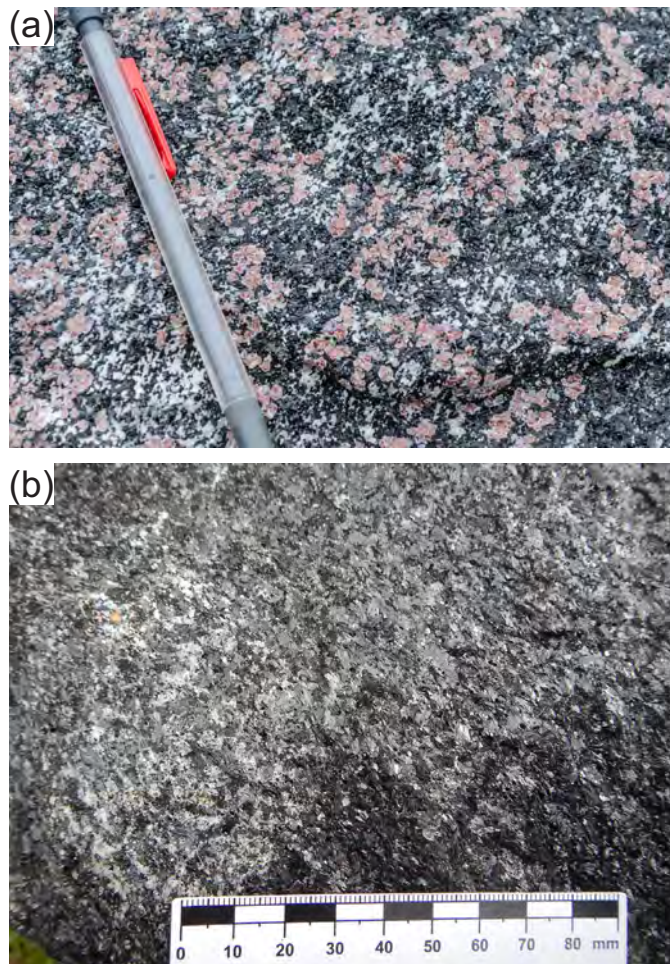


Fig. A2.12. Stop 4. Examples of Na-fenites, BS-1 cut, Upper Fir. **a)** Garnetiferous amphibolite with Na-Ca amphibole, albite and Na-rich clinopyroxene. **b)** Holomelanocratic hornblendite made up of magnesiohastingsite with minor interstitial carbonate.

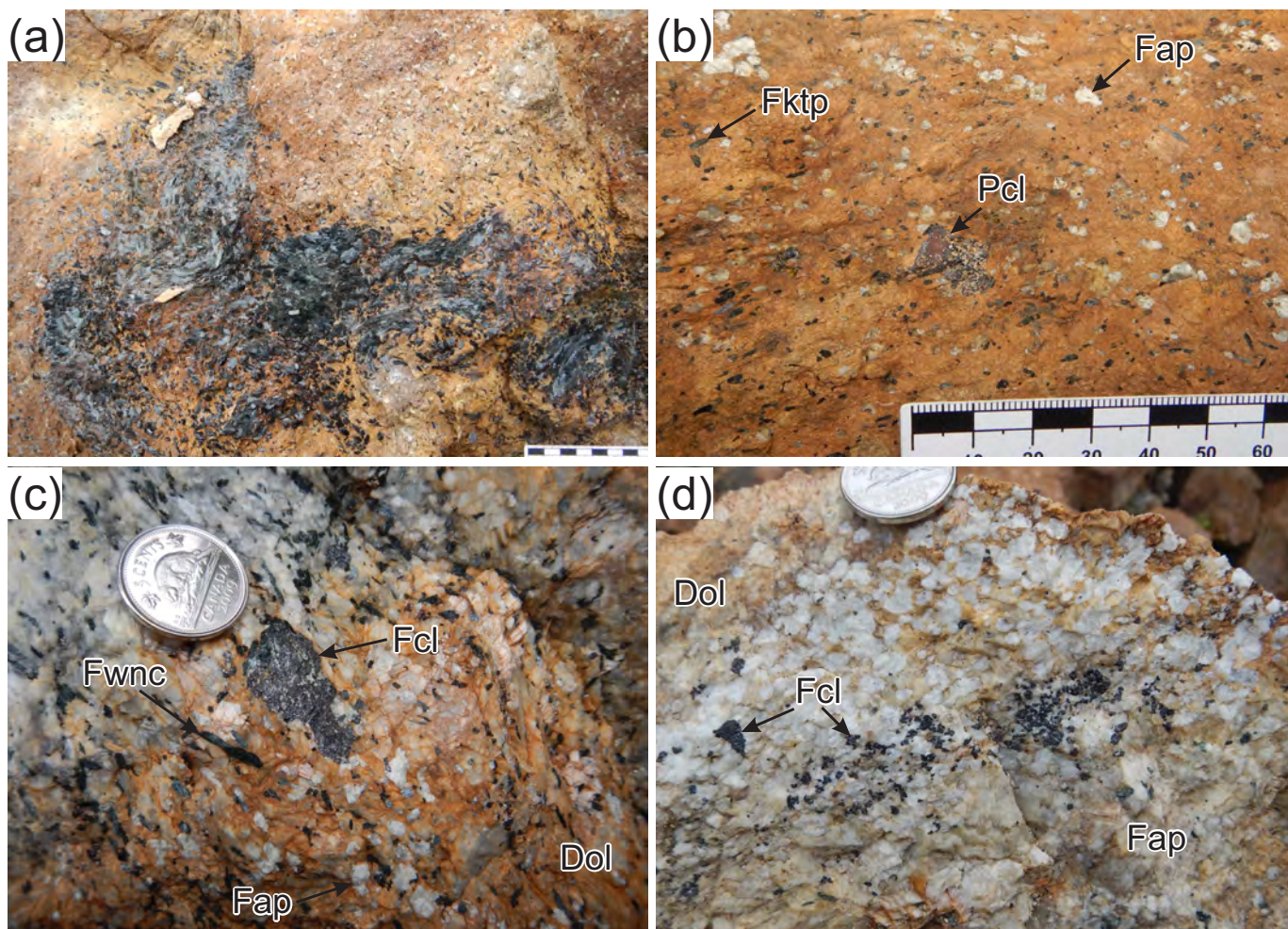


Fig. A2.13. Examples of textures and mineralization in carbonatites at Upper Fir. **a)** Folded amphibole segregation in dolomite carbonatite, BS-1 cut (Stop 4). **b)** Coarse euhedral U-Ta-rich pyrochlore (Pcl) in foliated, porphyroclastic dolomite carbonatite, containing ferrikatophorite (Fktp) and fluorapatite (Fap), BS-2 cut. **c)** Coarse ferrocolumbite (Fcl) in gneissic dolomite (Dol) carbonatite containing abundant fluorapatite and ferriwinchite (Fwnc), Landing site 2. **d)** Ferrocolumbite concentrated in fluorapatite segregation in granoblastic, anchimonomineralic dolomite carbonatite, Landing site 2.

0.53 km. Retrace north along the lower ramp road. Turn left (SW) on BS-1 Rd at Y jct.

0.58 km. Proceed southwest on BS-1 Rd and turn left (south) on Upper Bulk Sample Rd at Y jct.

1.00 km. Continue south on Upper Bulk Sample Rd. Turn left (NE) on the connector road at Y jct.

1.12 km. Proceed northeast (upslope) on the connector road. Keep straight (left) on the connector road at Y jct with 2900 Rd South Spur.

1.16 km. Proceed northeast. Turn right (NE) on the connector road at Y jct with 2900 Rd North.

1.19 km. Continue northeast to vehicles parked at Landing site. We leave for Blue River at **4:00 PM.**

Retrace to Yellowhead Hwy 5 by driving southwest down on L600 road, on Gum Creek FSR, and then northwest on Bone Creek FSR. Turn left (SW) on Yellowhead Hwy 5 and drive 19.1 km towards Blue River. Turn left (SE) on Harrwood Dr. Proceed southeast 71 m, then turn left (NE) on Harrison Rd and proceed 78 m to MWHS main lodge. Dinner at **6:30 PM** at Saddle Mountain restaurant.

Day 3. Core shack in Blue River and return to Vancouver

7:30 AM: breakfast at Saddle Mountain restaurant.

Check out and assemble by the main lodge. We depart for Commerce Resources Corp.'s core facility in Blue River at **9:00 AM**.

0.0 km. From Mike Wiegele Helicopter Skiing main lodge, turn right (NW) on Harrwood Dr.

0.07 km. Proceed northwest on Harrwood Dr. Turn left on Blue River East Fronting at intersection.

Drive 350 m southwest on Blue River East Fronting and continue 600 m straight south on Cedar St. to the Commerce Resources Corp. blue board in front of two white and blue buildings (field office) and a beige hangar (core facility) on the left side.

1.02 km. Stop 1: 52°6'17.76"N, 119°18'26.89"W.

Commerce Resources Corp. core facility.

We will examine representative core intervals from the Commerce Resources Corp.'s Upper Fir drillholes F10-198 (72.33-129.56 m; collar NAD83 UTM zone 11 coordinates: 352813 m E, 5796902 m N; elevation: 1201 m; plunge: 60° E) and F10-208 (7.32-230.19 m; NAD83 UTM zone 11 coordinates: 352967 m E, 5796622 m N, 1268 m, 75° E). Note texturally and mineralogically diverse dolomite carbonatites and calcite carbonatites containing up to 0.87 wt% Ta, 12.29 wt% Nb, and 6.7 wt% P₂O₅, amphibole-diopside± calcite± phlogopite skarn veins, exocontact-metasomatic calcite-amphibole glimmerites (phlogopite fenites) and calcite-pyroxene amphibolites (outer Na-fenites) with up to 68 ppm Mo, unaltered country gneisses, schists, amphibolites of the Mica Creek assemblage, and late syntectonic pegmatites. See downhole profiles for details (Appendix 1). Stop for **1 hour**.

We depart for Vancouver at 10:00 AM for arrival at Vancouver Convention Centre West by 7:30 PM.

Appendix 3. Upper Fir east-west cross sections (same location as Fig. 13a).

These cross sections show the 99th percentile assay results for selected elements from drill-core samples (typically 1 m intervals), gridded by the inverse-distance 3D interpolation method using GOCAD® software. (**a, b, c, d, e** by LiBO_4 fusion - HNO_3 digestion and inductively coupled argon plasma emission spectroscopy (**a – c**) or inductively coupled argon plasma mass spectrometry (**d** and **e**); **f** by $2\text{HNO}_3:2\text{HCl}:2\text{H}_2\text{O}$ (v/v) acid solution and inductively coupled argon plasma mass spectrometry): **a**) CaO/MgO (wt.%). **b**) total Fe expressed as Fe_2O_3 (wt.%). **c**) P_2O_5 (wt.%). **d**) Nb (ppm). **e**) Ta (ppm). **f**) Mo (ppm); also showing Mo assay results for individual drill-core intervals.

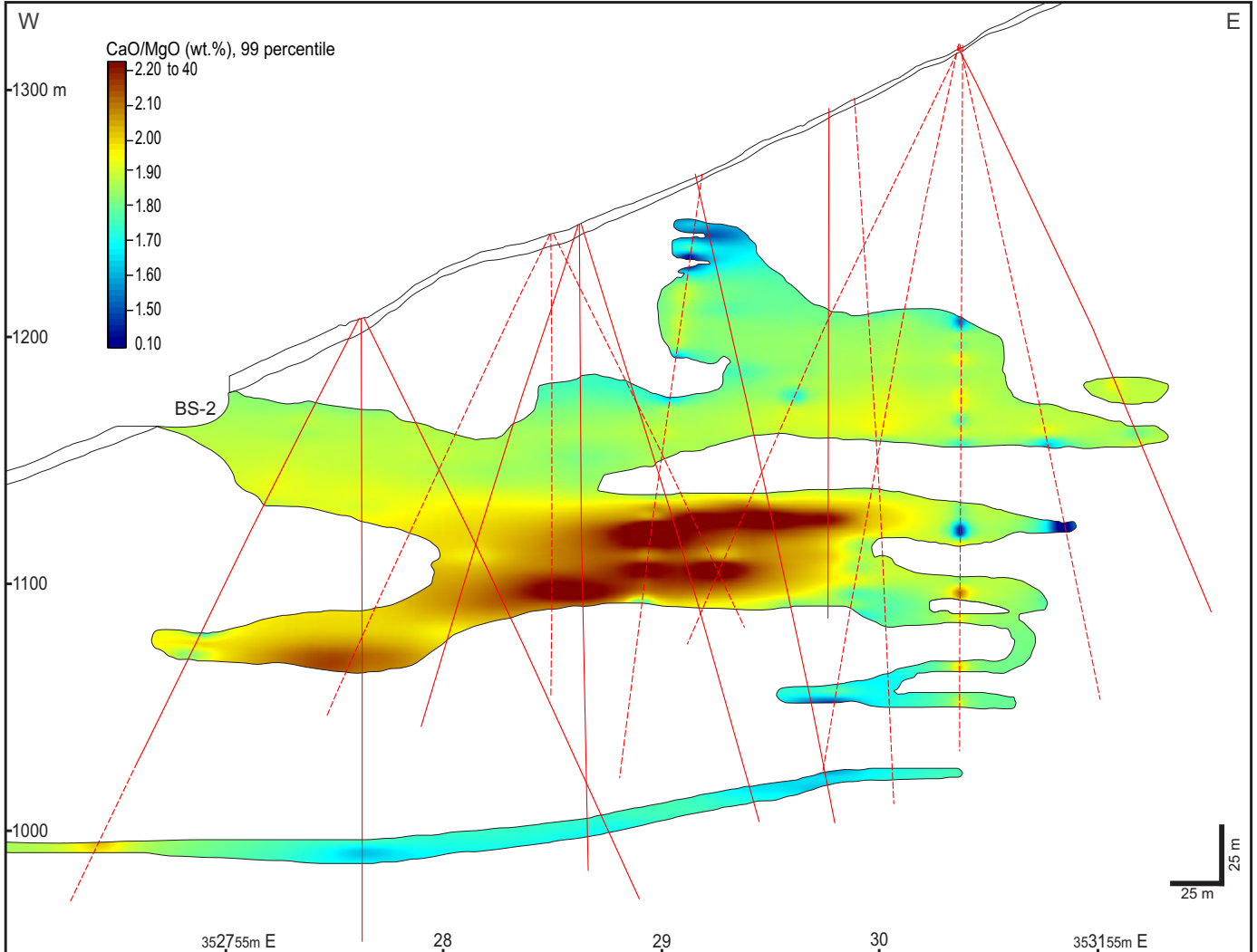


Fig. A3 a)

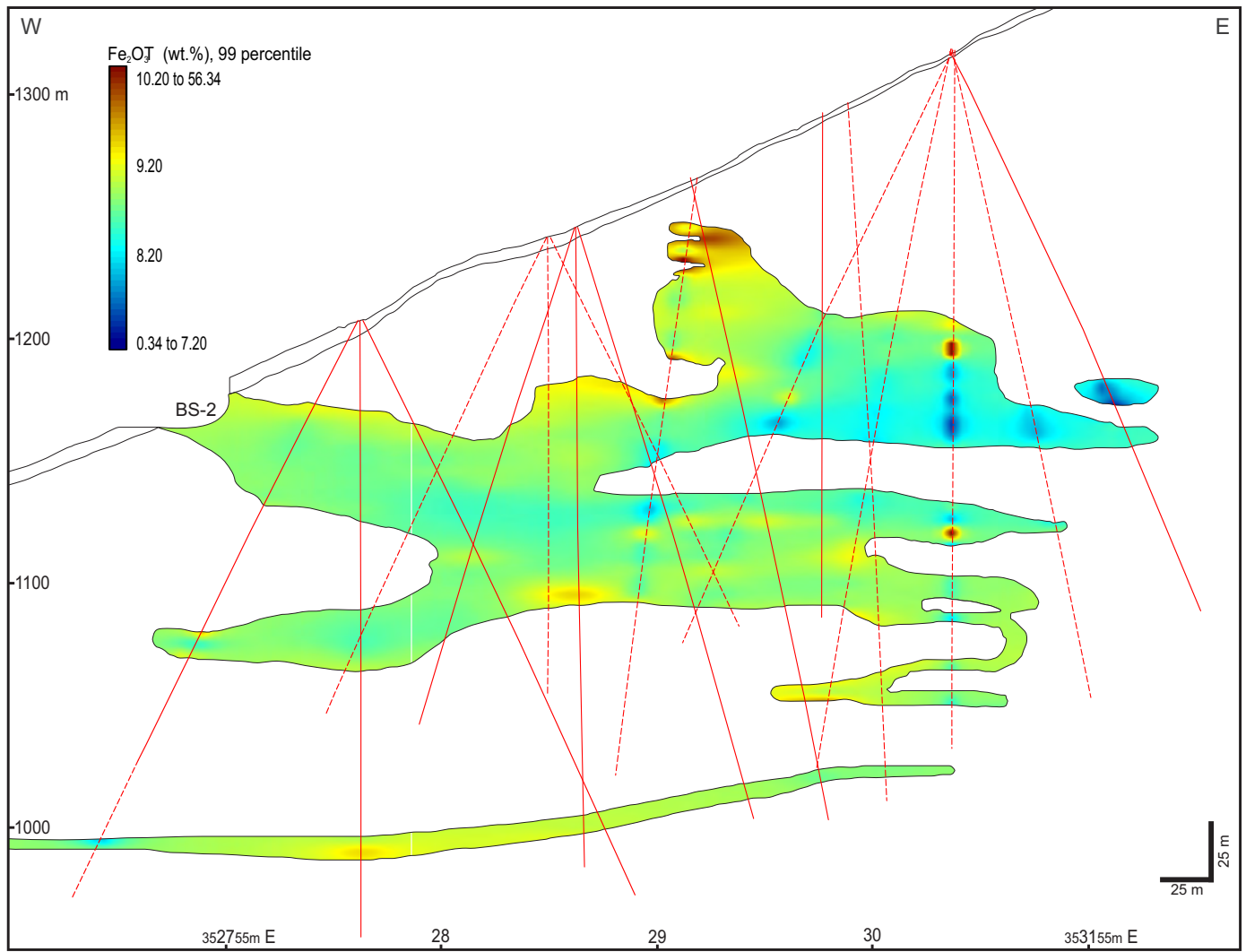


Fig. A3 b)

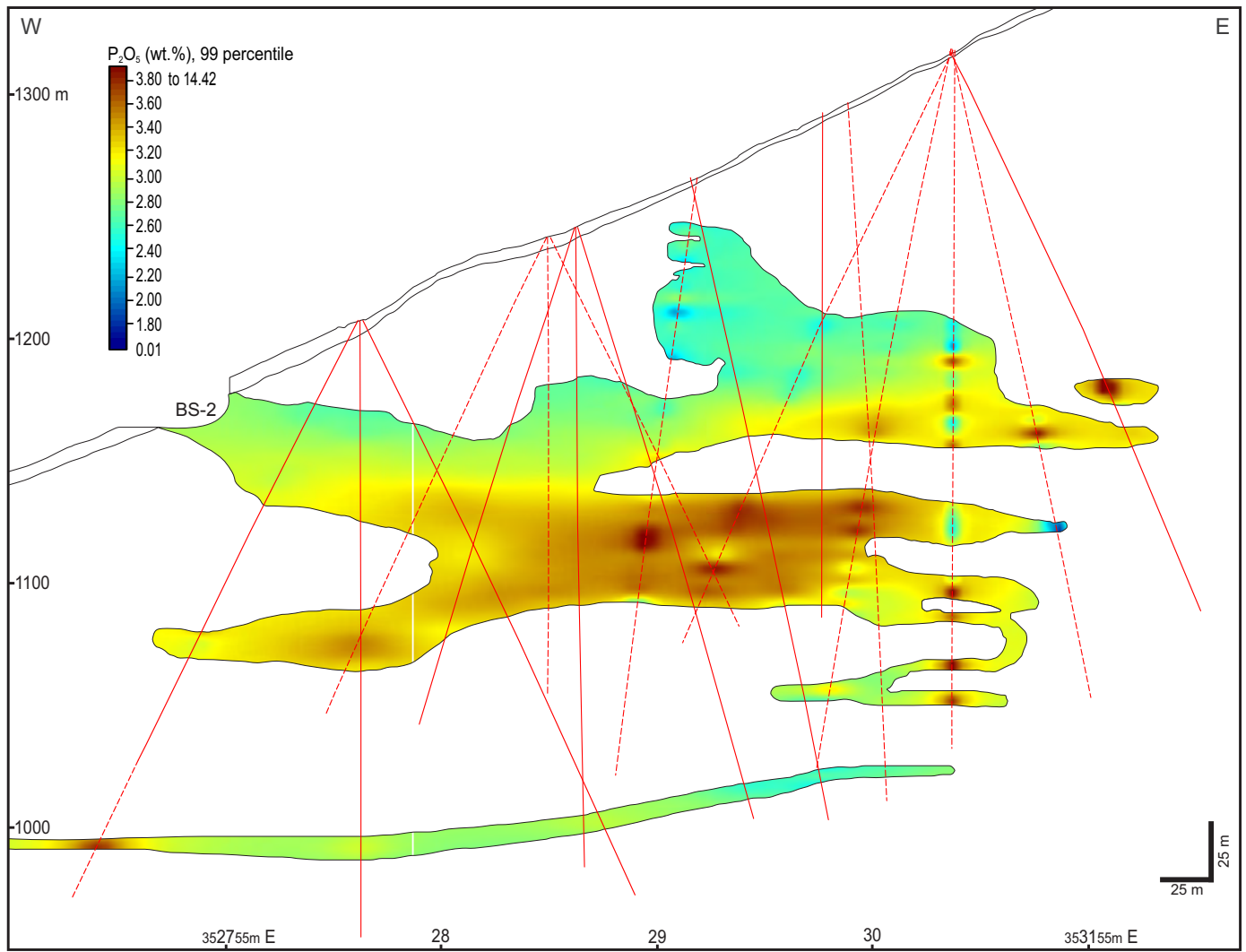


Fig. A3 c)

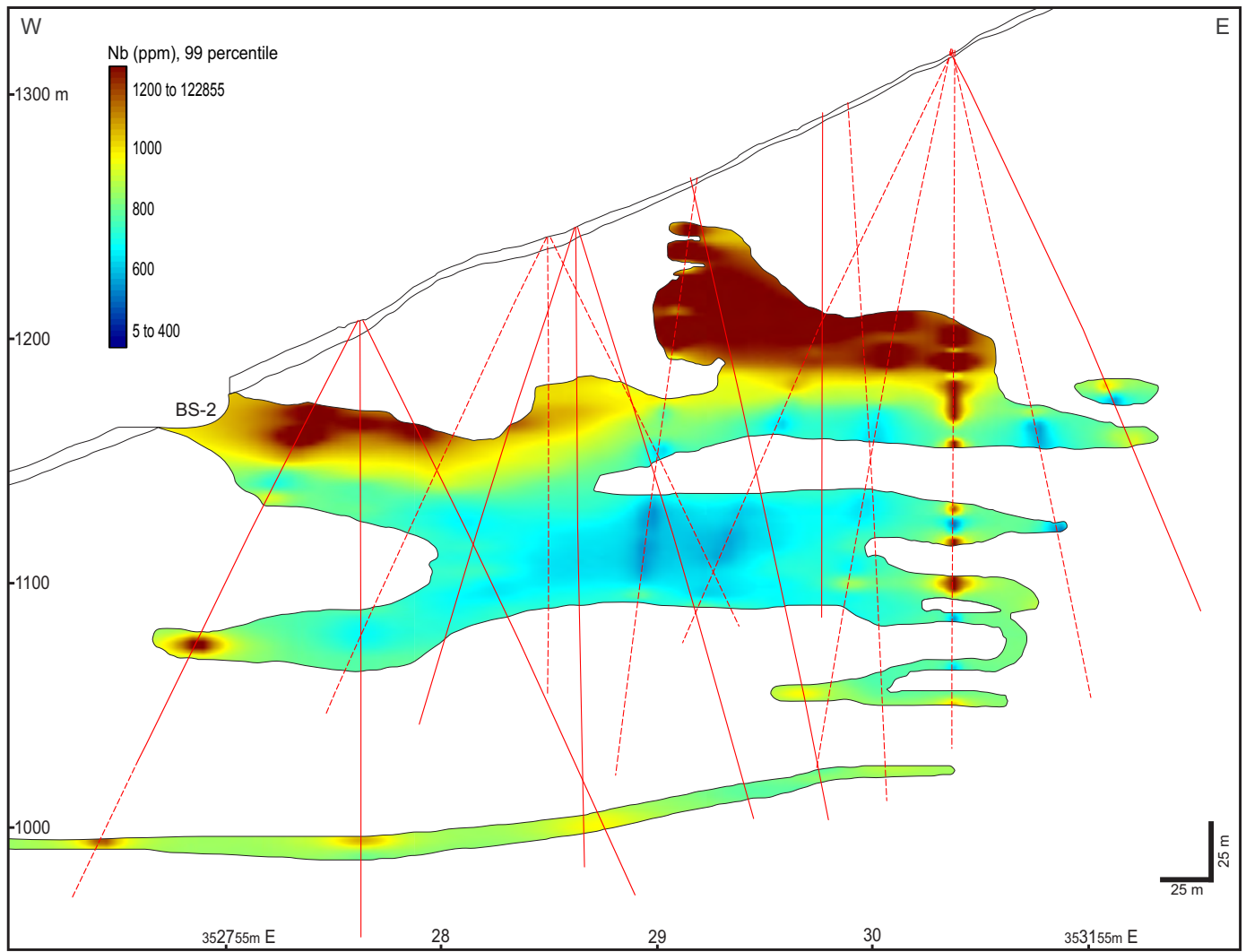


Fig. A3 d)

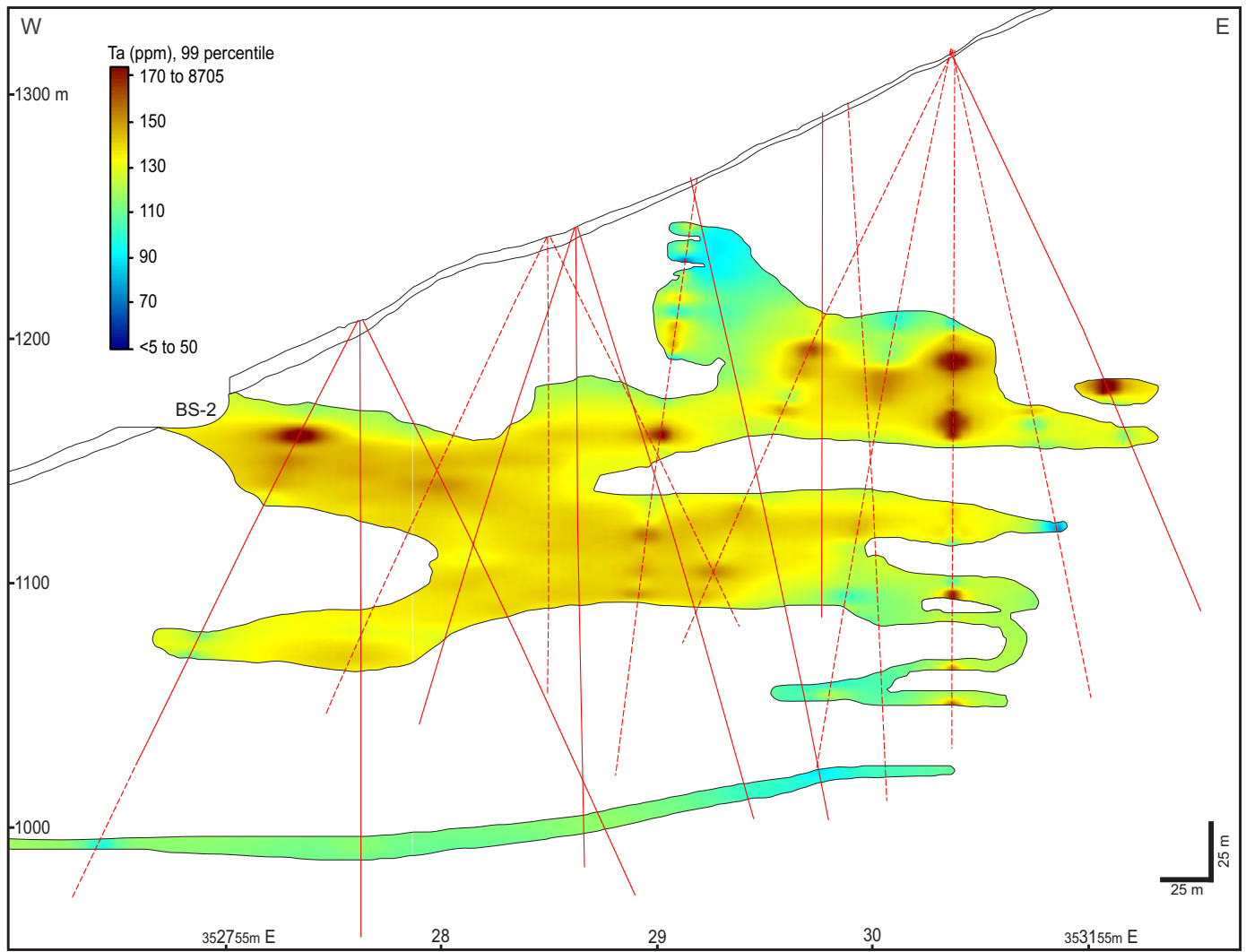


Fig. A3 e)

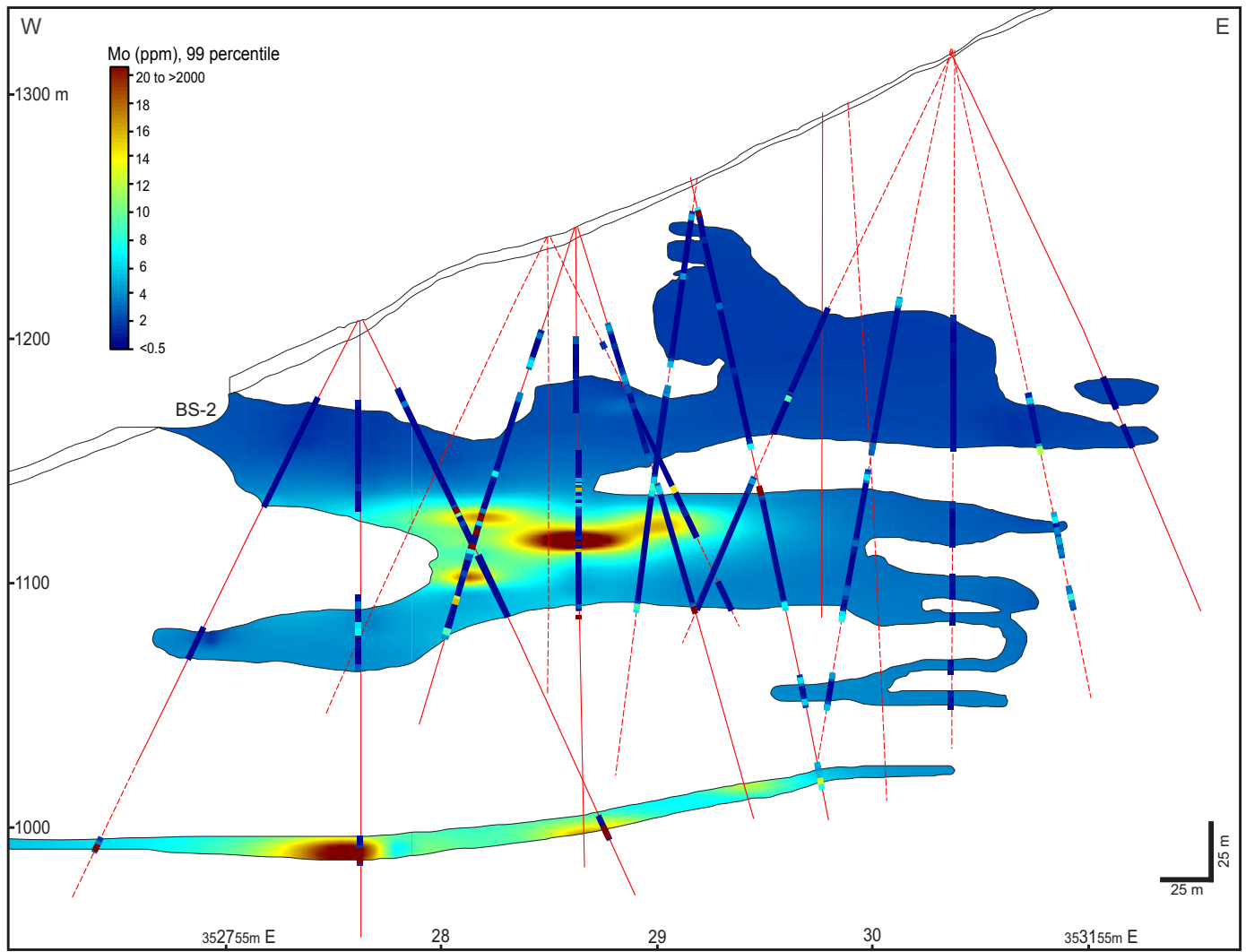


Fig. A3 f)

British Columbia Geological Survey
Ministry of Energy, Mines and Petroleum Resources
www.empr.gov.bc.ca/geology

